Cooperative Transmission for Downlink Distributed Antenna in Time Division Duplex System

A Thesis Submitted to The University of Kent
For The Degree of Doctor of Philosophy
In Electronic Engineering

By

Ashim Khadka

December, 2017

Supervisor

Professor Jiangzhou Wang

Dedication

I would like to dedicate this thesis to my family ...

Acknowledgements

This thesis would not be complete without the guidance and support of several individuals, who, in one way or the other, have left a lasting impression on me during the completion of this study.

I would like to thank my supervisor Prof. Jiangzhou Wang, for leading me to the area of distributed antenna system, for providing the comfortable environment and for his invaluable guidance. Without his comments and contributions the work of this thesis could not be achieved. I would like to thank Dr. Huiling Zhu, for her help advice, insightful questions and constructive feedback on my research. I admire her critical eye for important research topics.

I especially thank Dr. Koichi Adachi, who inspired on my research and provided invaluable advices during my research. I am indebted to him for carefully reading my manuscripts and patiently working with me on my writing. I would not have been able to complete my research without the benefit of his vast knowledge, experience, and valuable comments. I would like to thank Dr. Sun Sumei, for her collaboration on my research project, for ARAP Grant and for inviting me at Institute for Infocomm Research (I2R), Singapore during 2013-2014. Her attention to detail has always amzamed me. I have learnt how to treat research with rigorousness and intelligence and will remember for the rest of my life.

I would like to extend my thank to Dr. Junyuan Wang and Dr.Zhun Ye for providing valuable feedback and for many technical conversations. Undoubtedly, I have enjoyed every single moment talking with them.

Finally, I would like to thank the colleagues in the lab and school for their support and friendly environment.

List of Publications

1. A. Khadka, K. Adachi, S. Sun, J. Wang, H. Zhu and J. Wang, "Cooperative Transmission Strategy Over Users' Mobility for Downlink Distributed Antenna Systems," submitted to *IEEE Trans. Wireless Commun.*

2. A. Mahbas, A. Khadka, H. Zhu and J. Wang, "Challenges Imposed by User Mobility in Ultra-Dense HetNets," submitted to *IEEE Commun. Magazine.*

3. A. Khadka, K. Adachi, S. Sun, J. Wang, H. Zhu and J. Wang, "Cooperative Transmission Strategy Over Users' Mobility for Downlink Distributed Antenna Systems," in *Proc. IEEE Globecom,* Dec., 2017.

4. A. Khadka, K. Adachi, S. Sun, H. Zhu and J. Wang, "Cooperative Transmission Strategy for Downlink Distributed Antenna Systems Over Time-Varying Channel," in *Proc. IEEE Globecom,* Dec., 2015.

Abstract

Multi-user distributed antenna system (MU-DAS) systems play the essential role in improving throughput performance in wireless communications. This improvement can be achieved by exploiting the spatial domain and without the need of additional power and bandwidth. In this thesis, three main issues which are of importance to the data rate transmission have been investigated.

Firstly, user clustering in MU-DAS downlink systems has been considered, where this technique can be efficiently used to reduce the complexity and cost caused by radio frequency chains, associated with antennas while keeping most of the diversity advantages of the system. The proposed user clustering algorithm which can select an optimal set of antennas for transmission. The capacity achieved by the proposed algorithm is almost same as the capacity of the optimum search method, with much lower complexity.

Secondly, interference alignment in MU-DAS downlink systems has been studied. The inter-cluster interference is uncoordinated and limits the system performance. The inter-cluster interference should be eliminated or minimized carefully. The interference alignment is proposed to consolidate the strong inter-cluster interference into smaller dimensions of signal space at each user and use the remaining dimensions to transmit the desired signals without any interference. The performance of single cluster is better than the proposed algorithm due to the absence of inter-cluster interference in the single cluster. The numerical shows that the proposed algorithm is more suitable in multi-cell DAS environment due to the presence of inter-cell interference.

Finally, the impact of different user mobility on TDD downlink MU-DAS has been studied. The downlink data transmission in time division duplex (TDD) systems is optimized according to the channel state information (CSI) which is obtained at the uplink time slot. However, the actual channel at downlink time slot may be different from the estimated channel due to channel variation in mobility environment. Based on mo-

bility state information (MSI), an autocorrelation based feedback interval adjustment technique is proposed. The proposed technique adjusts the CSI update interval and mitigates the performance degradation imposed by the user mobility and the transmission delay. Cooperative clusters are formed to maximize sum rate. In order to reduce the computational complexity, a channel gain based antenna selection and signal-to-interference plus noise ratio (SINR) based user clustering are developed. A downlink ergodic capacity is derived in single user clustering. The derived analytical expressions of the downlink ergodic capacity are verified by system simulations. Numerical results show that the proposed scheme can improved sum rate over the non cooperative system and no MSI knowledge. The proposed technique has good performance for a wide range of user speed and suitable for future wireless communications systems.

Contents

Acknowledgements **iv**

List of Publications **v**

Abstract **vii**

List of Figures **x**

List of Tables **xiv**

List of Abbreviations **xv**

1 Introduction **1**
1.1 Motivation 1
1.1.1 Overview of the DAS 4
1.1.2 Types of DAS Communication Systems 5
1.1.3 Modes of Channel Operation 8
1.2 Challenges 10
1.3 Contribution of the Thesis 14
1.4 Structure of the Thesis 15

2 Background Theory **17**
2.1 Wireless Channel 17
2.1.1 Time Variant Channel 18
2.1.2 Jakes' Model 19
2.1.3 Rayleigh Fading Distribution 21

2.2 Time Division Duplex 23
2.3 Literature Review 25
2.3.1 Users' Mobility 25
2.3.2 TDD support User mobility 27
2.3.3 Multi-user DAS 28
2.3.4 Transmit precoding vectors 32
2.3.5 Per antenna power constraint 35
2.3.6 Interference Alignment 37

3 User clustering in MU-DAS 40
3.1 Introduction 40
3.1.1 Contribution 41
3.2 System Model 41
3.2.1 Cluster Formation 44
3.3 Numerical Results 46
3.4 Summary 51

4 Interference Alignment in Inter-cluster of MU-DAS 52
4.1 Introduction 52
4.1.1 Contribution 53
4.2 System Model 54
4.3 Cooperative Cluster Formation 55
4.3.1 User Clustering 55
4.3.2 Cooperative Clustering 56
4.3.3 Single Cluster 58
4.3.4 No Cluster Selection 59
4.4 Beamforming Design 59
4.4.1 Transmit Beamforming 59
4.4.2 Receive beamforming 60
4.5 Numerical Results 60
4.6 summary 64

5 Cooperative transmission over user mobility for MU-DAS 66
5.1 Introduction 66
5.1.1 Contribution 67
5.2 System Model 68
5.3 Cooperative Cluster Formation 73
5.3.1 Antenna Selection (AS) Phase 74
5.3.2 User Clustering (UC) Phase 75
5.3.3 Cluster based Sub-problem Formulation 78
5.4 Feedback Interval Allocation 83
5.5 Downlink Rate Analysis 88
5.6 Numerical Results 95
5.6.1 Average Sum Rate over User's Mobility 95
5.6.2 Average Sum Rate over the Number of Users . . . 98
5.6.3 Average Sum Rate over the Number of RAUs . . . 101
5.7 summary 102

6 Conclusions and Future Research 104
6.1 Summary of Contributions 104
6.2 Future Research 105

Appendices 107

Bibliography 113

List of Figures

1.1 Global mobile traffic growth 2
1.2 Options for improving the system capacity 4
1.3 Illustration of a cellular DAS, where RAUs are distributed over the cell and connected to the CU 6
1.4 Different DAS in the cellular network. 6
1.5 Modes of channel operation 9
1.6 Comparision of TDD with FDD 10
1.7 Autocorrelation of channel where users have different mobility. 12
1.8 The MU-DAS with outdated CSI due to user mobility/transmission delay. 13

2.1 Wireless multipath propagation. 18
2.2 Doppler shift of n^{th} incoming wave on the mobile receiver. 19
2.3 Jakes' ring model. The scatterers in the environment are distributed, at equal distances from a user. 20
2.4 Carrier frequency - velocity curve for various levels of normalized Doppler and fixed symbol duration $T = 100\mu s$. . 22
2.5 Carrier frequency - velocity curve for various levels of symbol duration and fixed normalized Doppler $f_dT = 0.1$. . . 23
2.6 Illustration of feedback interval 24
2.7 Illustration of data transmission delay 24
2.8 Illustration of single-user clustering where $K = 3$, $N_t = 3$ and three clusters are formed. 30

2.9 Illustration of multi-user clustering where $K = 3$, $N_t = 3$ and two clusters are formed. 31
2.10 Illustration of one clustering where $K = 3$, $N_t = 3$ and one cluster is formed. 32
2.11 The MU-DAS with zero-forcing linear precoding. 33
2.12 Illustration of sum rate of ZF precoding with $K = 2$ and $N_t = 7$ as a function of normalized Doppler. 34
2.13 Interference alignment - Toy example of [94]. 38

3.1 DAS architecture in cell 43
3.2 Illustration of sum rate comparison between CAS and DAS cellular networks under different user clustering scheme, where $K = 7$ and $N_t = 7$. 47
3.3 Illustration of CDF of proposed cluster and exhaustive cluster scheme at different transmit power, where $K = 7$ and $N_t = 7$. 48
3.4 Illustration of PDF of actual transmit power of One cluster and proposed cluster scheme, where $K = 7$ and $N_t = 7$. 49
3.5 Run time comparison of proposed and exhaustive user clustering with 2 users. 50

4.1 Comparison of CDF of sum rate of cluster selection when $N_t = 6$, $K = 6$, $N_r = 2$ at 20 dBm, where number of selected users is 3 62
4.2 CDF of difference between sum rate of norm based selection and sum rate of random based selection (delta sum rate) when $N_t = 6$, $K = 6$, $N_r = 2$ at 20 dBm, where number of selected users is 3 63
4.3 Comparison of CDF of difference between maximum user rate and minimum user rate of norm base and random based cluster selection (Delta rate) when $N_t = 6$, $K = 6$, $N_r = 2$ at 20 dBm, where number of selected users is 3 65

5.1 DAS architecture in cell 70

5.2 Illustration of antenna selection where user is assigned to RAU based on channel gain. 75
5.3 An example that strong cross link causes large interference. 77
5.4 An example of user clustering where strong cross link provide cooperative gain. 77
5.5 Illustration of cooperative clustering for 12 users and 400 RAUs where clustering threshold is 20dB. 78
5.6 Illustration of Average sum rate of different users mobility with various clustering threshold where $N_t = 400$ and user target SINR is 50 dB at feedback time slot. 80
5.7 Comparison of sum rate of exhaustive search and proposed algrothim where $v = 0$ m/s and $K = 4$. 83
5.8 Illustration of feedback interval with user speed between 2 to 4 m/s where radio frame duration is 10 ms. 85
5.9 Illustration of feedback interval of different mobility users where minimum autocorrelation coefficient is 0.8. 86
5.10 Illustration of time slot allocation. 87
5.11 Illustration of single user clustering for 12 users and 400 RAUs. 89
5.12 Illustration of Ergodic user rate of different mobility users over number of uplink time slots, N_u, where $K = 2$ and $N_t = 400$. 94
5.13 Illustration of Average sum rate over changing mobility of the users, where $\rho_o = 0.8$ $K = 2$ and $N_t = 400$. 96
5.14 Illustration of Average user rate over autocorrelation threshold, where $K = 4$ and $N_t = 400$. 97
5.15 Illustration of Ergodic sum rate of different mobility users where user speed is fixed. 100
5.16 Illustration of Average sum rate of different users mobility with and without MSI where cooperative clustering formed. 101

5.17 Illustration of Average sum rate of different users mobility with and without cooperative clustering where clustering threshold is 20dB and user target SINR 50 dB at feedback time slot. 102
5.18 Illustration of Average sum rate of different users mobility over network size, N_t with various user speed. 103

List of Tables

2.1 Effects of system parameters on the normalized Doppler frequency f_dT. 22

3.1 Simulation Parameters 46

4.1 Norm value of selected user from interfering cluster 56
4.2 Strong interference cancel for selected user 57
4.3 Cluster with the smallest interference 57
4.4 Simulation Parameters 61

5.1 Feedback parameters: $\rho_o = 0.8$ 86
5.2 Simulation Parameters 96
5.3 Feedback parameters: adaptive autocorrelation threshold . 98

List of Abbreviations

1G	First Generation
4G	Fourth Generation
5G	Fifth Generation
AS	Antenna Selection
AWGN	Additive White Gaussian Noise
BS	Base Station
CSI	Channel State Information
CU	Central Unit
D2U	Downlink to Uplink
DAS	Distributed Antenna System
DN	Dense Network
DoF	Degrees of Freedom
DPC	Dirty Paper Coding
FDD	Frequency Division Duplex
HetNets	Heterogeneous Networks
i.i.d	Independent and Identically Distributed
IA	Interferenve Alignment

ICI	Inter-Cell Interference
IUI	Inter-User Interference
JP	Joint Processing
LOS	Line of Sight
MGF	Moment Generating Function
MIMO	Multiple Input Multiple Output
MMSE	Minimum Mean Square Error
mmWave	Millimetre Wave
MSI	Mobility State Information
MU-DAS	Multi-User Distributed Antenna System
MU-MIMO	Multi-User Multiple Input Multiple Output
OCI	Other Cell Interference
PDF	Probability Density Function
QoS	Quality of Service
RAU	Remote Antenna Unit
RF	Radio Frequency
RF	Radio Frequency
SINR	Signal to Interference plus Noise Ratio
SNR	Signal to Noise Ratio
SU-DAS	Signle-User Distributed Antenna System
TDD	Time Division Duplex
TDMA	Time Division Multiple Access

U2D	Uplink to Downlink
UC	User Clustering
WH	Walsh-Hadamard
ZF	Zero-Forcing

Chapter 1

Introduction

1.1 Motivation

Wireless communication systems are evolving continuously. From the first generation (1G) system to the fourth generation (4G) system, the technologies have been advanced to cater to the needs of customers. However, the demands of the high data rate has been growing with the rapid development of smartphones as shown in Fig.1.1. The social networking, real-time video, entrainment and interactive games, will progressively be delivered over wireless communication systems. These developments will grow exponentially over the next decade [1–3]. The rapid growth of mobile data access requires huge demand for high data rate transmission and coverage extension with limited transmit power and bandwidth. The system capacity can be improved via three main approaches as shown in Fig.1.2.

1. **Spectral efficiency:** Multiple Input Multiple Output (MIMO) is promising approach to enhance the spectral efficiency by increasing the spatial dimensions in macro base stations (BSs). The number of antenna can be either co-located or distributed in the cell [4]. In massive MIMO, few hundred antennas are co-located to increase data rate and enhance reliability [5, 6]. In distributed antenna systems (DAS), a number of remote antenna units (RAUs) are deployed at geographical separated locations. Each RAU is connected to the central unit (CU) via optical fibre link [7, 8]. The DAS can ex-

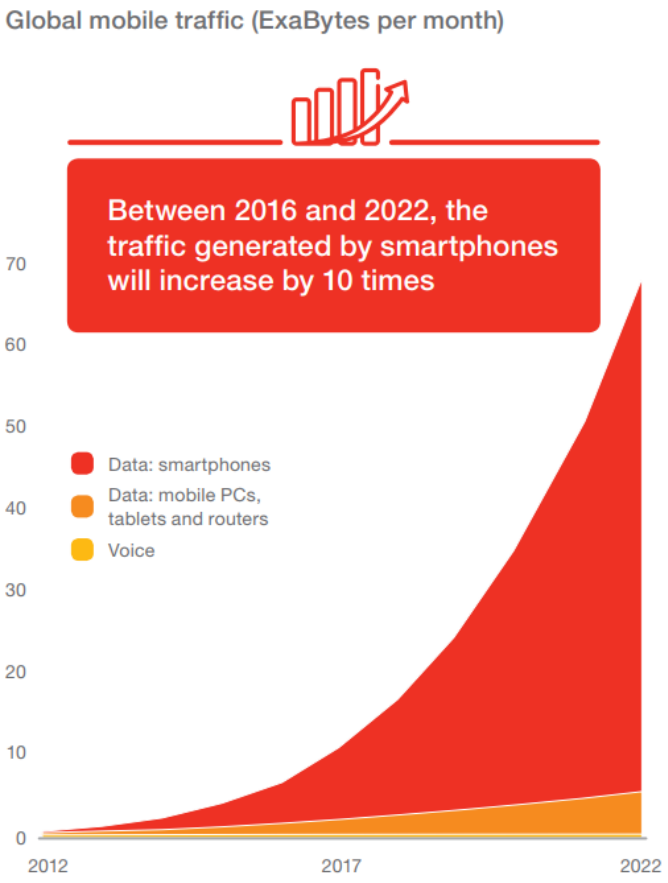

Figure 1.1: Global mobile traffic growth [Source: Ericsson, November 2016].

tend coverage area, improve spectral efficiency and reduce overall transmit power by reducing the distance between the user and the RAU [4, 8–14].

2. **Dense Network (DN):** The dense network has been proposed to effectively ease the traffic demand of macro BS by developing a number of small cell base stations in the network. The DN improves data rate by shortening the distance between the user and the BS [15, 16]. However, introducing a large number of small cells not only strength desired signal but also increases interference from other cells due to reuse of spectrum [16, 17].

3. **Spectrum extension:** One approach to increase the system capacity is to simply increase the system bandwidth, a resource which is limited in the well established centimetre wave spectrum. Alternatively, the untapped idle spectrum can be used from the millimetre wave (mmWave) spectrum to fulfil the fifth generation's (5G) capacity growth promise. Initial studies on the mmWave have shown the promising gains with the appropriate dense network [18, 19] and Massive MIMO [20]. While the mmWave do provide several challenges due to high propagation losses, and the necessity of Line of Sight (LOS) between a transmitter and receiver pair.

Recent studies have shown that the DAS can extend coverage area, improve spectral efficiency and reduce overall transmit power by reducing the distance between the transmitter and the receiver [21–24]. Moreover, by applying the frequency reuse technique [25, 26] and adaptive transmission schemes [27–29] to multi-cell DASs, it has been demonstrated that the inter-cell interference (ICI) in a DAS can be much lower than that in a co-located antenna systems, especially for cell-edge users [25], if the transmission scheme is elaborately designed. Therefore, the DAS is regarded as a promising system for future mobile communications.

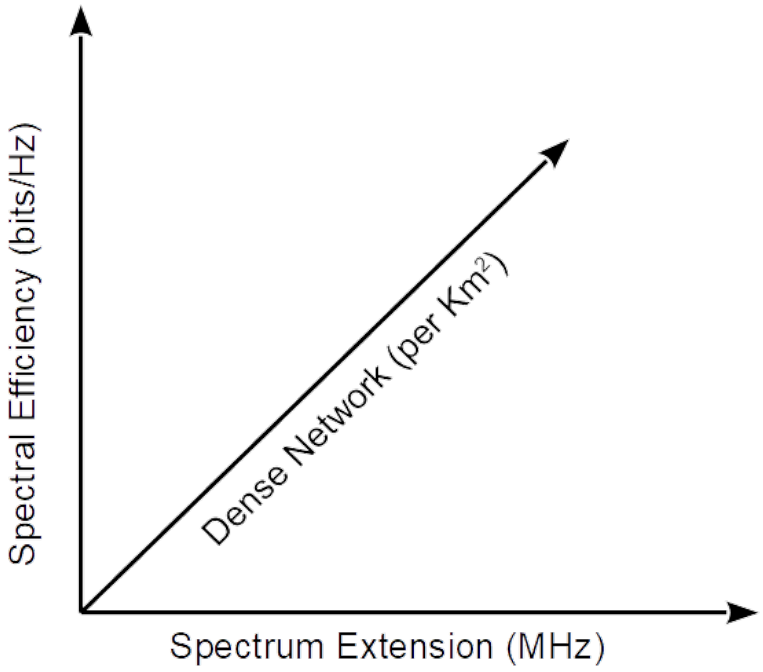

Figure 1.2: Options for improving the system capacity.

1.1.1 Overview of the DAS

The concept of DAS was originally proposed to cover dead spots in indoor wireless communication [30]. By placing the number of RAUs inside the building not only covers the dead spots, also enhance the signal quality [31, 32]. In 1990s, the DAS was adapted to outdoor cellular systems due to the flexible structure, high spectral efficiency, low transmit power and reduce transmission distance [33–35]. The DAS also improves battery life of mobile due to low transmit power. In a cellular DAS, a number of RAUs are geographically distributed and connected to the CU by fiber or coaxial cable, as shown in Fig. 1.3. The RAUs in the DAS are only simple antenna units carrying out radio transmission and reception for the CU. Thus, multiple RAUs provide spatial diversity by sending the same data to the user. Since the RAUs are distributed within a cell, it eliminates the correlation between RAUs [36]. All RAUs have different independent channel characteristics because the signals from

different RAUS to a user experience different large scale fading and different small scale fading. DAS's channels are typically modelled as the composite channels including uncorrelated large- and small-scale fading channels, which are a crucial part of motivation of the DAS technique and differentiate the DAS from MIMO techniques. In the DAS, the transmitter cannot allocate power arbitrarily across the RAUs, as each RAU has its own power budget. The downlink capacity of Multi-user MIMO (MU-MIMO) channels with a per antenna power constraint has been investigated in [37].

In DAS, the following issues will need to be addressed.

- **Transmission delay:** In DAS, the RAU is distributed over the network. One of the RAU is always close to the user, so the propagation delay is negligible. With 25 to 900 RAUs, the intra-antenna distance that is a minimum distance of neighboring RAUs varies from 30 m to 200 m, which is the coverage of small cells, where the propagation delay is not critical issues.
- **Feedback (signaling) overhead:** The channel state information (CSI) of all users is required at the CU to cancel the inter-user interference (IUI). The signaling overhead can be effectively reduced by the antenna selection, user clustering and feedback allocation.
- **Mobility Management:** While a user is moving, its RAU selection will be adjusted dynamically to support its movement at feedback/uplink timeslot, which is different from the traditional mobility management.

1.1.2 Types of DAS Communication Systems

Communication systems can be divided into single-user DAS (SU-DAS) and Multi-user DAS (MU-DAS),as shown in Fig. 1.4.

1.1.2.1 Single-user DAS

Point-to-point transmission was initially studied where all the signals at both ends of the communication link can be processed cooperatively.

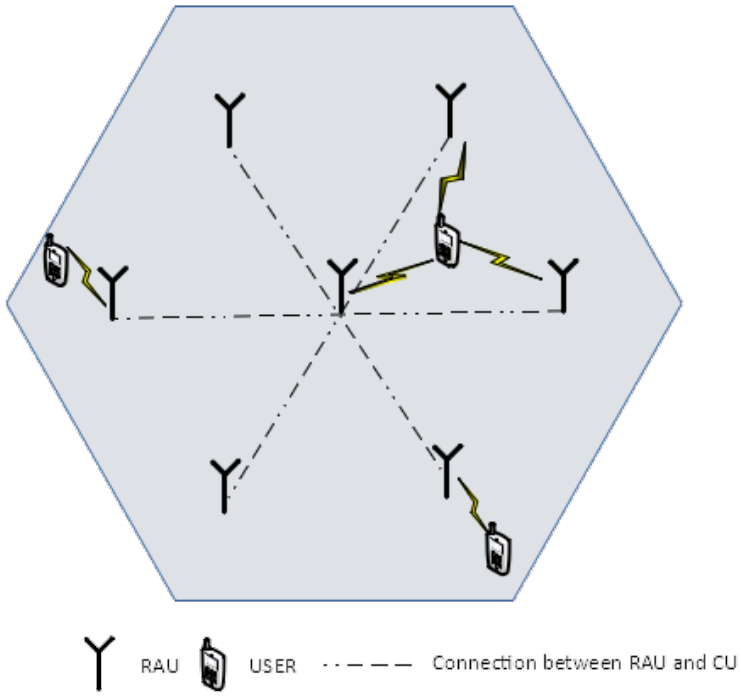

Figure 1.3: Illustration of a cellular DAS, where RAUs are distributed over the cell and connected to the CU.

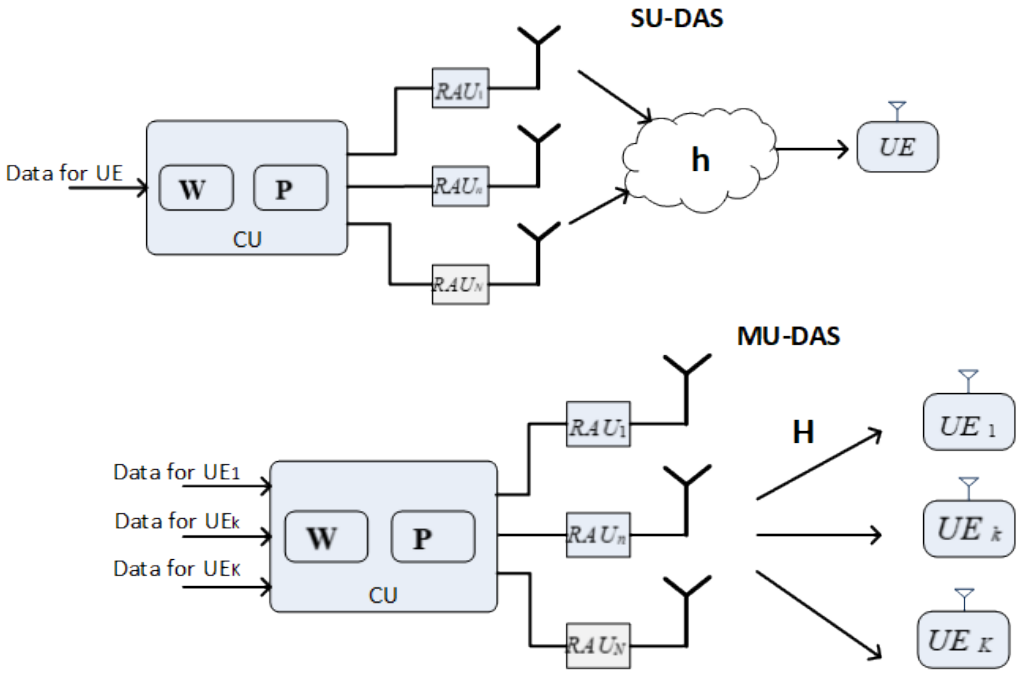

Figure 1.4: Different DAS in the cellular network.

With single-user spatial multiplexing, a single user is served on a given time-frequency resource employing all available antenna elements of the DAS. SU-DAS has been shown to yield higher sum rates then collocate antenna [38]. Depending on the average received Signal-to-Noise Ratio (SNR), SU-DAS can be used either to increase the reliability of data transmission through maximising spatial diversity gain or increase the system capacity through spatial multiplexing. For the single user multicell DAS, a downlink capacity gain obtained by reducing other-cell interference was investigated from an information theoretic point of view [27]. The paper [39] analyzed the downlink performance of the DAS with random antenna layout, where an asymptotic approximation of the ergodic capacity was derived by adopting random matrix theory.

Transmit precoding techniques with CSI at the transmitter, are shown to improve the performance of the system in fading channels, by using complex weights at transmit antennas. The beamforming improves the SNR and also achieves higher array gains with perfect CSI at the transmitter. However, these gains are shown to be degraded if the channel estimation at the transmitters is erroneous.

1.1.2.2 Multi-user DAS

Multiple users are served in parallel over a given time-frequency resource by means of spatial multiplexing [40, 41]. MU-DAS is considered as an extension of SU-DAS to increase the spectral efficiency. The spectral efficiency of DAS has been mainly studied [13, 27, 28, 42, 43]. In [42], the authors show proportional relationship between spectral efficiency and the number of RAUs. For more users to be served the RAUs can simultaneously communicate with different users, and the system capacity expands when the full frequency reuse is utilized among antennas, i.e., each RAU transmits signals to a distinct user using the same radio resource. Interference is one of the reasons that reduce the throughput of MU systems. Precoding schemes are key to mitigate the interference caused by the existence of multiple users in the system. Furthermore, CSI at the CU is critical for precoding in multiple users systems. Like sin-

gle user systems, multiple users systems also suffer the imperfect channel estimations, because, with imperfect CSI, the precoding scheme cannot mitigate interference effectively [44, 45].

In the DAS, the users are uniformly distributed where some users may be far away from some RAUs. If all RAUs are activated to transmit the signal to the user. The CU requires more transmit power to compensate high path loss for the user which is far from the RAU. Consequently, the concept of user selection has emerged as a pioneering technology to improve the average sum rate for MIMO systems. With the availability of partial or complete knowledge of the channel, the CU can select the best set of users to communicate with the set of RAUs. Based on matrix theory and linear algebra concepts, several prominent algorithms have been designed to select the optimal set of users under ZF approach, whereby data streams are cleared of interference and sent to the terminal users.

1.1.3 Modes of Channel Operation

There are three basic modes for operating a communication channel, namely: simplex, half duplex and full duplex as shown in Fig. 1.5. In the case of a simplex mode, the information can be sent only through one direction i.e., communication is unidirectional. For examples are loudspeaker, television and radio broadcasting. A half duplex mode can send and receive, but not at the same time. This means one entity transmits at a time while the other entity listens, and vice versa. This technique is used in walkie-talkie radio where only one person can talk at a time. Information that travels in both directions simultaneously is referred to as a full duplex mode. The two entities can receive and transmit at the same time. Notable examples landline telephones and cell phones. There are two ways of achieving this. One is to use frequency separation (frequency division duplex, FDD, and the other is to use time, time division duplex, TDD.

The FDD system uses the idea that the transmission and reception of signals are achieved simultaneously using two different frequencies so

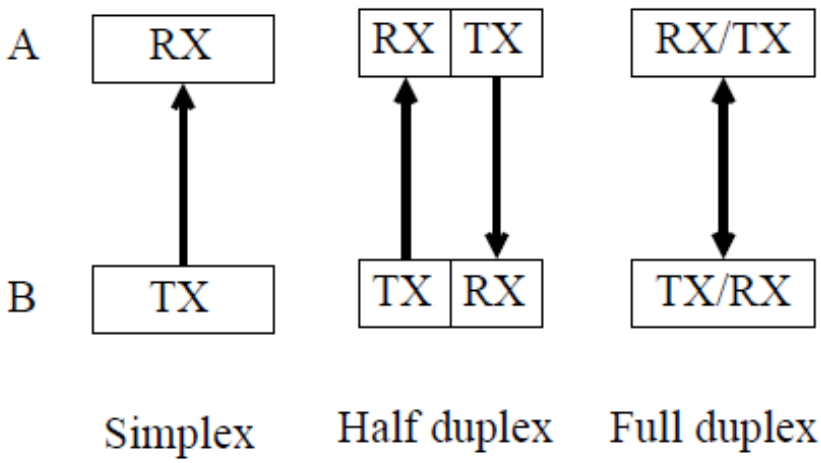

Figure 1.5: Modes of channel operation.

as to eliminate cross–talk. This means the full duplex channel is accomplished by two independent simplex modes. In contrast, a TDD system uses a single frequency and shares the time slot between transmission and reception. It emulates full duplex communication over a half duplex mode. The basic mechanism of TDD and FDD are shown in Fig. 1.6. In wireless communication, the direction from the BS to the user is referred to as the downlink. Similarly, the direction from the user to the BS is the uplink.

The FDD system represents a true full duplex channel which does not need any coordination between uplink and downlink transmission. However, two separate channels are required and this may not always use the available spectrum efficiently. For example, when a user downloads a file, the uplink channel is underused which results in the waste of expensive radio resources. In comparison, the TDD technique does not represent a true full duplex channel. It ideally supports services which basically only require an asymmetric half duplex mode. For example, when the user downloads file, the number of time slots should be greater in the downlink direction. Using a TDD system, it is possible to change the capacity in either direction by changing the number of time slots allocated to each direction. Therefore, the TDD becomes a more desir-

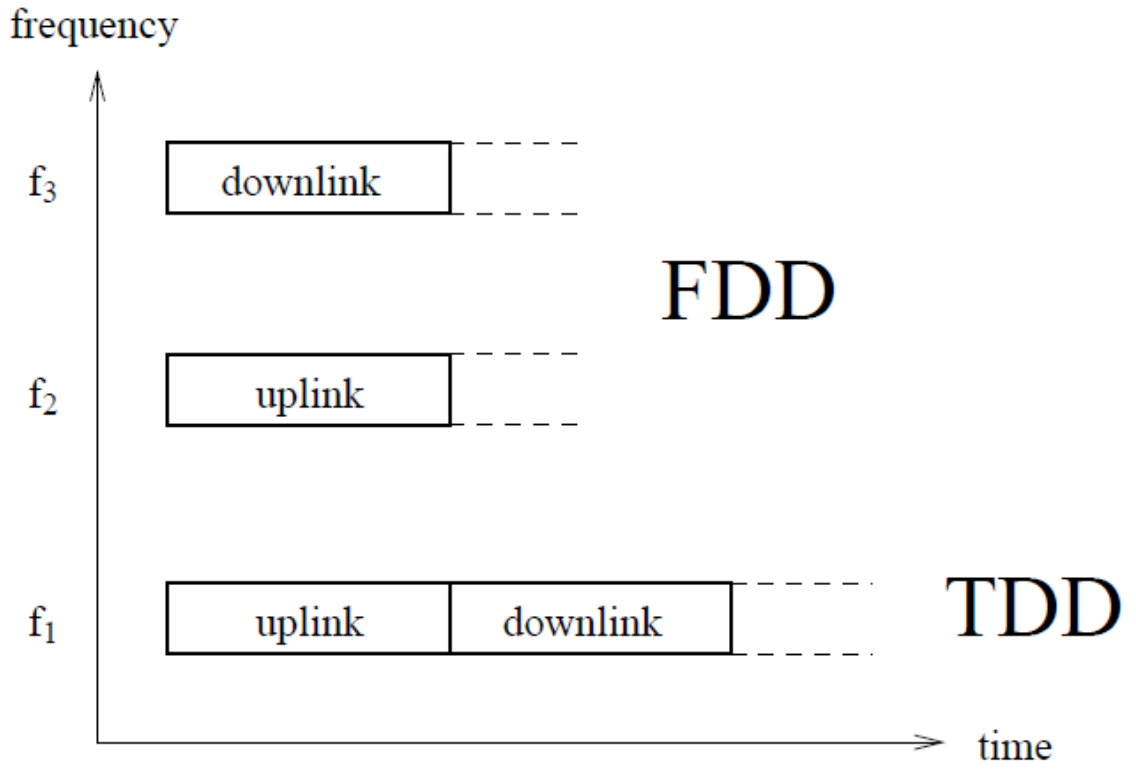

Figure 1.6: Comparision of TDD with FDD.

able duplexing technology for the future wireless communication due to asymmetric traffic between uplink and downlink transmissions and the shortage and cost of the spectrum.

1.2 Challenges

In a practical scenario, every user may exhibit different mobility characteristic. For different mobility users, the DAS is arguably better suitable than small cell. This is because a user is always near to one of the RAUs and the same signal is transmitted by multiple RAUs which reduces handoffs. When a user moves, the channel from the RAU to the user becomes a time-varying channel. In this situation, the transmitted signal is subjected to the Doppler effect and hence experiences frequency offset. When the mobility speed increases or the transmission delay increases,

the correlation between the actual channel and the estimated channel decreases as shown in Fig. 1.7, and this results in the severe degradation of the transmission performance. Thus, accurate CSI from all users at the CU are necessary to enable high bit rate transmission. However, the CSI obtained by the CU may be outdated in practice due to either channel variation in mobility environment and/or the transmission delay between the uplink time slot in which the CSI is estimated and the downlink time slot in which the downlink data transmission takes place. If the channel varies slowly relative to the time frame (low mobility), the CSI can update infrequently with minimal impact on channel throughput. For highly mobility users, however, the CSI becomes increasingly outdated, leading to low effective channel capacities. Such a capacity degradation metric is obviously linked to capacity under imperfect CSI where the initial channel estimate is in error [46–48]. The unique goal of this thesis is to improve spectral efficiency for the transmission delay/ moving user beyond which an initial channel estimate is no longer suitable for communications. The high mobility requires more CSI to improve channel capacity, which will require a large number of uplink time slots at expense of the number of downlink time slots.

In this thesis, we develop solutions for these challenging problems based on MU-DAS. Multi-user transmission in wireless communication causes IUI. Linear precoding like zero-forcing (ZF) [49] and minimum mean square error (MMSE) [50], has been introduced to mitigate the IUI. However, these precoding techniques require CSI from all users at the CU. Since the accurate CSI is a prerequisite for interference management, this will raise the problem of designing precoding because of user mobility or long transmission delay. However, with such channel mismatch error due to outdated/ imperfect CSI at the CU, there will be residual inter-user interference due to an imperfect spatial separation between different users as shown in Fig 1.8. In this thesis, we will investigate the impact of channel mismatch error on the performance of MU-DAS and propose adaptive strategies to improve the system sum rate.

In DAS, the RAUs are connected to another device which is the ra-

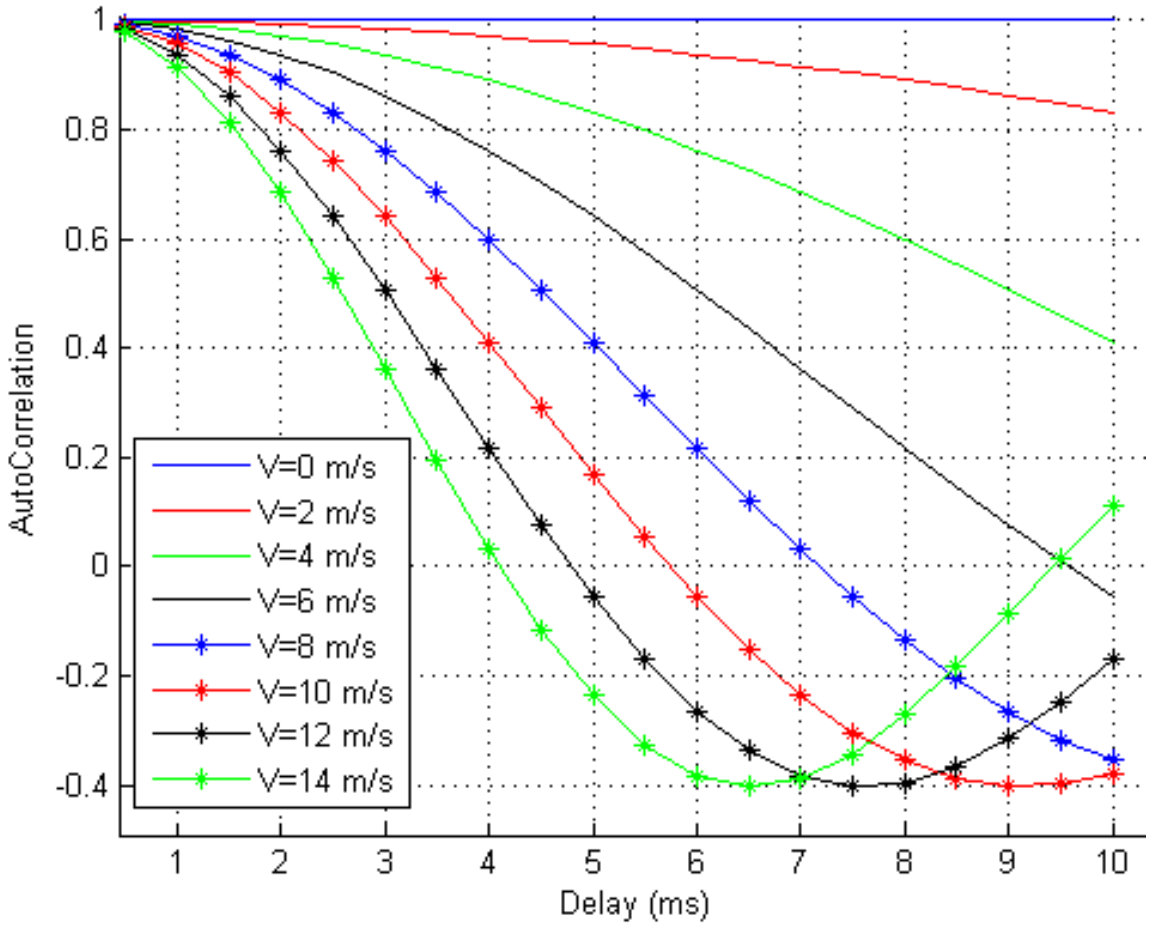

Figure 1.7: Autocorrelation of channel where users have different mobility.

dio frequency (RF) components in order to achieve the transmission process. That means if the DAS is equipped with N_t RAUs, the number of complete RF chains must be the same, including N_t devises of Analog-to-Digital (A/D) converters which are involved in the design of these chains. Compared to RAU elements, RF chains are considerably expensive. Moreover, deploying more RF components will increase the power consumption in the system. Scaling up the number of antennas in MIMO system to improve the performance of wireless transmission must be accompanied by increasing the number of RF switches, and leading to more expenses and power consumption in the system. To cope with this problem, user clustering technology comes to reduce the cost and

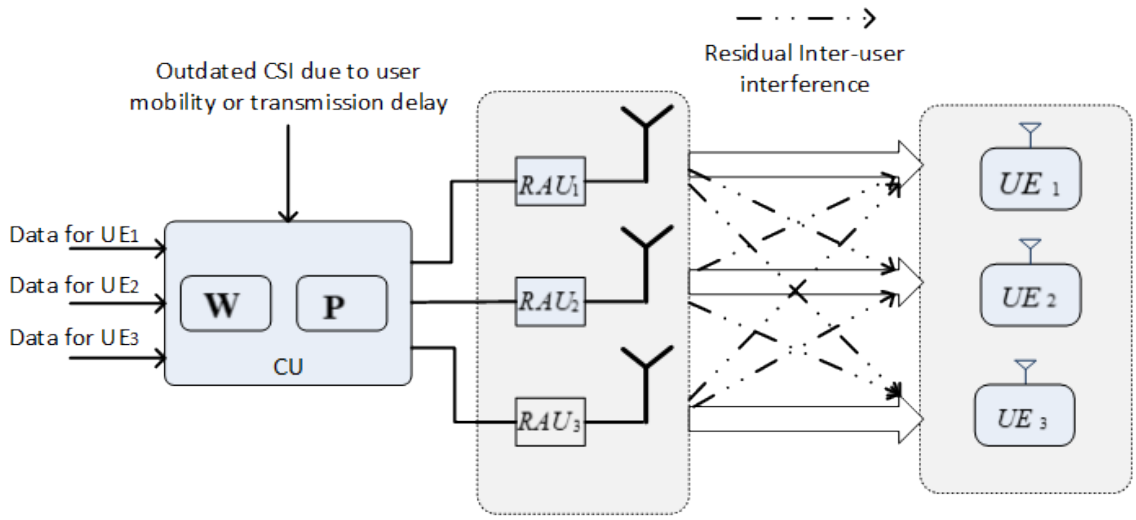

Figure 1.8: The MU-DAS with outdated CSI due to user mobility/transmission delay.

complexity of DAS architecture, while keeping most of its benefits. Considerable algorithms based on technical and mathematical concepts have been proposed to achieve either RAU selection or joint RAU/user selection.

Another important issue in DAS, the user experiences different channels from RAUs due to different large scale fading. Similarly, the user data mainly depend on the channel gain between user and RAU. This motivates us to consider antenna selection among RAUs and select users by user clustering. This will reduce the system computational complexity while designing precoding matrix by selecting a subset of RAUs and users. This will also reduce the number of active RF chains in user cluster. The active RF chain number will be same as the dimension (number of columns) of the precoding matrix. This thesis will also investigate user clustering strategies to reduce high complexity cause by handling large size of users or RUAs.

1.3 Contribution of the Thesis

The objective of this thesis is to study the spectral efficiency of downlink MU-DAS with per-antenna power constraint and per-user signal to interference plus noise ratio (SINR) constraint is studied by taking into account the different mobility speed ranges. The contributions of this thesis are summarized as follows:

1. **User clustering:** A capacity based user clustering is proposed in MU-DAS downlink systems, where this technique can be efficiently used to reduce the complexity and cost caused by RF chains, associated with antennas, while keeping most of the diversity advantages of the system. The algorithm designs its precoders using zero-forcing in order to nullify the inter-user interference. The performance and complexity of the proposed algorithm is compared to two other algorithms; the exhaustive search algorithm and the single-user algorithm. The performance of MU-DAS is better than co-located MIMO in both exhaustive and proposed user clustering. Simulation results show that the proposed algorithm achieve almost the same performance obtained by the exhaustive search algorithm.

2. **Interference alignment:** The intra-cluster interference within the cluster is eliminated by using ZF precoding. However, the inter-cluster interference is uncoordinated and limits the system performance. The inter-cluster interference should be eliminated or minimized carefully. Each cluster receives different power level interference from the RAUs of the other clusters due to the large scale fading. The interference alignment is proposed to consolidate the strong inter-cluster interference into smaller dimensions of signal space at each user and use the remaining dimensions to transmit the desired signals without any interference.

3. **Cooperative transmission over user mobility:** The CSI feedback interval reduction technique is proposed to improve the system throughput cause by channel mismatch error. The channel mis-

match error is controlled by adjusting the threshold values. Thus, the estimated channel can remain unchanged, while feedback interval is adjusted. A user grouping technique is proposed which divides the users into multiple groups based on mobility state information (MSI). In the DAS, the sum rate mainly depends on the channel between RAU and user whose channel gain is high. Thus, the antenna selection of RAUs and interference power based user clustering is proposed to maximize sum rate within a mobility group. A cooperative clustering is proposed to mitigate the inter-group interference which limits the average sum rate of the system. Each cooperative cluster serves a subset of users of its own mobility group and has a subset of users of the other groups to coordinate the interference. Accurate closed-form approximations are derived for the single-user cluster.

1.4 Structure of the Thesis

This thesis is organized into six Chapters and an Appendix, as follows:
Chapter 1, provides the overview of MU-DAS and TDD. The motivation and challenges of users' mobility in MU-DAS are discussed. The main contributions of the thesis to address these challenges are then summarized. Also the structure of the thesis is given.
In chapter 2, theoretical basis of time-varying channel, TDD, user clustering are presented. Moreover, the state-of-the-art literature on user's mobility and cooperative transmission in a DAS is surveyed.
In chapter 3, the user clustering for MU-DAS downlink systems is studied. The system model of MU-DAS downlink is presented. Then, the capacity based user clustering algorithm is explained. Finally simulation results evaluate the performance of the proposed algorithm compared to other algorithms.
In chapter 4, the interference alignment technique is poropsed to coordinate strong inter-cluster interference in $N_r - 1$ dimension. The weak inter-cluster interference is treated as noise. The performance of the

proposed algorithm is compared to other algorithms; single cluster algorithm, random user cluster and norm based cluster.
In chapter 5, the DAS architecture and system model is introduced, followed by explaining the proposed antenna selection and user clustering decomposes the original problem into multiple problems to reduce the system computational complexity. The autocorrelation based feedback allocation scheme is developed to minimize the channel mismatch error. It also shows that the derived ergodic rate of single user clustering approximately matches with the numerical results. The numerical results of multi-user clustering is compared with non-cooperative clustering.
In chapter 6 concludes the thesis with a summary of contents and the conclusions derived throughout. Moreover, future research lines within the framework of this thesis are also presented.
The list of related publications to this research is provided on page vi of this thesis.

Chapter 2

Background Theory

In this chapter, we introduce the background information and the related work of this thesis. Although the focus of this thesis is on user's mobility and cooperative transmission in a distributed antenna system.

2.1 Wireless Channel

In wireless communication, the signal is transmitted at the presence of multiple propagation paths between the transmitter and receiver as illustrated in Fig. 2.1. The combination of multiple copies of the transmitted signal affects many characteristics of the received signal. In general, the effects of a wireless channel can be categorized into two types: large-scale fading (or path loss, attenuation) and small-scale fading (typically referred simply to as fading). The large-scale fading is due to signal attenuation by large objects such as buildings, hills, etc that occur over relatively large distances and is typically frequency independent [51]. The small-scale fading is due to the constructive and destructive combinations of the multiple signals arrived over different propagation paths at the receiver. Dealing with small-scale fading is one of the most challenging issues in designing a robust wireless communication system.

In wireless communication systems, the transmitter or the receiver is mobile with significant velocities. These situations give rise to time variations of the wireless channel due to the Doppler effect.

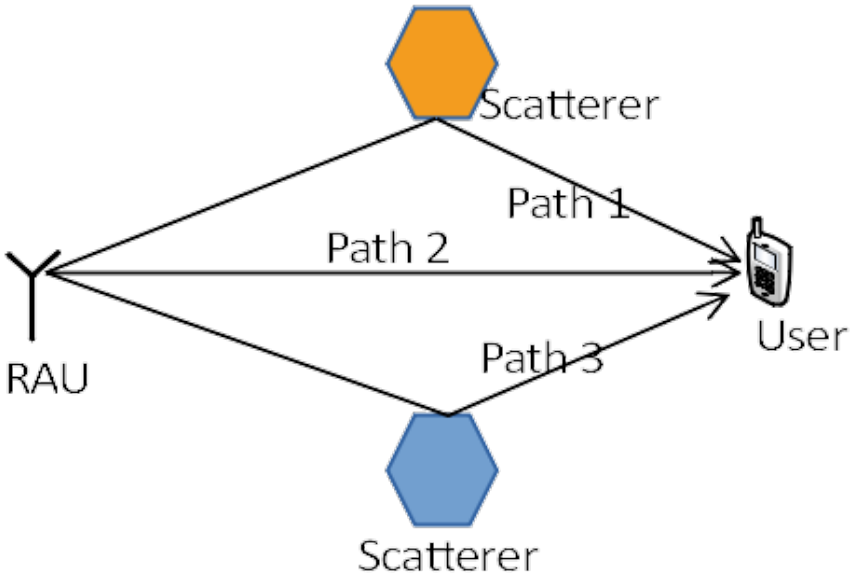

Figure 2.1: Wireless multipath propagation.

2.1.1 Time Variant Channel

A time-variant channel is a channel which has the property of changing over time. The time-variant channel has the characteristic of a signal which changes at the same rate as the changes in the communication signal, or even faster. The channel normally has the Doppler effect which caused by Doppler spread of multipath wave interference, arising from multiple scattering of the waves [52]. Let $h(t)$ be a time-variant channel with N_0 plane waves at a moving receiver with arrival angles α_n. Each plane wave has associated with it a Doppler shift depending on the mobile speed, the carrier frequency, and the angle its propagation vector makes with the mobile velocity vector. A diagram of this simple model is shown in Fig. 2.2 with plane waves from stationary scatterers incident on a mobile travelling in the x-direction with velocity v. The vehicle motion introduces a Doppler shift in n wave:

$$\omega_n = \frac{2\pi f_c v}{c} \cos \alpha_n = \omega_{max} \cos \alpha_n \tag{2.1}$$

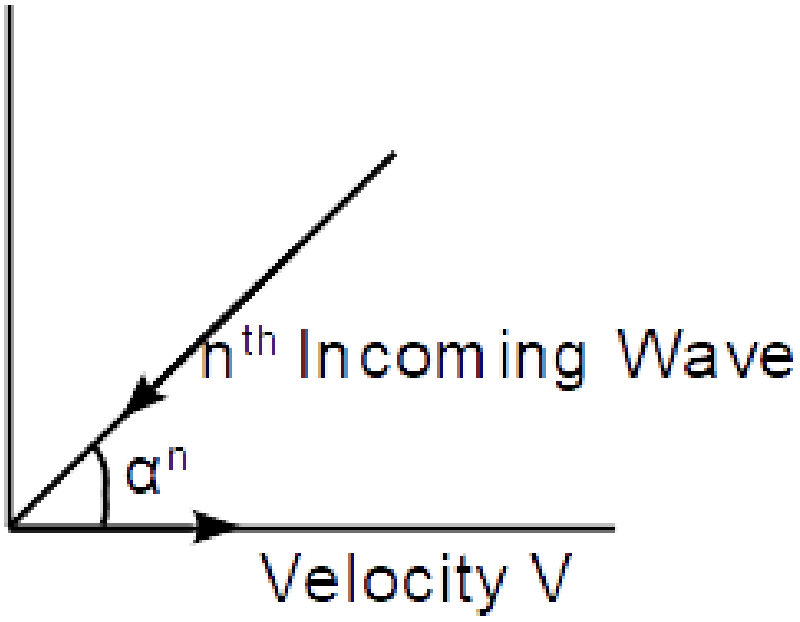

Figure 2.2: Doppler shift of n^{th} incoming wave on the mobile receiver.

where f_c is the carrier frequency, v is the user speed, c is the speed of light and ω_{max} is the maximum Doppler frequency shift. We also assume that the receiver is moving at a constant velocity v.

2.1.2 Jakes' Model

In a practical wireless channel, there may be relative motion between the transmitter and the receiver, with no direct line-of-sight between them. The simulation of the flat fading channel is done using Jakes' model [52–54]. In this system, the received signal is mainly composed of the scattered signals and diffracted signals from different obstacles. The channels can be simulated by assuming that the received signal is a sum of several horizontal plain waves, with random angles of arrival and random phases distributed in the interval $[-\pi, +\pi)$. A model that is used for this purpose is as shown in Fig. 2.3. The scatterers are assumed to be uniformly distributed around the user, at equal distances from the user,

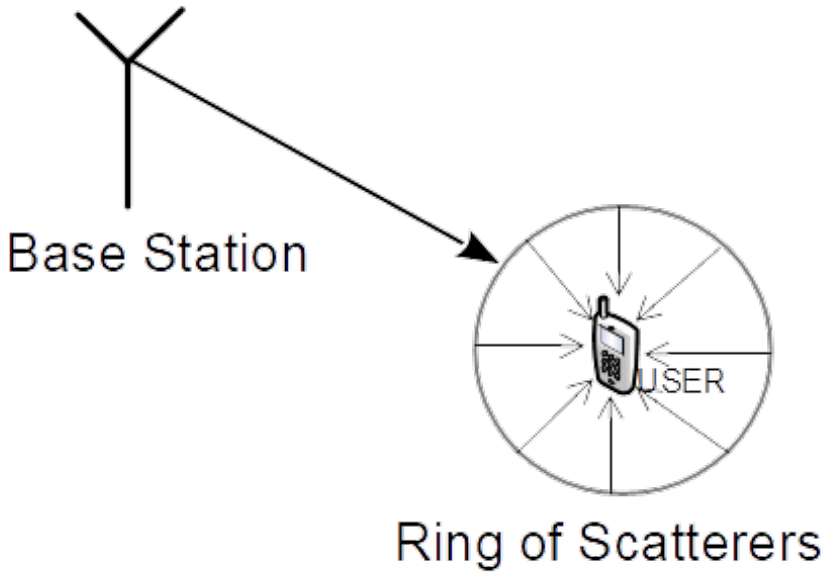

Figure 2.3: Jakes' ring model. The scatterers in the environment are distributed, at equal distances from a user.

like in a ring. Jakes' model assumes that all the components arriving plain waves at the receiver will have equal strengths.

The plain wave cross-correlation is determined by the sum of the product of the oscillator coefficients, which can be viewed as a vector inner product. Orthogonal vectors, such as Walsh-Hadamard (WH) codewords, give zero inner product values with one another. The small-scale fading of j-th plain wave is generated using [52]

$$h_j(t) = \sqrt{\frac{2}{N_0}} \sum_{n=1}^{N_0} \mathbf{A}_j(n)[\cos(\beta_n) + i\sin(\beta_n)]\cos(\omega_n t + \theta_n) \qquad (2.2)$$

where $\mathbf{A}_j(n)$ is an orthogonal vector of Walsh-Hadamard codewords (± 1 values) to generate multiple uncorrelated waveforms at moving user, $\beta_n = \frac{\pi n}{N_0}$ is a phase and gives zero correlation between the real and imaginary parts of $h_j(t)$, θ_n is oscillator phase. The arrival angle is given by $\alpha_n = \pi(n - 0.5)/2N_0$. The Jakes' model is a continuous time wireless Rayleigh flat fading channel [55].

2.1.3 Rayleigh Fading Distribution

In a wireless channel, the receiver gets a large number of reflected and scattered signals with random amplitudes, i.e., none of signal paths is dominant and each multipath of the signal will vary and can have an impact on the overall signal at the receiver. Each path can be modelled as a circularly symmetric complex random variable. The sum of such circularly symmetric complex random variable paths can be modelled as a zero-mean Gaussian random variable following the central limit theorem. $|h_j|^2$ follows a chi-squared distribution with degree of freedom of 2 and its probability density function (pdf) is given by [56]

$$f_{|h_j|^2}(x) = e^{-x}, x > 0 \tag{2.3}$$

It has to be mentioned that the Rayleigh model only describes small-scale fading. Large-scale fading due to path loss and shadowing is not described by this model. The path loss describes the distance-dependent power decay of waves. Let us model the attenuation factor as $d^{-\alpha}$, where d is the distance from user to transmitting RAU and α denotes the path loss exponent, which is typically assumed to lie between 2 and 4. The path loss in decibels is then obtained as $P_L = 10\alpha \log_{10}(d)$. In this thesis, only path loss is considered as large-scale fading.

Due to the assumption of relative motion with constant velocity between transmitter, receiver, and objects in the environment, the fading becomes temporally correlated. The autocorrelation function ρ is given by [53]

$$\rho = J_0(2\pi f_d T) \tag{2.4}$$

where $J_0(\cdot)$ is the zeroth-order Bessel function of the first kind, T is the time duration of a symbol and $f_d = \frac{v}{c} f_c$. Clearly, when the carrier frequency or the mobile velocity increase, the normalized Doppler ($f_d T$) increases proportionally. We illustrate the interplay between these parameters in Figs. 2.4 and 2.5. Table 2.1 summarizes the effects of changing system parameters on the normalized Doppler frequency.

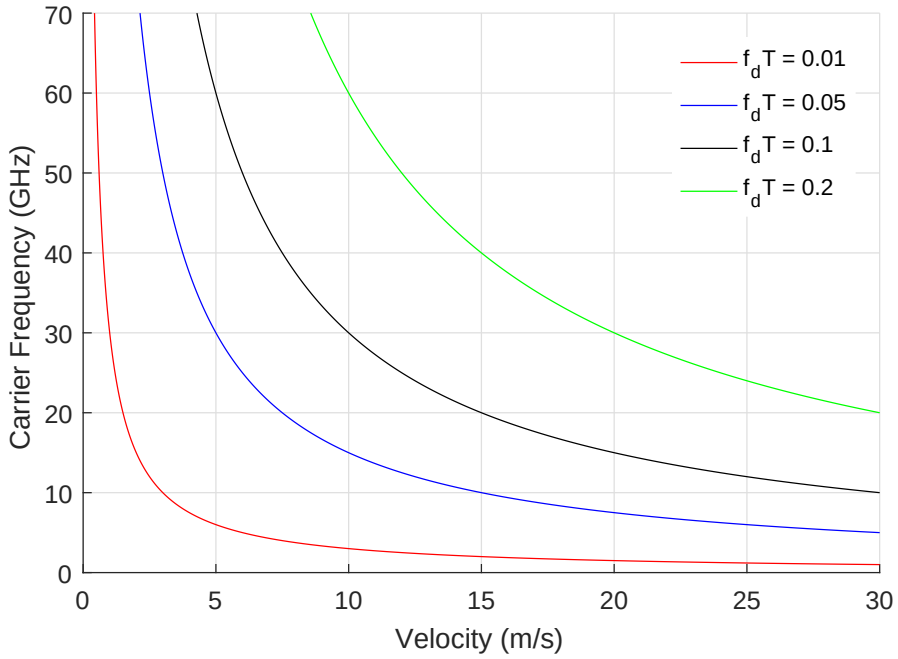

Figure 2.4: Carrier frequency - velocity curve for various levels of normalized Doppler and fixed symbol duration $T = 100\mu s$.

Table 2.1: Effects of system parameters on the normalized Doppler frequency f_dT.

Parameter	Effect on f_dT
User mobility ↑	↑
Carrier frequency ↑	↑
Symbol time duration ↑	↑

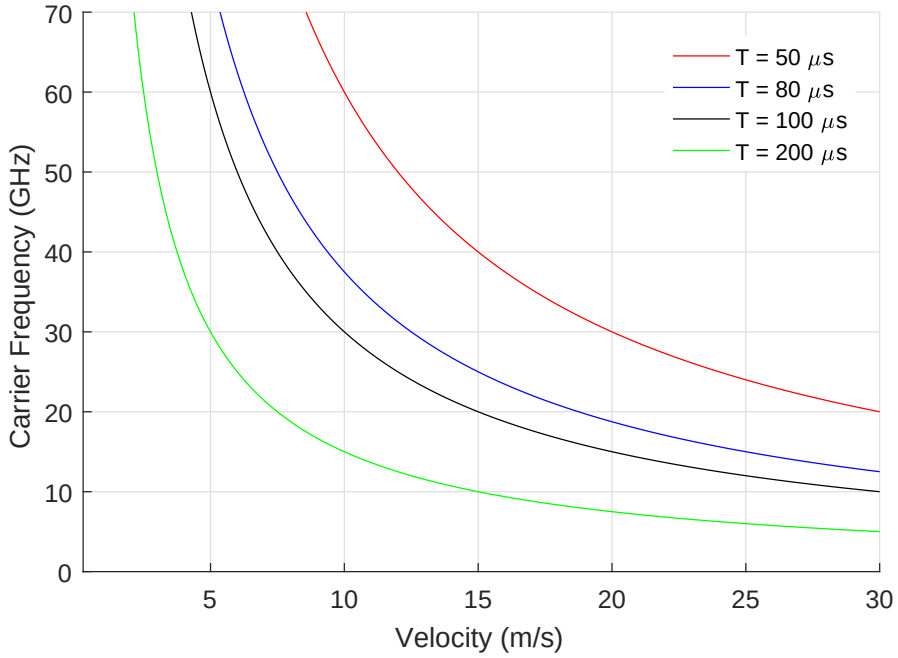

Figure 2.5: Carrier frequency - velocity curve for various levels of symbol duration and fixed normalized Doppler $f_d T = 0.1$.

2.2 Time Division Duplex

The feedback interval is the time duration between two uplink time slots where the CU estimates the CSI as shown in Fig. 2.6. In the TDD system, the CU estimates the CSI at the uplink time slot and then uses it via channel reciprocals to generate transmit precoder for downlink transmission [57]. There exists a delay τ from the instant when CSI is obtained for downlink transmission as illustrated in Fig. 2.7. In the FDD system, the CSI for the CU is provided by separate frequency band, where the user should estimate and quantize the pilot signal. The increasing demand of high data rate is mainly due to the use of multimedia services such as social networking, real-time video and interactive games. These services require asymmetric traffic between uplink and downlink. The asymmetric traffic in FDD system requires extra system bandwidth, whereas TDD can fit it into any single spectrum by allocating uplink and downlink time slots according to the traffic condition [58, 59].

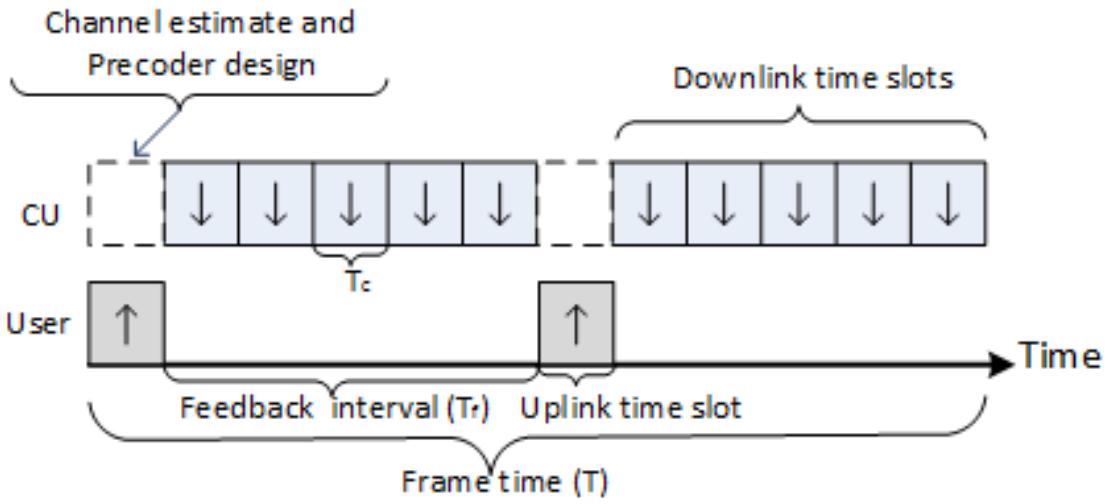

Figure 2.6: Illustration of feedback interval.

In this thesis, we assume that the CU can perfectly estimate the CSI of all users at the uplink transmit slot and the MSI of the user. When the channel is time-varying, especially when it is under severe fading, the transmission delayed will affect the performance of system dramatically.

Suppose that $\mathbf{h}(t)$ is the vector consisting of the accurate channel coefficients at continuous time instant t, and its delayed vector can be denoted as $\mathbf{h}(t-\tau)$ when transmission is delayed by τ duration. The

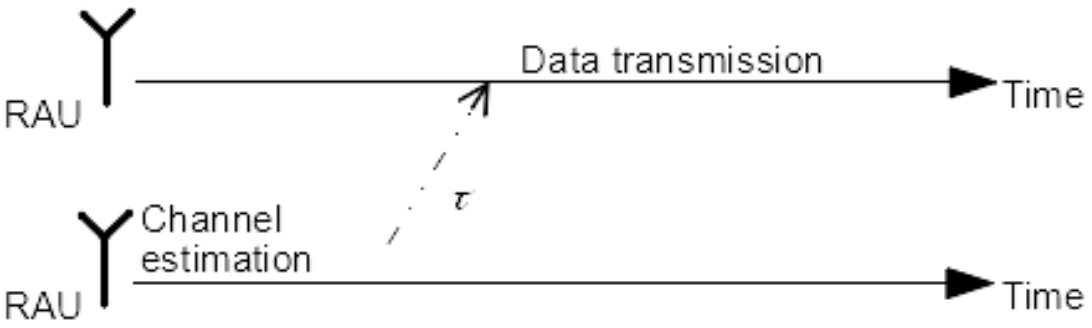

Figure 2.7: Illustration of data transmission delay.

relation between actual channel and estimated channel is modelled by [60, 61]

$$\mathbf{h}(t) = \rho\mathbf{h}(t-\tau) + \sqrt{(1-\rho^2)}\mathbf{e}(t) \tag{2.5}$$

where $\mathbf{h}(t-\tau)$ is the estimated channel vector, where its element is obtained from (2.2) , $\mathbf{e}(t)$ is the error in the estimate that is uncorrelated with $\mathbf{h}(t-\tau)$ and ρ is the autocorrelation function of a fading channel with motion at a constant velocity, and $0 \leq \rho \leq 1$. It can be seen that $\rho = 0$ represents no CSI, whereas $\rho = 1$ corresponds to perfect CSI. The autocorrelation coefficient between the actual channel gain and its estimate [53], which is given by

$$\rho = \frac{\mathbb{E}[h(t)h^H(t-\tau)]}{\sqrt{\mathbb{E}[|h(t)|^2|h(t-\tau)|^2]}} \tag{2.6}$$

The value of ρ depends on the length of the transmission delay and the user velocity. When the channel is under Rayleigh fading, ρ can be calculated as

$$\rho = J_0(2\pi f_d \tau) \tag{2.7}$$

where f_d is the Doppler frequency, which reflects the velocity of the users.

2.3 Literature Review

2.3.1 Users' Mobility

When the mobility speed increases or the transmission delay increases, the correlation between the actual channel and the estimated channel decreases, and this results in the severe degradation of the transmission performance. For a multi-user system with linear precoding, the mismatch between the actual channel and the precoder happens. Since the accurate CSI is a prerequisite for interference management, this will raise the problem of designing precoding because of user mobility or long transmission delay. The effect of quantized and delayed CSI on the average achievable rate for both joint transmission processing and

coordinated beamforming systems was studied in [62] for homogeneous cellular scenarios, and the impact of the other cell interference (OCI) has been considered in [63]. In [64], it has been shown that the interference increases and the performance of the precoding system degrades as the channel correlation decreases. The performance of the precoded system finally approaches that of the non-precoding systems, when the channel correlation is beyond the correlation threshold. In [65], the effects of the imperfect CSI on the ergodic capacity performance was studied, and it has been concluded that the performance of the MU-MIMO system strongly depends on the correlation between the actual channel and the CSI estimated at the transmitter. In [66], the MU-MIMO system was considered in the presence of imperfect CSI. The authors have concluded that only predictable (low mobility) users can be served jointly, where space-time coded transmission is adopted to unpredictable (high mobility) users. The effect of the user mobility in multi-user heterogeneous networks (HetNets) has been investigated [67], where low and high mobility users can be served simultaneously without affecting other users' rate. In HetNets, the high mobility users are served by macrocell BSs and the low mobility users are served by small-cell BSs, where the precoding is coordinated across the cells to suppress ICI. In [68], users were classified into low mobility user group and high mobility user group based on channel variance. The system performance is improved by using frequency selective scheduling in low mobility user group and frequency diversity scheduling in high mobility user group. In [69] the authors address the impact of the estimation error on the throughput and derive some asymptotic behavior in the regime of high SNR and of a large number of users. In [70], the impact of a feedback delay on the multiuser diversity is examined in a broadcast channel with multiple antennas at a transmitter. Both in [69] and [70], an optimal rate allocation is proposed such that the effective average throughput, taking into account the outage probability, should be maximized.

2.3.2 TDD support User mobility

The low mobility user implicitly has high channel temporal correlation and the channel mismatch is relatively small within a feedback interval because the channel varies slowly. On the other hand, the high mobility user may be subjected to large channel mismatch due to the fact that the channel significantly varies during the feedback interval. Thus, the channel mismatch becomes larger as the mobility speed increases. The channel mismatch can be reduced by reducing the feedback interval. By reducing the feedback interval in the TDD system, the number of time slots allocated to the uplink transmission increases at the expense of the reduction of the number of time slots for the downlink transmission. In this thesis, we assume that the users have no data to transmit in the uplink direction and hence the uplink time slot is used for channel estimation only. In [71] and [72], all the users were divided into multiple groups based on their channel strength. The different number of feedback time slots were allocated to each group in order to maximize the sum rate. In [73], the amount of feedback overhead has been optimized for the sum rate maximization of the MU-MIMO in the TDD system. The transmission scheme has been developed to unveil the trade-off between the cost and the gains associated with feedback.

In [74], the traffic share between uplink and downlink time slot is periodically assessed. The configuration which represents most closely this traffic share is then chosen. It is shown that the faster the slot reconfiguration time, the better the session throughput performance, since the TDD allocations can capture the uplink time slots and downlink time slots traffic dynamics of the cell more accurately. A similar approach is taken in [75] but the configuration is chosen based on the weighted sum of the instantaneous uplink/downlink buffer status and the previous uplink/downlink traffic statuses. In [76], the flexibility introduced by dynamic TDD is exploited and the problem of same-entity interference is mitigated via appropriate cell clustering. Neighbouring cells are grouped in a cluster, such that all cells within that cluster use the same TDD slot

configuration. This TDD configuration can then be collectively reconfigured by all the cells inside that cluster based on longer term traffic statistics.

2.3.3 Multi-user DAS

In downlink transmission, the multiple users may be served by multiple RAUs by sending the signals simultaneously. Serving multiple users simultaneously using the same radio resources incurs IUI. The IUI can be mitigated by using precoding like dirty paper coding (DPC) [77], zero-forcing (ZF) [49,78,79] and minimum mean square error (MMSE) [50,80]. However, these precoding techniques require CSI from all users at the CU.

In the DAS, a CU can apply the joint processing (JP) and scheduling over all RAUs. The sum capacity is achieved by the DPC proposed by Caire and Shamai [77]. However, due to the high computation complexity, especially when the number of users is large, the DPC is hardly used in the practical system. As a suboptimal precoding strategy, ZF precoding can easily be implemented in practice and its performance is comparable to that of DPC. In [81], it has been shown that when the number of users is sufficiently large, due to the multiuser diversity effect, its sum rate performance comes close to that of DPC. Under the ZF strategy, selecting the best set of users improves the performance of this scheme significantly, which comes from multiuser diversity gain [82]. However, due to the high complexity of selecting the best set given by exhaustive search over all possible combinations, some suboptimal methods with low complexity have been developed [45]. As the most efficient algorithm, the greedy algorithm proposed in [83] that selects the users in each step has the much lower complexity compared to the exhaustive search. This algorithm selects the user greedily according to the achieved capacity. A suboptimal power control method and a simple antenna selection (AS) method are proposed to improve the spectral efficiency [13]. In the AS, in the first stage, the best user that has the largest channel gain always is the first selected user. This system structure remarkably

increases the degree of freedom available for multiuser precoding since widely separated RAUs exhibit low antenna correlation. This configuration is also suitable for MU-MIMO, which can further enhance system capacity. It is not simple to apply MU-MIMO to DAS if there are many RAUs because the calculation overhead imposed by multiuser precoding is excessive. This cost can be significantly reduced by forming clusters which consisting of only a few RAUs that working cooperatively via MU-MIMO.

In JP, user data is available to all the RAUs belonging in the cluster. The CU schedules the RAUs that will participate in the JP based on the interference based on user clustering. The CU will decide on the power levels and the precoding weights. In UC not all the RAUs transmit user information unless they belong to the active set of the UC. The active set of UC changes its cardinality based on the interference based on the UC algorithm. More specifically, each user is assigned a RAU which is the one with the highest channel gain. The remaining users are added in the cluster only if their SINR are less than a clustering threshold. The value of the threshold is specified by the CU and choosing a value will lead to a single-user cluster, multi-user cluster and one cluster.

2.3.3.1 Single-user cluster

The single-user cluster consists of one pair of user and its associated RAU. For the single-user cluster, the RAU always transmits the signal with maximum power of RAU due to per antenna power constraint. In single-user clustering, a user receives data only from RAU which is assigned during AS as shown in Fig. 2.8.

For a user k the received signal y_k is given as

$$y_k = h_{k,k} w_k s_k + \sum_{k=1, i \neq k}^{K} h_{k,i} w_i s_i + n_k \tag{2.8}$$

where $h_{k,i} \in \mathbb{C}^{1\times 1}$ channel vector that is formed between the user k and the RAU associated with user i, $w_k \in \mathbb{C}^{1\times 1}$ denotes the precoding for

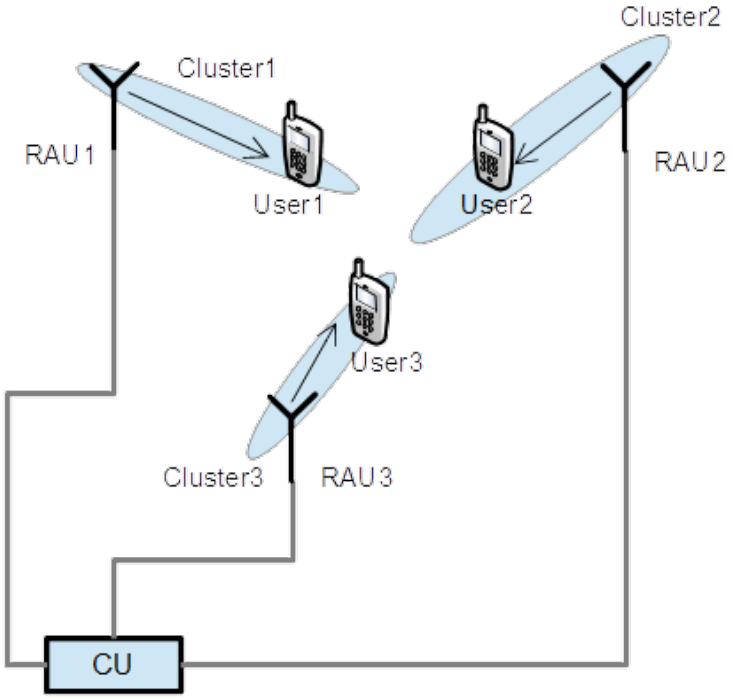

Figure 2.8: Illustration of single-user clustering where $K = 3$, $N_t = 3$ and three clusters are formed.

user k, $s_k \in \mathbb{C}^{1\times 1}$ is a transmit symbol for user k with $\mathbb{E}\{|s_k|^2\} = 1$ and $n_k \sim \mathcal{CN}(0, \sigma^2)$ is the additive White Gaussian noise (AWGN).

The received SINR of user k is calculated as

$$\gamma_k = \frac{|h_{k,k}w_k|^2}{\sigma^2 + \sum_{k=1,i\neq k}^{K} |h_{k,i}w_i|^2} \tag{2.9}$$

Since the clustering threshold is low. The SINR is mainly affected by inter-cluster interference which limits the system sum performance.

2.3.3.2 Multi-user cluster

In multi-user clusters, multiple users are jointly served by multiple RAUs by using MU-MIMO precoding. The number of users in each cluster is depended based on the clustering threshold as shown in Fig. 2.9. As the clustering threshold increases, cluster size increases and the number of clusters decreases. The received SINR of user k of cluster c is calculated

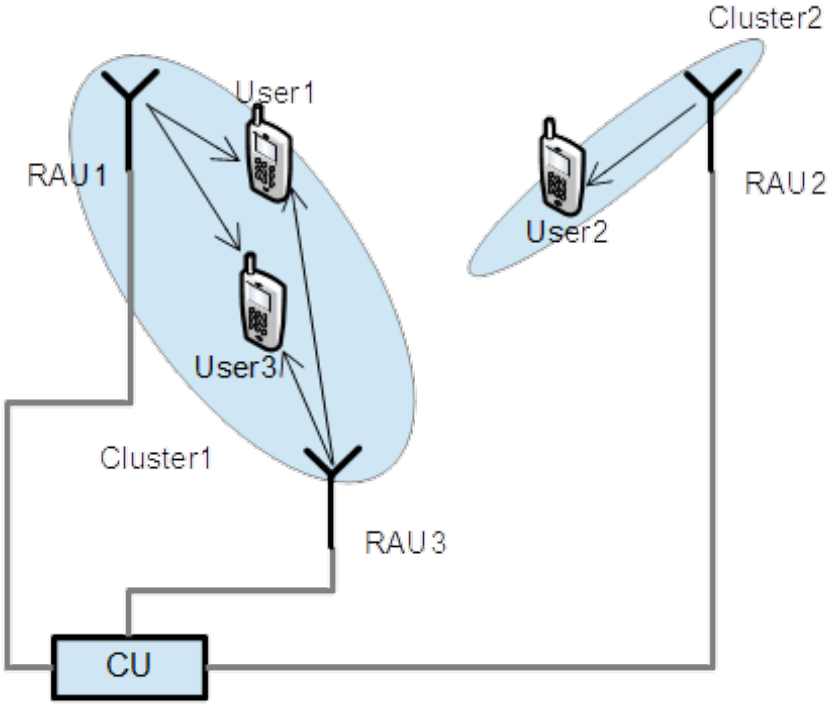

Figure 2.9: Illustration of multi-user clustering where $K = 3$, $N_t = 3$ and two clusters are formed.

as

$$\gamma_{k,c} = \frac{|\mathbf{h}_{c,c}^{k}\mathbf{w}_{k,c}|^2}{\sigma^2 + \sum_{i \neq k} |\mathbf{h}_{c,c}^{k}\mathbf{w}_{i,c}|^2 + \sum_{j \in \mathcal{C}, j \neq c} |\mathbf{h}_{c,j}^{k}\mathbf{W}_j|^2} \tag{2.10}$$

where $\mathbf{h}_{c,c}^{k} \in \mathbb{C}^{1 \times |\mathcal{N}_c|}$ is a channel vector from RAUs of cluster c to user k in the cluster c, $\mathbf{W}_j \in \mathbb{C}^{|\mathcal{N}_j| \times |\mathcal{C}_j|}$ denotes the precoding matrix for cluster j, $\mathbf{h}_{c,j}^{k}$ is interfering channel vector from RAUs of cluster j to user k of cluster c. The entries of $\mathbf{h}_{c,c}^{k}$ and $\mathbf{w}_{i,c}$ are zeros except those entries that are corresponding to the serving RAU.

2.3.3.3 One cluster

At the high clustering threshold value, the system forms one cluster as shown in Fig. 2.10. In the one cluster, all users are jointly served using MU-MIMO precoding. The received SINR of user k is calculated as

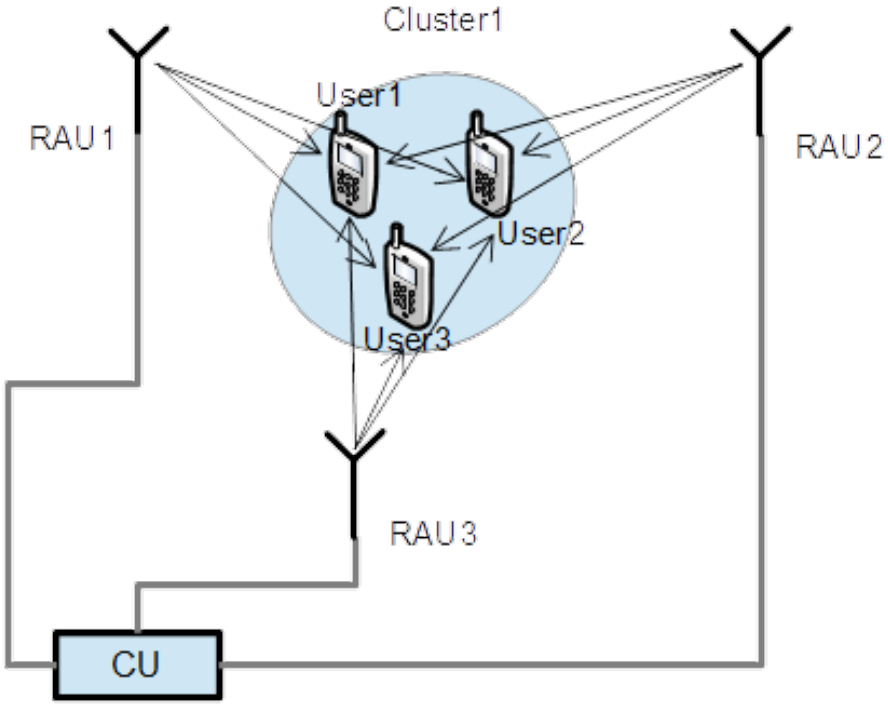

Figure 2.10: Illustration of one clustering where $K = 3$, $N_t = 3$ and one cluster is formed.

$$\gamma_k = \frac{|\mathbf{h}_k \mathbf{w}_k|^2}{\sigma^2 + \sum_{i \neq k} |\mathbf{h}_k \mathbf{w}_i|^2} \tag{2.11}$$

where $\mathbf{h}_k \in \mathbb{C}^{1 \times N_t}$ is a channel vector from RAUs to user k, $\mathbf{w}_i \in \mathbb{C}^{N_t \times K}$ denotes the precoding vector. The entries of $\mathbf{h}_k$ and $\mathbf{w}_i$ are zeros except those entries that are corresponding to the serving RAU. The SINR is close to SNR due to the elimination of inter-cluster interference. By increasing the clustering threshold, sum rate can be improved while the computational complexity also increases due to increment of precoding matrix size.

2.3.4 Transmit precoding vectors

Precoding [84] is a suboptimal strategy that can serve multiple users at a time like DPC, but with much reduced complexity. In precoding, each user stream is coded independently and multiplied by a beamforming weight vector for transmission through multiple antennas. Despite its reduced complexity, precoding has been shown to achieve a fairly large

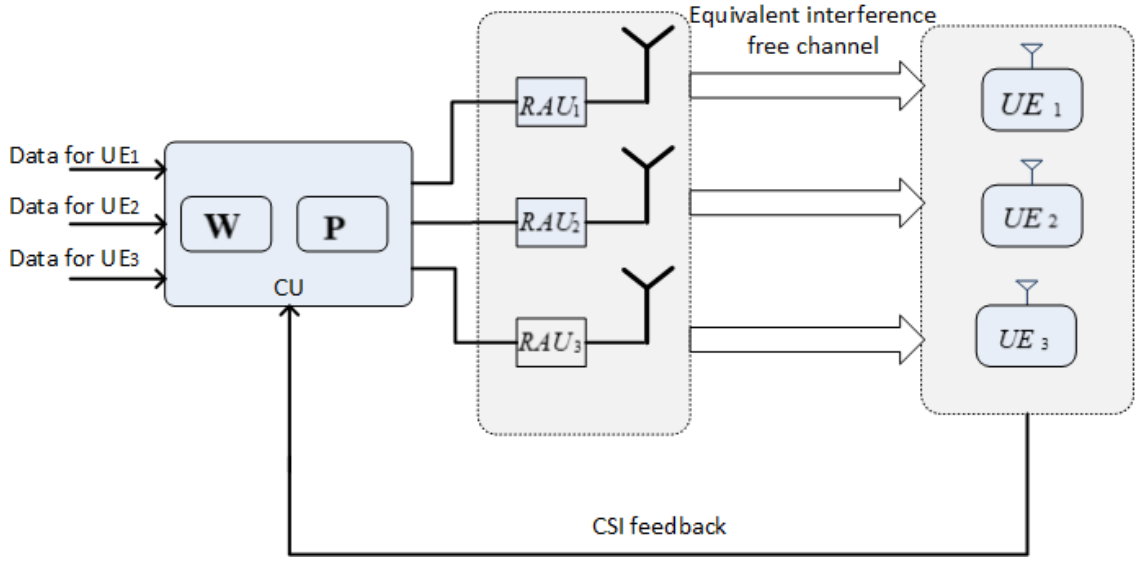

Figure 2.11: The MU-DAS with zero-forcing linear precoding.

fraction of DPC performance when the system has multiple antennas and each user has a single antenna [84–86].

In this thesis, we consider a suboptimal strategy, zero-forcing (ZF) precoder that follows the maximization of the SINR criterion. The ZF precoding is designed to put nulls in the directions other than the user of interest which results in minimizing the interference between neighbouring users as shown as Fig. 2.11. It is then possible to encode users individually. For the ZF precoding $\mathbf{W}$ is the well known matrix containing the pseudo-inverse of the channel matrix $\mathbf{H}$ [49], i.e.,

$$\mathbf{W} = \mathbf{H}^H(\mathbf{H}\mathbf{H}^H)^{-1} \tag{2.12}$$

In precoding, user streams are separated by different beamforming directions. Let s_k, $\mathbf{w}_k$, p_k be a transmit vector symbol, a precoding weight vector and a power normalization factor of RAU respectively and define $\mathbf{W} = [\mathbf{w}_1 \cdots \mathbf{w}_K]$ and $\mathbf{P} = \text{diag}\{p_1 \cdots p_K\}$. For user k, the received signal is given by:

$$y_k = \mathbf{h}_k \mathbf{w}_k \sqrt{p_k} s_k + \mathbf{h}_k \sum_{i \neq k} \mathbf{w}_i \sqrt{p_i} s_i + n_k \tag{2.13}$$

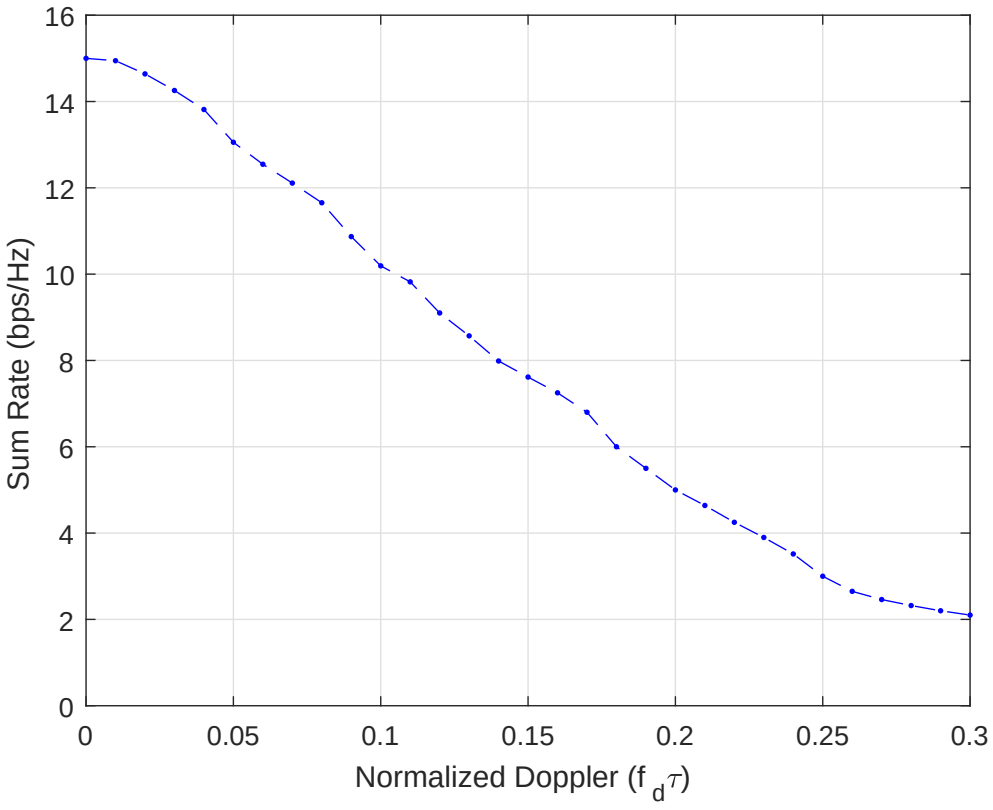

Figure 2.12: Illustration of sum rate of ZF precoding with $K = 2$ and $N_t = 7$ as a function of normalized Doppler.

The achievable sum rate is

$$R = \sum_{k=1}^{K} \log_2 \left(1 + \frac{p_k |\mathbf{h}_k \mathbf{w}_k|^2}{\sigma^2 + \sum_{i \neq k} p_i |\mathbf{h}_k \mathbf{w}_i|^2} \right) \tag{2.14}$$

In ZF precoding [49, 85, 86], precoding vectors are selected such that $\mathbf{h}_k \mathbf{w}_i = 0$ for $i \neq k$ and $\mathbf{h}_k \mathbf{w}_k = 1$. Then (2.14) becomes

$$R = \sum_{k=1}^{K} \log_2 \left(1 + \frac{p_k}{\sigma^2} \right) \tag{2.15}$$

2.3.4.1 Zero-forcing in Time varying channel

Fig. 2.12 shows the effect of outdated CSI due to time varying channel at the transmitter (CSI) on the performance of the ZF precoding. The plots are generated assuming that the transmitter has an outdated channel knowledge ($\tilde{\mathbf{H}}$), and its correlation coefficient to the true channel ($\mathbf{H}$)

is given by $\rho = J_0(2\pi f_d \tau)$, where τ is the feedback delay. Inaccuracy in CSI destroys semi-orthogonality of users in a group, i.e., $\mathbf{h}_k \mathbf{w}_i > 0$ and results in a poor performance of ZF precoding. Therefore, the high channel accuracy at the transmitter is required for zero-forcing precoding that use multiple beams at the same time.

2.3.5 Per antenna power constraint

The capacity of a wireless channel depends on the constraints on the transmit power and on the availability of the CSI at the transmitter and receiver. With sum power constraint across all transmit antennas, the capacity and optimal signalling are well established [87–89].The per-antenna power constraint is more realistic than sum power in practice because of the constraint on the individual RF chain connected to each antenna.

In DAS, the RAUs located at different physical nodes that cannot share power with each other. Thus understanding the capacity and the optimal signalling scheme under per-antenna power constraint can be useful. In [37], the optimization problem of a multiuser downlink channel is considered with per-antenna power under a minimum-power precoding design for downlink channels with a single antenna at each remote user and a capacity-achieving transmitter design for downlink channels with multiple antennas at each remote user. In [90], downlink zero-forcing precoding was derived to maximize the minimum user rate under per-antenna power constraint.

Suppose that the maximum power at each RAU becomes $P = P_t/N_t$. Giving the precoding vectors $\mathbf{w}_k$, $k = 1, \cdots, K$, such per-antenna power constraints correspond to

$$\max_j \sum_{k=1}^{K} \left[\mathbf{w}_k p_k \mathbf{w}_k^H\right]_{j,j} \leq P \quad j = 1, \cdots, N_t \tag{2.16}$$

where p_k is power normalization factor of RAU. Therefore, the transmit

power of RAU j is given by

$$\begin{aligned} P_j &= |w_{j,k}\sqrt{p_k}|^2 \\ &= |w_{j,k}|^2 \frac{P}{\max\limits_j \sum_{k=1}^{K} \left[\mathbf{w}_k \mathbf{w}_k^H\right]_{j,j}} \end{aligned} \tag{2.17}$$

Special case

1. **Single-user cluster**: Each RAU serves one user based on the channel condition, i.e., the user selects the RAU who has highest channel gain. In this case number of clusters is same as total number of users. Within a cluster, there is no inter-user interference. The RAU always transmit signal with maximum power of RAU which is given as

$$\begin{aligned} P_k &= |w_{k,k}\sqrt{p_k}|^2 \\ &= |w_{k,k}^2| \frac{P}{|w_{k,k}|^2} \\ &= P \end{aligned} \tag{2.18}$$

2. **One cluster**: The one cluster scenario corresponds to a situation in which all RAUs cooperatively transmit the signal to all users simultaneously In this case number of cluster is one. Within a cluster, the intra-cluster interference is cancelled by precoding. The transmit power of RAU j in cluster is given as

$$\begin{aligned} P_j &= \sum_{k=1}^{K} |w_{j,k}\sqrt{p}|^2 \\ &= P \frac{\sum_{k=1}^{K} |w_{j,k}|^2}{\max\limits_j \sum_{k=1}^{K} |w_{j,k}|^2} \end{aligned} \tag{2.19}$$

   The per antenna power constraint becomes strict because if one of the RAUs transmit power of the cluster exceeded the constraint, then the transmit power of all RAU of the cluster will be normalized.

This means only single RAU can transmit signal with maximum power. For example, the system forms a one cluster with two users and RAUs, and the total power is 20 mW. The transmit power of first RAU and second RAU are 5 mW and 15 mW respectively. Here the maximum power per RAU is 10 mW and the transmit power of the second RAU exceeds the constraint. After normalization the transmit power of first RAU and secod RAU become $5*10/15 = 3.34$ mW and $15 * 10/15 = 10$ mW respectively.

2.3.6 Interference Alignment

The wireless networks become more efficient where many users share the same radio resources. As a result of the existence of multiple users in the same radio resources, interference is one of the biggest challenges that limits the performance of wireless communications. Interference alignment (IA) is an inspiring technique, recently proposed in [91, 92]. In order to understand what IA could achieve, consider the toy example of [93] which is motivated by the wireless interference channel. Let us assume a conference in a room with K speakers, who will present their talks. Each listener must be able to hear his/her desired speaker with no interference from other $K - 1$ speakers. In order to be fair to each speaker, we should allow each user equal amounts of time to talk to his/her audience. Considering all of these issues, we should answer the question: What is the maximum amount of time that each speaker can talk while causing no interference to another speaker's audience? Using traditional interference management techniques, one could let each speaker talk for $1/K$ of the total session time. This corresponds to the idea of time division multiple access (TDMA) in wireless networks. However, it is suggested in [93] that each speaker can speak 1/2 of the total time without causing any interference. This seemingly impossible result can be made possible by the concept of IA which can be achieved in time, frequency or space. However, IA has many practical issues. It has been shown in the pioneering papers of IA [91, 92, 94, 95] that perfect alignment of interference requires perfect channel estimation and feedback.

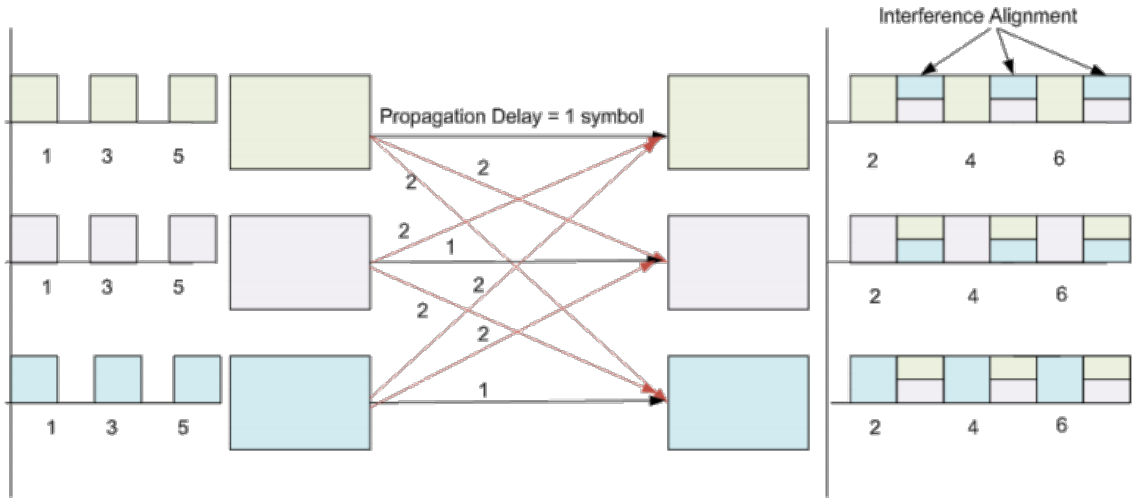

Figure 2.13: Interference alignment - Toy example of [94].

Dimensionality is also a very important problem in IA systems [96]. As the interference is aligned using precoding vectors, the system should have enough dimensions to align all interfering sources within a same subspace.

The main idea of the IA, which is originated from the linear algebra. However, it is not very easy to implement IA because of many disruptive challenges we encounter during implementation. Consider a system of linear equations such that [94]

$$\begin{aligned} y_1 &= h_{11}x_1 + h_{12}x_2 + \cdots + h_{1K}x_K \\ y_2 &= h_{21}x_1 + h_{22}x_2 + \cdots + h_{2K}x_K \\ &\cdots \\ y_B &= h_{B1}x_1 + h_{B2}x_2 + \cdots + h_{BK}x_K \end{aligned} \tag{2.20}$$

where B received signals $y_1, y_2, \cdots, y_B$ which are linear combinations of K symbols with channel coefficients h_{ij}.

We assume N to be the number of transmitters and B to be the bandwidth or signalling dimensions. Since the channel is linear, each signalling dimension produces a linear combination of the transmitted information symbols. Thus, a receiver has access to B signalling dimen-

sions. Before IA, a total of N signalling dimensions are used so that each receiver is able to resolve its desired one dimensional signal, i.e., the total bandwidth is divided among the K users so that each user gets $1/K$-th of the resources.

IA provides $1/2$ of the total available time interference free to all pairs, instead of $1/K$. This huge gain may seem impossible at first. This seemingly impossible result is made possible by the concept of IA which can be made in time, frequency or space. Let us consider K user interference channel where there is a propagation delay from transmitter i to receiver j, which is denoted as T_{ij} [94]. Suppose the locations of the transmitters and receivers can be configured such that the delay T_{ii} from each transmitter to the intended receiver is an even multiple of a basic symbol duration T_s, while the signal propagation delays $T_{ij}, (i \neq j)$ from each transmitter to all unintended receivers are odd multiples of symbol duration. The communication strategy is as seen in the Fig. 2.13, such that all transmissions occur simultaneously at even symbol durations. Note that with this policy, each receiver sees its own transmitter's signal interference-free over even time periods, while it sees all interference signals simultaneously over odd time periods. That is why, each user is able to achieve $1/2$ degrees of freedom and the total degrees of freedom achieved is equal to $K/2$.

Chapter 3

User clustering in MU-DAS

3.1 Introduction

Providing faster and reliable data transmission has drawn big attention in recent wireless technologies with taking into account the cost and complexity which may limit of solutions presented in this field. Conducting researches found that the data bit rate and spectral efficiency is an increasing function with the number of antennas. One main issue with scaling up transmit antenna relates to the cost and complexity of RF components that are deployed with antenna elements. To override this problem, antenna selection (AS) technique comes to reduce the number of analog components required, likewise preserves most of the advantages of MIMO systems such as diversity to improve the reliability of the system, or spatial multiplexing to increase the sum data rate of the system. The principal idea of AS scheme is to select a subset of antennas optimally among all available antennas in the transmitter [97–99]. However, equipping MIMO with more antennas leads to increase the complexity of the system due to the high number of computations required to achieve optimal antenna selection. By selecting best transmit antennas for the user, the number of transmit antenna and receiver will decrease dramatically which reduce the system computational complexity.

Since optimum method of AS requires exhaustive search over all possible combinations of antenna subsets which makes it impractical to use when there is a large number of antennas, any algorithm of AS should be

designed to reduce the complexity of selection process as well as achieve the required level of efficiency. Motivated by the idea of selecting RAUs for user, a transmit antenna selection algorithm for downlink multiuser DAS is proposed. AS involves various criteria such as channel capacity [100–104], squared Frobenius-norm of effective channels [105], channel's minimum singular value [106], and antennas with the highest SINR have to be chosen [97, 98, 107, 108]. The proposed algorithm selects an optimal subset of RAUs among the total RAUs available in the CU for transmission. In this paper, we propose suboptimal user and RAU selection algorithms for ZF with the aim of maximizing the total throughput while keeping the complexity low. Each selected set is updated with time according to the instantaneous channel information at the CU.

3.1.1 Contribution

The thesis contains the following contributions:

1. We investigate the antenna selection in MU-DAS downlink systems. We propose a user and antenna selection algorithm which aims at reaching the performance obtained by the exhaustive-search algorithm (optimum method) but with lower complexity. The performance of proposed algorithm is compared with multi-user distributed and co-located MIMO.

2. With in cluster, the proposed algorithm uses ZF precoding design to precancel the inter user interference.

3. The performance and complexity of the proposed algorithm have been validated and compared to two other algorithms; the exhaustive search algorithm and the single-user algorithm.

3.2 System Model

Consider a single-cell downlink environment which consists of N_t RAUs and K users, as shown in Fig. 3.1. $N_t \geq K$ is assumed. Each user is equipped with a single antenna. The users are randomly and uniformly

distributed within the cell. The RAUs are distributed with a circular layout with radius r and located at $r\cos\left[\frac{2\pi(i-1)}{N_t-1}\right], r\sin\left[\frac{2\pi(i-1)}{N_t-1}\right]$. Since all transmit antennas are spaced apart by a distance, the channel model involves not only fast fading but also path loss. We assume that the CU can perfectly estimate the CSI of all users. Let $\mathcal{K}$ denote the user set, i.e., $\mathcal{K} = \{1, \cdots, K\}$ and $\mathcal{N}$ denote the RAU set, i.e., $\mathcal{N} = \{1, \cdots, N_t\}$. Under these assumptions, the received signal of user k is given by:

$$y_k = \mathbf{h}_k(\mathbf{a}_k \circ \mathbf{w}_k)\sqrt{p_k}s_k + \mathbf{h}_k \sum_{i\in\mathcal{K}, i\neq k} (\mathbf{a}_i \circ \mathbf{w}_i)\sqrt{p_i}s_i + n_k \tag{3.1}$$

where $\mathbf{h}_k \in \mathbb{C}^{1\times N_t}$ is a channel vector for user k from all RAUs, $\mathbf{a}_k \in \mathbb{C}^{N_t\times 1}$ is a binary antenna selection vector for user k whose $(j,1)$-th element $a_{j,1} = 1$ if the RAU j is selected for user k , and $a_{j,1} = 0$ otherwise, $\mathbf{W} \in \mathbb{C}^{N_t\times K}$ denotes the precoding matrix whose j-th row and k-th column element is $w_{j,k}$, $\mathbf{s} \in \mathbb{C}^{K\times 1}$ is a transmit symbol vector whose k-th element denotes a transmit symbol for user k with $\mathbb{E}\{|s_k|^2\} = 1$ and $n_k \sim \mathcal{CN}(0, \sigma^2)$ is the AWGN. The j-th element of the channel vector $\mathbf{h}_k$ represents the channel from RAU j to user k, which consists of path loss and small scale fading and is given by

$$h_{k,j} = d_{k,j}^{-\frac{\alpha}{2}}(t) \cdot \tilde{h}_{k,j} \tag{3.2}$$

where α is path loss exponent and $d_{k,j}(t)$ is distance between user k and RAU j, $\tilde{h}_{k,j}$ is small scale fading from RAU j to user k and is independently and identically distributed (i.i.d).

The achievable user rate R_k for user k is

$$R_k = \log_2\left(1 + \frac{p_k|\mathbf{h}_k(\mathbf{a}_k \circ \mathbf{w}_k)|^2}{\sigma^2 + \sum_{i\neq k} p_i|\mathbf{h}_k(\mathbf{a}_i \circ \mathbf{w}_i)|^2}\right) \tag{3.3}$$

The contribution of this thesis is to maximize the sum rate by designing the beamforming with per-antenna power constraints. The opti-

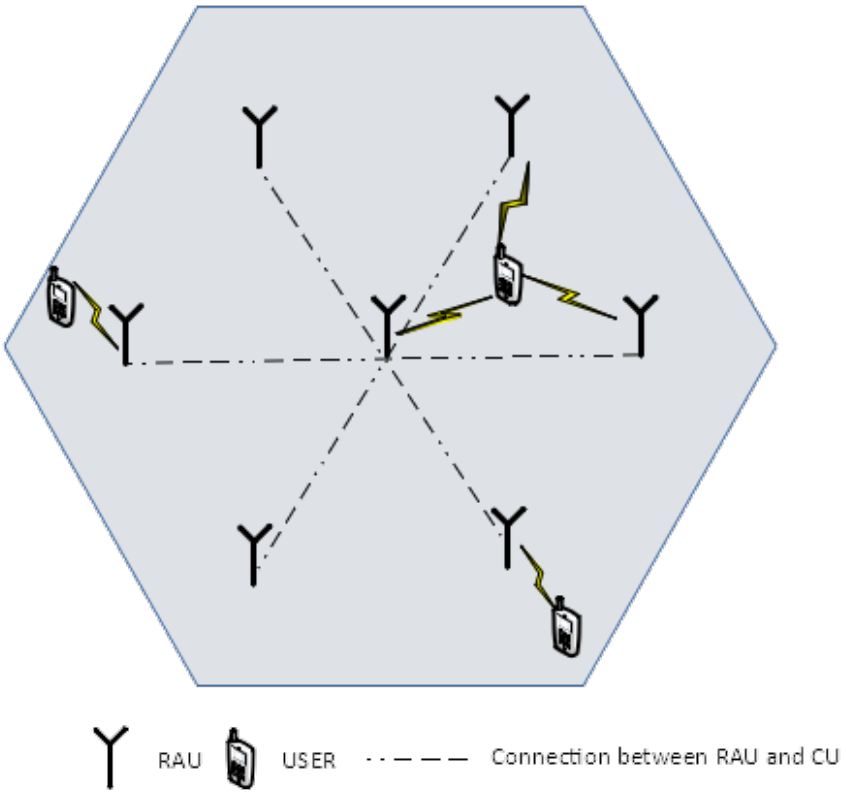

Figure 3.1: DAS architecture in cell.

mization problem for multiuser DAS is formulated as

$$\max_{\{\mathbf{a}_k,\mathbf{w}_k\}} \sum_{k=1}^{K} \log_2\left(1+\frac{p_k|\mathbf{h}_k(\mathbf{a}_k\circ\mathbf{w}_k)|^2}{\sigma^2+\sum_{i\neq k}p_i|\mathbf{h}_k(\mathbf{a}_i\circ\mathbf{w}_i)|^2}\right) \tag{3.4a}$$

$$\text{s.t } \max_{j} \sum_{k=1}^{K} \left[(\mathbf{a}_k\circ\mathbf{w}_k)p_k(\mathbf{a}_k\circ\mathbf{w}_k)^H\right]_{j,j} \leq P \tag{3.4b}$$

$$R_k(\mathbf{a}_k,\mathbf{w}_k) \geq R_0 \ \forall k \tag{3.4c}$$

where P is the maximum transmit power of each RAU and R_0 is target rate which is common for all users. (3.4a) is the objective function; (3.4b) follows a per-antenna power constraints, (3.4c) are per-user rate constraints, i.e., quality-of-service (QoS) constraints;

3.2.1 Cluster Formation

Optimum user clustering is performed by exhaustively searching over all possible antenna combinations, i.e.,

$$S_{optimum} = C_{N_t}^{N_s} \tag{3.5}$$

where $S \subset \{1, 2, ..., K\}$ denotes a set of users which can be served simultaneously by the CU, N_s is number of active RAUs. Hence, the sum rate for all possible combinations of the users and the antennas is calculated. The combination with the highest sum rate is selected. It is clear from (3.5) that the exhaustive search becomes impractical to use when the number of transmit antennas is large. Many suboptimal algorithms are proposed to reduce the computational complexity, also to achieve as close as possible to the optimum method. In this thesis, we proposed user clustering algorithms whose performance is very close to the exhaustive search method with much lower complexity.

3.2.1.1 Capacity Based Suboptimal User Cluster Algorithm

Let cluster c is formed to serve the set of user $\mathcal{C}_c$, which is subset of $\mathcal{K}$. Let $\hat{\mathbf{H}}_c = \mathbf{H}_c\mathbf{W}_c$ denote the effective channel after precoding for user $k \in \mathcal{C}_c$ then the cluster rate achieved with ZF applied to the user set $k \in \mathcal{C}_c$ is expressed as

$$R_c = \max \sum_{k \in \mathcal{C}_c} \log_2 \left| \mathbf{I} + \frac{1}{\sigma^2} \hat{\mathbf{H}}_c \hat{\mathbf{H}}_c^H \right| \tag{3.6}$$

Let $\mathcal{C}$ be the set containing all possible $\mathcal{C}_c$, i.e., $\mathcal{C} = \{\mathcal{C}_1, \mathcal{C}_2, \cdots\}$, then the sum rate R with ZF can be defined as

$$R = \max_{\{\mathcal{C}_c \in \mathcal{C}\}} R_c \tag{3.7}$$

The algorithm first selects the single user and antenna pair with the highest capacity. Then, from the remaining unselected users and antennas, it finds the user that provides the highest total throughput together with those selected users. The algorithm terminates when the

total throughput drops if more users are selected. Clearly, the proposed algorithm needs to search over no more than $N_t N_s$ user sets, which greatly reduces the complexity compared to the exhaustive search method $N_t^{N_s}$. Let s_i denote the user index selected in the ith iteration, i.e. $s_i \in \{1, 2, \cdots, K\}$. The capacity-based user clustering algorithm is described in Table 1.

Algorithm 1 Capacity based suboptimal user clustering algorithm

Initialize $\mathcal{K} = \{1, 2, \cdots, K\}$, $\mathcal{N} = \{1, 2, \cdots, N_t\}$ and $\mathcal{C} = \emptyset$. Let $s_1 = \arg \max_{\{k \in \mathcal{K}, n \in \mathcal{N}\}} \log_2 \left|\mathbf{I} + \frac{1}{\sigma^2}\mathbf{H}_k \mathbf{H}_k^H\right|$. Let $\mathcal{K} = \mathcal{K} - \{s_1\}$, $\mathcal{C} = \mathcal{C} + \{s_1\}$ and $R_{temp} = \max_{\{k \in \mathcal{K}, n \in \mathcal{N}\}} \log_2 \left|\mathbf{I} + \frac{1}{\sigma^2}\mathbf{H}_k \mathbf{H}_k^H\right|$.

for $i = 2 : K$ **do**
  for every $k \in \mathcal{K}$ **do**
    Let $\hat{\mathcal{C}}_k = \mathcal{C}_k + \{k\}$
    $R_k = \max_{\{j \in \hat{\mathcal{C}}_k\}} \log_2 \left|\mathbf{I} + \frac{1}{\sigma^2}\mathbf{H}_j \mathbf{H}_j^H\right|$
  end
  Update $s_i = \arg \max_{\{k \in \mathcal{K}, n \in \mathcal{N}\}} R_k$
  if $\max_{\{k \in \mathcal{K}, n \in \mathcal{N}\}} R_k < R_{temp}$ **then**
    The selected user set is $\mathcal{C}$
    Find the precoding matrix $\mathbf{W}_c$ for each $c \in \mathcal{C}$ and the effective channel $\hat{\mathbf{H}}_c = \mathbf{H}_c \mathbf{W}_c$
    $R_c = \max \sum_{k \in \mathcal{C}_c} \log_2 \left|\mathbf{I} + \frac{1}{\sigma^2}\hat{\mathbf{H}}_c \hat{\mathbf{H}}_c^H\right|$
  else
    Update $\mathcal{K} = \mathcal{K} - \{s_i\}$, $\mathcal{C} = \mathcal{C} + \{s_i\}$ and $R_{temp} = \max_{\{k \in \mathcal{K}\}} R_k$
  end
end

3.2.1.2 Single-user Cluster Algorithm

Each antenna serves one user based on the channel condition, i.e., the user selects the antenna that has highest channel gain. The user clustering is carried out at the CU based on the estimated channel. The CU estimates CSI for all users from all RAUs. The user k^* and RAU j^* are selected as follows

$$k^*, j^* = \arg \max_{j \in \mathcal{N},\ k \in \mathcal{K}} |h_{k,j}|^2 \tag{3.8}$$

Then, user k^* and RAU j^* are removed from the selection pool. This procedure is repeated until all users are assigned to the RAUs. Every RAU transmits the signal to the corresponding user simultaneously. Therefore, there is uncoordinated inter-cluster interference. In this algorithm, the number of clusters is same as the total number of users.

3.3 Numerical Results

We evaluate the rate performance for the downlink MIMO (co-located) and DAS cellular system. The simulation parameters are given in Table I. The users are randomly and uniformly distributed within the coverage area. The maximum total transmit power is varied from -30 dBm to 30 dBm. The channel between each RAU and each user is composed of the path loss (path loss exponent of 3) and small scale fading which is modelled as a frequency flat Rayleigh fading channel. Table 3.1 summarizes the MU-DAS system parameters for performance evaluation.

Table 3.1: Simulation Parameters

Parameter Settings	Value
Cell Model	Hexagonal grid1 km^2
Carrier Frequency	2 GHz
Number of RAUs	10
Number of users	2, 7
Users distribution	Uniform
Path loss exponent	3
Total transmit power (P_t)	from -30 dBm to 40 dBm
Noise power	-104 dBm
User speed range	0 m/s to 15 m/s
User target Rate	2 bps/Hz

Fig. 3.2 shows the comparison of the average sum rate of DAS and co-located MIMO cellular network as a function of the maximum total transmit power P_t dBm. The sum rate of the DAS cellular network is better than co-located MIMO in both exhaustive and proposed user clustering scheme. This is because in DAS, the user selects the RAU whose channel gain is the highest among the RAUs. Due to geographi-

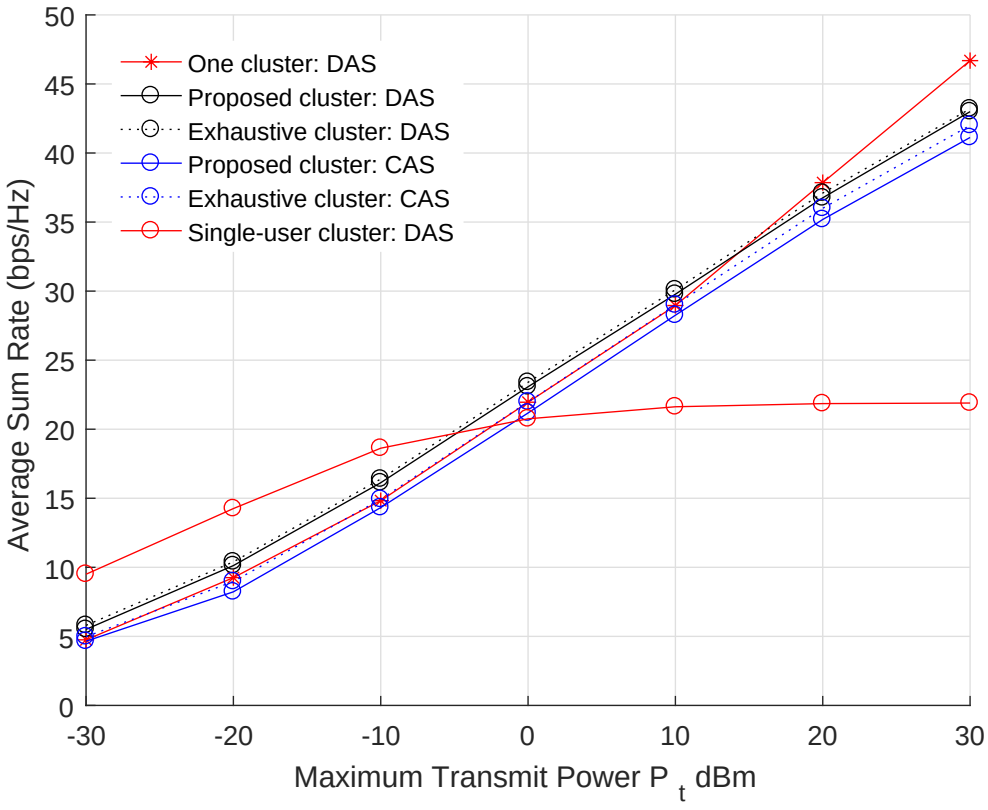

Figure 3.2: Illustration of sum rate comparison between CAS and DAS cellular networks under different user clustering scheme, where $K = 7$ and $N_t = 7$.

cal distribution of antennas in DAS, the path loss between selected users and RAUs will be reduced when large number of antennas are deployed. Therefore the DAS, RAUs can use more power to transmit the signal. On the other hand, in co-located MIMO, every antenna experiences the same path loss. Therefore, the transmit power needs to be used to compensate the path loss. In low transmit power regime, the received interference power is less than noise power. So the noise power is a dominant factor to limit the sum rate at low transmit power regime. Therefore, the single-user cluster scheme has better sum rate than other user clustering scheme at low transmit power regime. As the transmit power increases, the interference power becomes more dominant to limit the sum rate. Therefore, the sum rate becomes saturate in the single-user cluster scheme. In one cluster scheme, all users are jointly served by using MU-

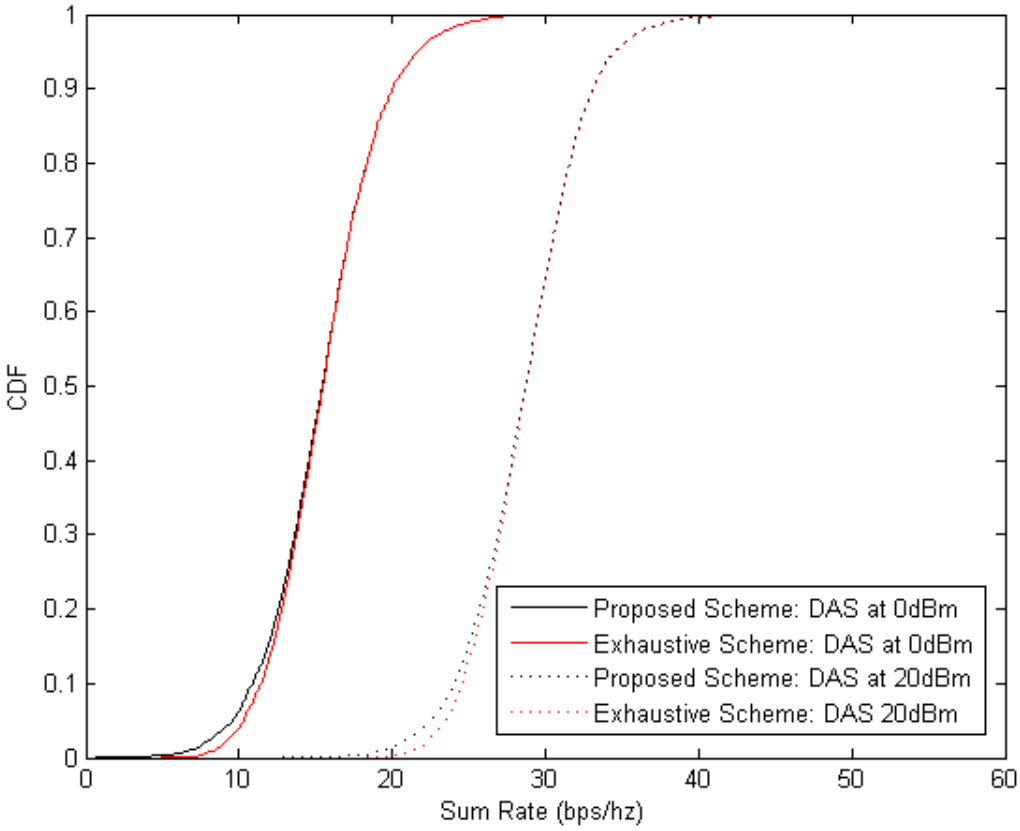

Figure 3.3: Illustration of CDF of proposed cluster and exhaustive cluster scheme at different transmit power, where $K = 7$ and $N_t = 7$.

MIMO precoding. The SINR is close to SNR due to the elimination of intra-cluster interference using ZF precoding. However, at low transmit power regime, the one cluster contains all users and RAUs including the worst channel gain between users and RAUs. So, more transmit power is used to compensate the worst channel gain between users and RAUs. Therefore, the proposed user clustering scheme provides better sum rate than a one cluster at low transmit power. However, when transmit power increases in the proposed technique, the inter-cluster interference power also increases. In case of one clutser, there is no inter-cluster interference and intra-cluster interference is cancelled by ZF precoding. Therefore, the one cluster scheme has better sum rate performance than the other user clustering schemes as the maximum transmit power increases.

Fig. 3.3 shows the CDF of the instantaneous sum rate of exhaustive

scheme and proposed scheme in DAS at different transmit power. Fig. 3.2 and 3.3 shows that the exhaustive scheme performance of DAS is slightly better than proposed scheme of DAS. Note that the exhaustive scheme needs to consider all possible user and antenna combinations. On the other hand, the proposed scheme only considers user and antenna sets whose channel gain is the highest.

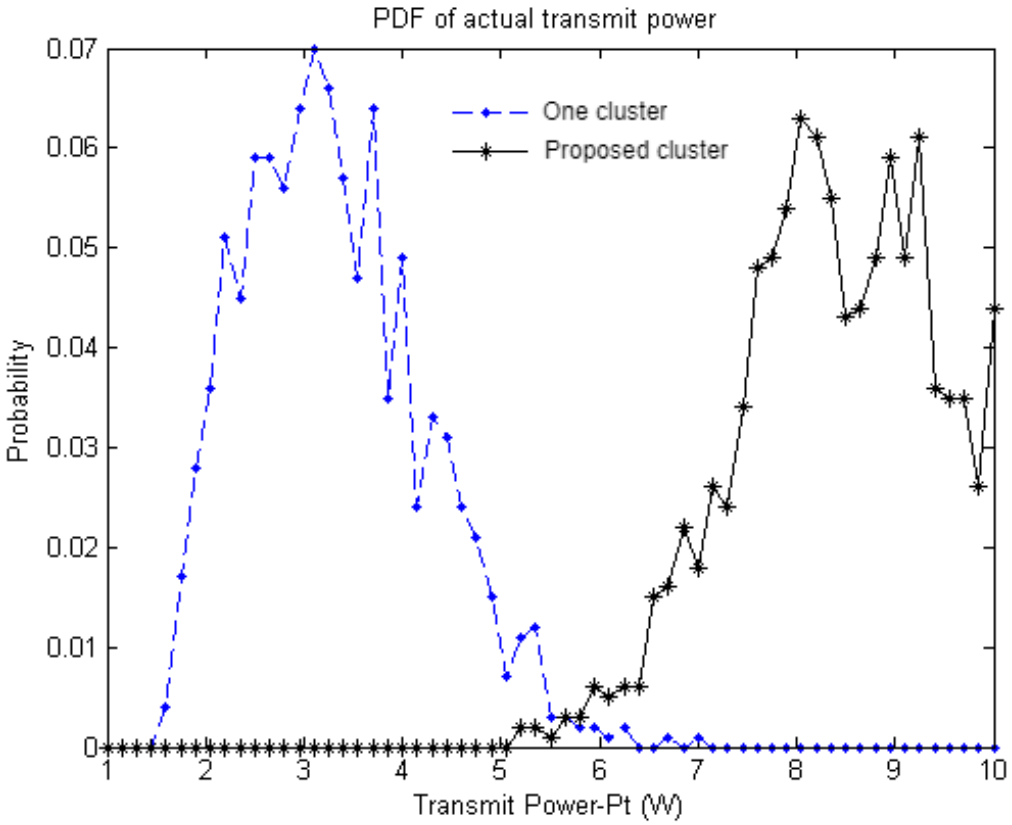

Figure 3.4: Illustration of PDF of actual transmit power of One cluster and proposed cluster, where $K = 7$ and $N_t = 7$.

We have considered per-antenna power constraint with same power normalization factor at each RAUs within a cluster. Fig. 3.4 shows that the proposed cluster technique can utilize more total transmit power than one cluster technique. This is because one cluster includes all users and RAUs with the worst channel gain. So, more transmit power is

required to compensate the worst channel gain between users and RAUs. However, in proposed algorithm, multiple cluster is formed with subsets of users and RAUs with high channel gain. Therefore, the system with proposed cluster utilizes more transmit power to transmit signal.

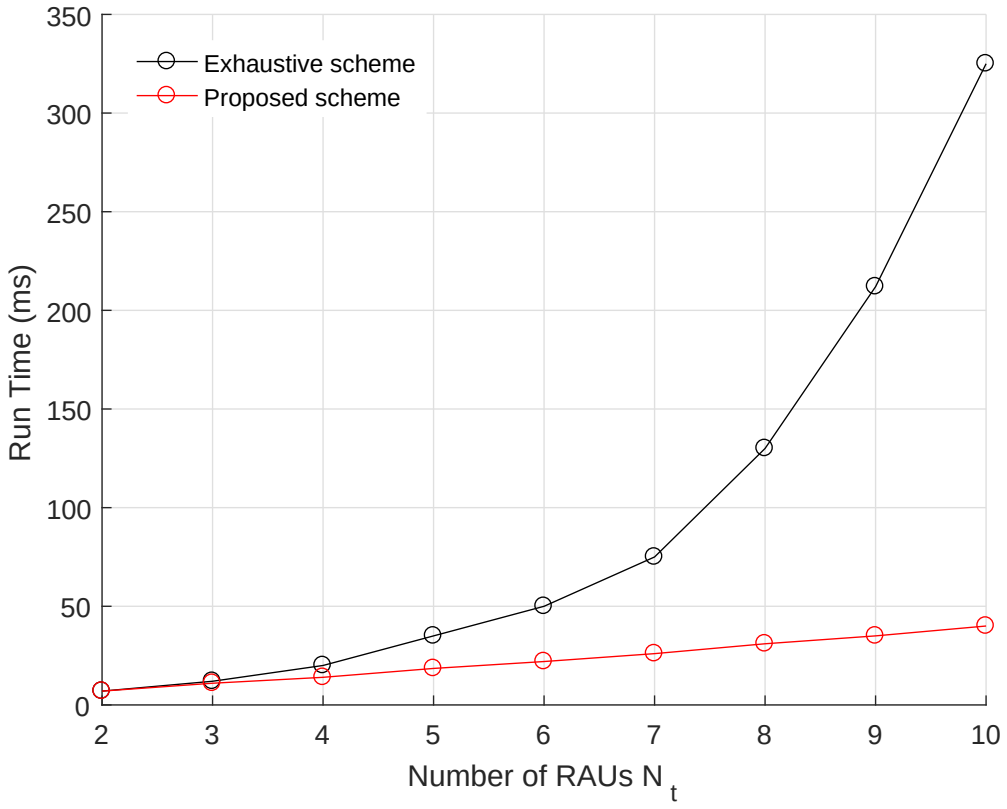

Figure 3.5: Run time comparison of proposed and exhaustive user clustering with 2 users.

In Fig. 3.5, the elapsed CPU time of the proposed scheme and exhaustive search scheme is plotted against the number of RAUs for two users. This result was attained by 3.4 GHz Core *i*7 CPU pc. As noted in the figure, the CPU runtime of the proposed scheme outperforms the exhaustive search but achieves almost same performance as the exhaustive search.

3.4 Summary

In this Chapter, we have studied the user clustering technique for downlink multi-user DAS. The objective is to design an algorithm which can almost achieve the same throughput obtained by the exhaustive search algorithm with lower complexity. Further, the zero-forcing precoding is used to cancel the inter-user interference in multiuser systems. Simulation results show that the proposed algorithm achieves very close to the optimal search algorithm with a considerable reduction in complexity.

Chapter 4

Interference Alignment in Inter-cluster of MU-DAS

4.1 Introduction

In the DAS, the sum rate can be increased by a cooperative transmission technique where, the multiple RAUs will transmit the independent massage signal to the multiple users simultaneously. To overcome inter-user interference due to simultaneous transmission, multiple RAUs form a cluster and cooperatively transmit the signal to all users. The intra-cluster interference within the cluster is eliminated by using Zero Forcing (ZF) precoding scheme. However, the inter-cluster interference is uncoordinated and can deteriorate the system performance and it should be eliminated or minimized carefully.

Interference management is one of the major challenging issues in DAS. IA is an inspiring technique, recently proposed in [91, 92]. IA eliminates the interference among multiple users by reducing the dimension of interference space [92]. This reduction is achieved by a careful design of precoding at each transmitter. IA is used to manage the inter-cell interference [109, 110]. However, the achievable sum rate of the system with IA decreases as the number of users within cell increases [111]. This degradation is because of large number of interference to the user. To overcome this problem, a user clustering is proposed [111], where the interference within each cluster is eliminated by IA. Although IA brings

significant performance gain in the high signal to noise ratio (SNR) region, IA can not provide sufficient gain in low SNR region [96, 109]. In the cellular system, the user located at the cell edge receives low signal power due to large propagation loss, therefore, the applicability of IA to cellular system is limited. To solve this problem, a combination of IA and DAS is proposed in [109]. In [109], multiple RAUs are deployed to increase the SNR at the cell edge so that IA can bring the gain.

4.1.1 Contribution

Suppose cellular network has N_t RAUs and K users. Each user is equipped with N_r antennas. The system sends K independent messages to K users in the cell, each user suffers from the inter-cluster interference i.e., K interfering symbol from the RAUs of the other cells. Each user can cancel only $N_r - 1$ inter-cluster interference symbol and still suffers from $K - N_r + 1$ inter-cluster interference symbol.

This issue can be solved by forming multiple clusters within a cell. Cluster is a subset of RAUs which serve multiple users simultaneously. The interference within a cluster i.e., intra-cluster interference will be eliminated by using ZF precoding. Each cluster receives different power level interference from the RAUs of the other clusters due to the large scale fading. The achievable sum rate of the cluster is mainly affected by strong interference received from the RAUs of the other clusters i.e., inter cluster interference. Eliminating weak inter-cluster interference by IA may not improve the achievable rate but requires additional subspace dimension to align these interference. Therefore, a cooperative cluster is formed to cancel the strongest inter-cluster interference by performing the IA. The proposed approach consists of two phases:

1. A number of users and RAUs form a cluster and ZF precoding is used to eliminate the intra-cluster interference.

2. IA is performed to eliminate the strongest inter-cluster interference by forming a cooperative cluster.

4.2 System Model

Consider a single cell downlink environment covered by N_t RAUs with radius R_c and K users, as shown in Fig. 3.1. Each RAU is equipped with a single antenna. Each user is equipped with N_r antennas. The users are uniformly distributed within a cell. The total K users within a cell are divided into M clusters i.e. $1 \leq M \leq K$ and $\sum_{k=1}^{M} |\mathcal{U}_k| = K$, where $\mathcal{U}_k$ is the index set of users for the cluster k. We assume each user and RAU belongs to only one cluster. Thus, $\mathcal{U}_k \cap \mathcal{U}_l = \phi$, for $k \neq l$. $\mathcal{N}_k$ will be a subset of RAUs which will serve $\mathcal{U}_k$ i.e $\mathcal{N}_k \cap \mathcal{N}_l = \phi$, for $k \neq l$. We assume that the CU can perfectly estimate the CSI of all users at the CU.

Each cluster will select a user from K users pool using the user selection scheme which is discussed in section 4.3. Let $\mathbf{y}_i \in \mathbb{C}^{N_r \times 1}$ be received signal vector of a user k of the cluster i can be written as

$$\mathbf{y}_i^k = \underbrace{\mathbf{H}_i^k \mathbf{W}_i \mathbf{s}_i}_{\text{desired signal}} + \underbrace{\sum_{\substack{j=1,\\ j\neq i}}^{M} \mathbf{G}_{i,j}^k \mathbf{W}_j \mathbf{s}_j}_{\text{inter-cluster interference}} + \mathbf{n}_i^k \tag{4.1}$$

where $\mathbf{G}_{i,j}^k \in \mathbb{C}^{N_r \times |\mathcal{N}_j|}$ is the interfering channel matrix from RAUs of the cluster j to the user k of the cluster i, $\mathbf{W}_i \in \mathbb{C}^{|\mathcal{N}_i| \times |\mathcal{U}_i|}$ is the transmit beamforming vector,where the design of the alignment beamforming will be explained in 4.4, $\mathbf{s}_i \in \mathbb{C}^{|\mathcal{U}_i| \times 1}$ is the transmitted signal data of cluster i and $\mathbf{n}_i^k \in \mathbb{C}^{N_r \times 1}$ denotes received Gaussian noise vector. The second term is the interference received at the user k of the cluster i from RAUs of the other clusters, i.e., inter-cluster interference.

The j-th vector of the channel matrix $\mathbf{H}_i^k$ represents the channel from RAU j to user k of the cluster i, i.e., $\mathbf{h}_{j,i}^k \in \mathbb{C}^{N_k \times 1}$, which consists of large scale fading and small scale fading is given by

$$\mathbf{h}_{j,i}^k = \mathbf{l}_{j,i}^k \cdot \tilde{\mathbf{h}}_{j,i}^k \tag{4.2}$$

where $\mathbf{l}_{j,i}^k$, $\tilde{\mathbf{h}}_{j,i}^k$ are large scale fading vector and small scale fading vector respectively from RAU j to user k of the cluster i. The large scale fading

$\mathbf{l}_{j,i}^{k}$ consists of path loss and shadowing from RAU j to all antennas N_r of user k which remain same. So, without loss of generality, the element of $\mathbf{l}_{j,i}^{k}$ can written as

$$l_{j,i}^{k} = d_{j,i}^{k^{-\frac{\alpha}{2}}} \psi \tag{4.3}$$

where $d_{j,i}^{k}$ denotes the path loss with path loss exponent α and distance $d_{j,i}^{k}$ between user k and RAU j of the cluster i. ψ denotes as shadowing and modelled as a log-normal random variable, given by $\psi = 10^{(\eta\sigma_{SF})/10}$, where σ_{SF} is the shadowing standard deviation in dB and η is a zero mean Gaussian random variable with unit variance.

Each user decodes the desired signal by multiplying the receive beamforming vector. Let $\mathbf{u}_i^k \in \mathbb{C}^{N_r \times 1}$ be receive beamforming vector at the user k of the cluster i, which is used to cancel the received interference. The received signal at the i-th cluster after receive beamforming vector, can be expressed as

$$\begin{aligned} \tilde{y}_i^k &= \left(\mathbf{u}_i^k\right)^H \mathbf{y}_i^k \\ &= \left(\mathbf{u}_i^k\right)^H \mathbf{H}_i^k \mathbf{W}_i \mathbf{s}_i + \left(\mathbf{u}_i^k\right)^H \sum_{j=1, j\neq i}^{M} \mathbf{G}_{i,j}^k \mathbf{W}_j \mathbf{s}_j + \left(\mathbf{u}_i\right)^H \mathbf{n}_i^k \end{aligned} \tag{4.4}$$

Each user needs to feedback its effective channel vector, i.e., $\tilde{\mathbf{H}}_i^k = \left(\mathbf{u}_i^k\right)^H \mathbf{H}_i^k \in \mathbb{C}^{1\times|\mathcal{U}_i|}$ to the CU, so that the cluster beamforming $\mathbf{W}_i$ is designed at each cluster.

4.3 Cooperative Cluster Formation

4.3.1 User Clustering

The cell consists of users K and each cluster supports one user. The purpose of the user selection algorithm is to select a suitable user to transmit which can maximize the system sum rate. The proposed selection algorithm is based on norm value of the user. The CU of DAS system has full knowledge about CSI of each user. Let $\mathbf{H}_i^k \in \mathbb{C}^{N_r \times|\mathcal{N}_i|}$ be the channel

matrix for the user k of the cluster i. The CU of DAS system calculates the squared frobenius norm for each user using its channel matrix ($\mathbf{H}_i$). The squared frobenius norm can be considered as the total power gain of the channel of the user.

$$||\mathbf{H}_i||_F^2 = \text{trace}(\mathbf{H}_i\mathbf{H}_i^H) \tag{4.5}$$

The CU of DAS system orders these norm values in descending form for each cluster. Each cluster selects the user which has the largest norm value from the order.

4.3.2 Cooperative Clustering

The purpose of cooperative cluster selection is to select a cluster where IA is not performed and also selects the strong interference for the selected cluster. Once the user is selected, the next step is to select a cluster where the IA will not be applied, but its strong interference will be cancelled by receive beamforming. We used two techniques to do cluster selection.

4.3.2.1 Norm based Selection

Each cluster can easily find out the norm value of its selected user to the other clusters, because cluster selection is done at the CU of DAS. This can be illustrated by Table 4.1. Let $K = 3$, $N_r = 2$, U_1, U_2 and U_3 be selected users for cluster C_1, C_2 and C_3 respectively.

Table 4.1: Norm value of selected user from interfering cluster

	C_1	C_2	C_3
U_1		0.0034	0.0228
U_2	0.02		0.0301
U_3	0.130	0.0136	

Each user can cancel one received interference by receive beamforming because each user has two receive antennas. Therefore, each user selects the interference with the highest power to be cancelled as shown in Table 4.2.

Table 4.2: Strong interference cancel for selected user

	C_1	C_2	C_3
U_1		0.0034	~~0.0228~~
U_2	0.02		~~0.0301~~
U_3	~~0.130~~	0.0136	

The cluster will be selected which has the smallest interference power for its selected user. The interference with the smallest power which will be treated as noise. Therefore, the IA is not performed on the selected cluster as shown in Table 4.3.

Table 4.3: Cluster with the smallest interference

	C_1	C_2	C_3
U_1		0.0034	
U_2	0.02		
U_3		0.0136	

The transmit beamforming for the selected cluster is fixed because the IA is not be applied and its value can be arbitrarily under the criterion of per antenna power constraint. Let us pick the transmit beamforming vector 2×1 be all ones and will be normalized under the criterion of per-antenna power constraint.

The interference alignment is performed for remaining two clusters. Each remaining cluster receives interference from the selected cluster and from the other one. Therefore, each remaining cluster will align the interference with interference receives from the selected cluster. Since the transmit beamforming of the selected cluster is already fixed, so the transmit beamforming for remaining cluster interference will be calculated based the transmit beamforming of the selected cluster.

4.3.2.2 Random Selection

The CU of DAS will randomly select the two clusters where IA is performed and one cluster where one interference is cancelled by using re-

ceived beamforming. Similarly, the interference is also selected randomly where received beamforming is used to cancel.

4.3.3 Single Cluster

The single group scenario corresponds to a situation in which all RAUs cooperatively transmit the signal to three selected users simultaneously. A linear precoding for single cluster is constructed based on the block diagonalization (BD) algorithm. The BD is used to null space the inter user interference. The received signal for the user k is given by:

$$\mathbf{y}_k = \mathbf{H}_k \mathbf{W}_k \mathbf{s}_k + \sum_{j=1, j \in k}^{K} \mathbf{H}_k \mathbf{W}_j \mathbf{s}_j + \mathbf{n}_k \tag{4.6}$$

The BD algorithm is an extension of the ZF method for multi-user MIMO systems where each user has multiple antennas. Each user's linear precoder and receiver filter can be obtained by twice SVD operations [112]. To eliminate all inter-user interference, the following constraint is imposed.

$$\tilde{\mathbf{H}}_k \mathbf{W}_k = 0 \tag{4.7}$$

$\tilde{\mathbf{H}}_k$ is defined as the channel matrix for all users other than the user k.

$$\tilde{\mathbf{H}}_k = \left[\mathbf{H}_1^T, \cdots, \mathbf{H}_{k-1}^T, \mathbf{H}_{k+1}^T, \cdots, \mathbf{H}_K^T\right]^T \tag{4.8}$$

By applying the SVD, the following value for the channel is obtained as

$$\tilde{\mathbf{H}}_k = \mathbf{U}_k \Sigma_k \left[\mathbf{V}_k^{(1)} \mathbf{V}_k^{(0)}\right]^H \tag{4.9}$$

where Σ_k is the diagonal matrix of which the diagonal elements are non-negative singular values of $\tilde{\mathbf{H}}_k$ and its dimension equals to the rank of $\tilde{\mathbf{H}}_k$. $\mathbf{V}_k^{(0)}$ contains vectors corresponding to the zero singular values, and $\mathbf{V}_k^{(1)}$ consists of the singular vectors corresponding to nonzero singular values. Thus, $\mathbf{V}_k^{(0)}$ is an orthogonal basis for the null space of $\tilde{\mathbf{H}}_k$. Define the SVD of $\tilde{\mathbf{H}}_k \tilde{\mathbf{V}}_k^{(0)}$ as

$$\tilde{\mathbf{H}}_k \tilde{\mathbf{V}}_k^{(0)} = \tilde{\mathbf{U}}_k \tilde{\Sigma}_k \left[\tilde{\mathbf{V}}_k^{(1)} \tilde{\mathbf{V}}_k^{(0)} \right]^H \tag{4.10}$$

Thus, we define the total precoding matrix as

$$\mathbf{W} = \left[\tilde{\mathbf{V}}_1^{(0)} \mathbf{V}_1^{(1)} \cdots \tilde{\mathbf{V}}_K^{(0)} \mathbf{V}_K^{(1)} \right]^H \tag{4.11}$$

4.3.4 No Cluster Selection

From user selection, each cluster selects the user which has the largest norm value. All three clusters serve its corresponding user simultaneously using the same radio resources incurs inter-cluster interference. The inter-cluster interference will be treated as noise.

4.4 Beamforming Design

4.4.1 Transmit Beamforming

Assuming perfect channel knowledge at the transmitter, pre-processing of the transmitted signal can be applied to align the interfering signals in a particular subspace. No interference alignment is necessary for selected cluster. Therefore, the transmit beamforming of the selected cluster for both selection scheme is fixed. The transmit beamforming for remaining cluster interference is calculated based the transmit beamforming of the selected cluster.

Let C_1, C_2 and C_3 be three cluster in a cell. Each cluster consist of two RAUs and one user. Let us consider C_2 cluster is the selected cluster and its transmit beamforming $\mathbf{w}_2 = \mathbf{1}_{2\times 1}$. The interference of cluster C_1, and C_3 is align into one dimension subspace. The transmit beamforming vector is calculated as follows.

For user of cluster C_1, the interference from cluster C_2 and C_3 are perfectly aligned

$$\begin{aligned} \mathbf{G_{13}} \mathbf{w}_3 &= \mathbf{G_{12}} \mathbf{w}_2 \\ \mathbf{w}_3 &= (\mathbf{G_{13}})^{-1} \mathbf{G_{12}} \mathbf{w}_2 \end{aligned} \tag{4.12}$$

For user of cluster C_3, the interference from cluster C_1 and C_2 are perfectly aligned

$$\begin{aligned} \mathbf{G_{31}}\mathbf{w}_1 &= \mathbf{G_{32}}\mathbf{w}_2 \\ \mathbf{w}_1 &= (\mathbf{G_{31}})^{-1}\mathbf{G_{32}}\mathbf{w}_2 \end{aligned} \tag{4.13}$$

The calculated transmit beamforming will be normalized under the criterion of per antenna power constraint.

4.4.2 Receive beamforming

The receive beamforming vector is designed at each user to cancel the received interference using the CSI. For the desired signal detection, the receive beamforming needs to satisfy the following condition:

$$\left(\mathbf{u}_i^k\right)^H \mathbf{G}_{i,j}^k = 0 \quad \forall j \neq i \tag{4.14}$$

4.5 Numerical Results

The users are randomly and uniformly distributed within the coverage area. The rate performance for the downlink DAS is evaluated. The total transmit power P_t is 20 dBm. The channel between each RAU and each user is composed of the path loss (path loss exponent of 3), shadowing (standard deviation $\sigma = 8$ dB) and small scale fading which is modelled as a frequency flat Rayleigh fading channel. The simulation parameters are given in Table 4.4.

Table 4.4: Simulation Parameters

Parameter Settings	Value
Direction	Downlink
Transmission bandwidth	10MHz
Cell Radius R_c	1Km
Distance between RAU d_r	$\frac{2R_c}{3}$
Number of total RAU	6
Number of users	6
Selected RAU per cluster	2
Selected user per cluster	1
Number of receive antennas	3
Users distribution	Uniformly
Path loss exponent	3
Shadowing (σ)	8 dB
Total transmit power P_t	20dBm
Noise power density	-104dBm/Hz

Fig. 4.1 shows the comparison of the CDF of sum rate of cluster selection at the maximum total transmit power $P_t = 20$ dBm. The sum rate of single cluster technique is better than other techniques. This is because in single cluster, the inter user interference has been cancelled. So, no further interference management is necessary. On other techniques, interference management is necessary. The sum rate of norm based cluster selection than random cluster selection and no cluster selection. This is because in norm based selection, the CU selects a cluster where IA is not performed the user of the cluster, which received the smallest interference power from RAUs of other cluster and also its strongest interference, which is cancelled by receive beamforming. The IA is applied two clusters, which has high power receive interference. On other the hand, the random selection selects a cluster where IA is not performed randomly. The selected cluster may not have smallest interference power. Also, it selects interference symbol randomly, where received beamforming is used to cancel. In no cluster selection, the interference for each cluster has been treated as noise. So its sum rate performance is worse than other cluster selection techniques. We observe that around 20% times

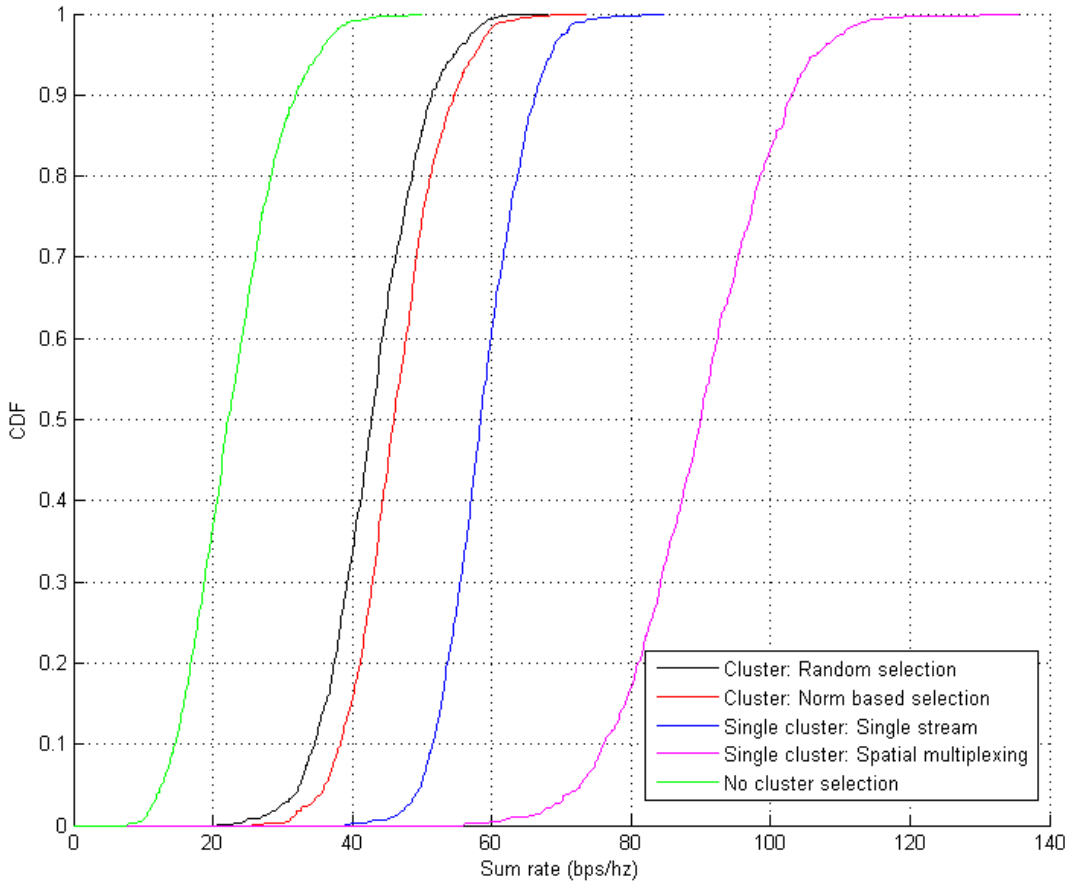

Figure 4.1: Comparison of CDF of sum rate between random cluster selection and proposed norm based cluster selection when $N_t = 6,\ K = 6,\ N_r = 2$ at 20 dBm, where number of selected users is 3.

random selection is better than the norm based selection which is shown in fig. 4.2, this may be due to the transmit beamforming is affected by interference vector. So the more transmit power is used to compensate the channel. Similarly, around 20% times random selection and norm based selection select same cluster where IA is not performed and also select same interference vector of select cluster, which is cancelled by receive beamforming. The delta sum rate represents the difference between sum rate of norm based selection and sum rate of random based selection.

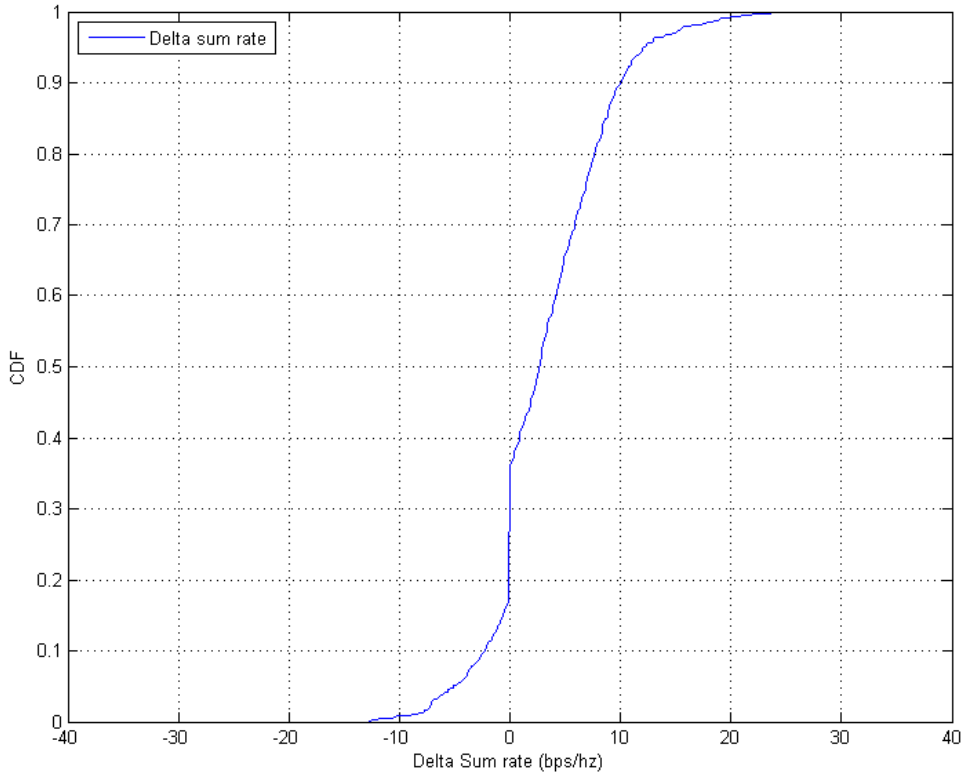

Figure 4.2: CDF of difference between sum rate of norm based selection and sum rate of random based selection (Delta sum rate) when $N_t = 6,\ K = 6,\ N_r = 2$ at 20 dBm, where number of selected users is 3.

Fig. 4.3 shows the comparison of CDF of difference between maximum user rate and minimum user rate of norm base and random based cluster selection. The difference between maximum user rate and minimum user rate of norm base cluster selection is less than random cluster selection. This is because random cluster selection selects a cluster randomly where IA is not performed. The selected cluster may not receive the interference with the smallest power. Due to this reason, the user rate of selected cluster may be less than norm based selection. Similarly, the user rate of remaining two clusters, where IA is performed, for both cluster selections may be different. This is because both schemes may select different cluster,where IA is not performed. Therefore the transmit beamforming for cluster will be different, which will affect the user rate.

4.6 summary

From the simulation result, the sum rate of single cluster is better than cluster selection techniques because inter user interference has been cancelled. We consider a single cell environment. So, no further interference management is necessary. If we consider multi-cell environment, the sum rate of single cluster will be reduced due to inter-cell interference. In multi-cell environment, the user near to the cell edge will receive not only interference from its cell, but also a considerable amount of interference from the other cells. So the propose cluster selection can used to select a cluster near to the cell edge where IA is not performed.

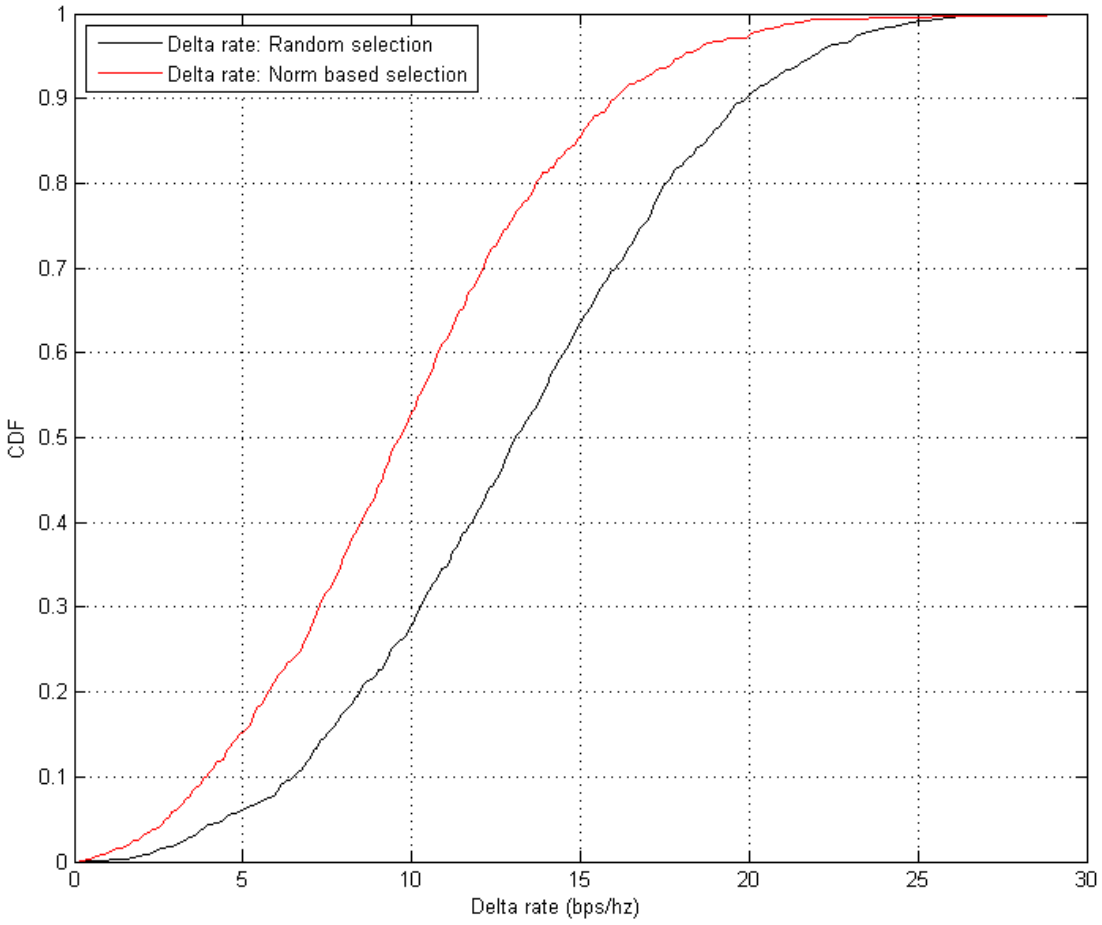

Figure 4.3: Comparison of CDF of difference between maximum user rate and minimum user rate of norm base and random based cluster selection (Delta rate) when $N_t = 6, K = 6$ at 20 dBm, where number of selected users is 3.

Chapter 5

Cooperative transmission over user mobility for MU-DAS

5.1 Introduction

The multi-user system with linear precoding requires accurate CSI to manage the inter-user interference. However, the CSI obtained by the CU may be outdated in practice due to either channel variation in mobility environment and/or the transmission delay between the uplink time slot in which the CSI is estimated and the downlink time slot in which the downlink data transmission takes place. So, the correlation between the actual channel and the estimated channel becomes small. The authors in [64] have been shown that the performance of the precoding system degrades as the channel correlation decreases. The performance of the precoded system finally approaches that of the non-precoding systems, when the channel correlation is beyond the correlation threshold. In [65], the effects of the imperfect CSI on the ergodic capacity performance was studied, and it has been concluded that the performance of the multi-user multiple-input multiple-output (MU-MIMO) system strongly depends on the correlation between the actual channel and the CSI estimated at the transmitter. In [66], the authors have concluded that only low mobility users can be served jointly, where high mobility users adopt single user space time coded transmission.

The low mobility user has small the channel mismatch error because

the channel varies slowly within a feedback interval. On the other hand, the high mobility user may have large channel mismatch due to the fact that the channel significantly varies during the feedback interval. The channel mismatch can be reduced by reducing the feedback interval. By reducing the feedback interval in the TDD system, the number of time slots allocated to the uplink transmission increases at the expense of the reduction of the number of time slots for the downlink transmission.

5.1.1 Contribution

In this thesis, the impact of channel mismatch error produced by the user mobility and the transmission delay in MU-DAS has been investigated, where all the users were classified into multiple groups based on the mobility speed. Within a group, feedback time slot is allocated to reduce the impact of the channel mismatch error.

Similarly, the spectral efficiency of downlink MU-DAS with per-antenna power constraint and per-user SINR constraint is studied by taking into account the different mobility speed ranges. The contributions of this paper are summarized as follows:

1. We propose the CSI feedback interval reduction technique to improve the system throughput. Since the channel mismatch severely degrades the system throughput, the channel mismatch error is introduced in the system model. The channel mismatch error is controlled by adjusting the threshold values. Thus, the estimated channel can remain unchanged, while feedback interval is adjusted.

2. A user grouping technique is proposed which divides the users into multiple groups based on MSI. The MSI of the user can be speed or acceleration information.

3. We consider antenna selection of RAUs and interference power based user clustering. To achieve the maximum sum rate within a mobility group, all the users should be jointly served. However, the sum rate mainly depends on the channel between RAU and user whose

channel gain is high in the DAS systems. The user clustering is carried out within the same mobility group. By this, the original problem can be decomposed into multiple cluster based problems.

4. We propose a cooperative clustering based strategy in order to mitigate the inter-group and inter-cluster interference which limits the average sum rate of the system. Each cluster serves a subset of users of its own mobility group and has a subset of users of the other groups to coordinate the interference.

5. Closed form of an analytical expression of single-user cluster conditioned on the user's location is derived. Simulation results show that the analysis is highly accurate.

5.2 System Model

Consider a single rectangular cell downlink environment which consists of N_t RAUs and K users, as shown in Fig. 5.1. $N_t \geq K$ is assumed. Each user is equipped with a single antenna. The users are randomly and uniformly distributed within the cell. We assume that the CU can perfectly estimate the CSI of all users at the uplink transmit slot and the MSI of the user. Let $\mathcal{K}$ denote the user set, i.e., $\mathcal{K} = \{1, \cdots, K\}$ and $\mathcal{N}$ denote the RAU set, i.e., $\mathcal{N} = \{1, \cdots, N_t\}$. Under these assumptions, the received signal at user k at time t is given by:

$$\begin{aligned} y_k(t) &= \mathbf{h}_k(t)\mathbf{W}(t)\sqrt{\mathbf{P}(t)}\mathbf{s}(t) + n_k(t) \\ &= \mathbf{h}_k(t)\mathbf{w}_k(t)\sqrt{p_k(t)}s_k(t) \\ &+ \mathbf{h}_k(t)\sum_{i\in\mathcal{K}, i\neq k}\mathbf{w}_i(t)\sqrt{p_i(t)}s_i(t) + n_k(t) \end{aligned} \tag{5.1}$$

where $\mathbf{h}_k(t) \in \mathbb{C}^{1\times N_t}$ is a time-varying channel vector, $\mathbf{W} \in \mathbb{C}^{N_t\times K}$ denotes the precoding matrix whose j-th row and k-th column element is $w_{j,k}$, $\mathbf{P} \in \mathbb{R}^{K\times K}$ is a diagonal matrix of power normalization factor of each RAU, $\mathbf{s} \in \mathbb{C}^{K\times 1}$ is a transmit symbol vector whose k-th element denotes a transmit symbol for user k with $\mathbb{E}\{|s_k|^2\} = 1$ and

$n_k \sim \mathcal{CN}(0, \sigma^2)$ is the AWGN. The j-th element of the channel vector $\mathbf{h}_k(t)$ represents the channel from RAU j to user k at time t, i.e, $h_{k,j}(t)$, which consists of path loss and small scale fading and is given by

$$h_{k,j}(t) = l_{k,j}(t) \cdot \tilde{h}_{k,j}(t) \tag{5.2}$$

where $l_{k,j}(t) = d_{k,j}^{-\frac{\alpha}{2}}(t)$ denotes the path loss with path loss exponent α and distance $d_{k,j}(t)$ between user k and RAU j at time t, $\tilde{h}_{k,j}(t)$ is small scale fading from RAU j to user k at time t and is independently and i.i.d. The $\tilde{h}_{k,j}(t)$ is assumed to be Rayleigh distributed and modelled as Jakes fading model [52] where N_0 plain waves arrive at moving user with uniformly distributed arrival angles α_n, such that plain wave n experiences a Doppler shift $\omega_n = \frac{2\pi f_c v}{c} \cos \alpha_n$ where f_c is the carrier frequency, v is the user speed, c is the speed of light. The small scale fading is given by

$$\tilde{h}_{k,j}(t) = \sqrt{\frac{2}{N_0}} \sum_{n=1}^{N_0} \mathbf{A}_j(n)[\cos(\beta_n) + i \sin(\beta_n)] \cos(\omega_n t + \theta_n) \tag{5.3}$$

where $\mathbf{A}_j(n)$ is an orthogonal vector of Walsh-Hadamard codewords to generate multiple uncorrelated waveforms at moving user, $\beta_n = \frac{\pi n}{N_0}$ is a phase and gives zero correlation between the real and imaginary parts of $h_{k,i}(t)$, θ_n is oscillator phase. The arrival angle is given by $\alpha_n = \pi(n - 0.5)/2N_0$.

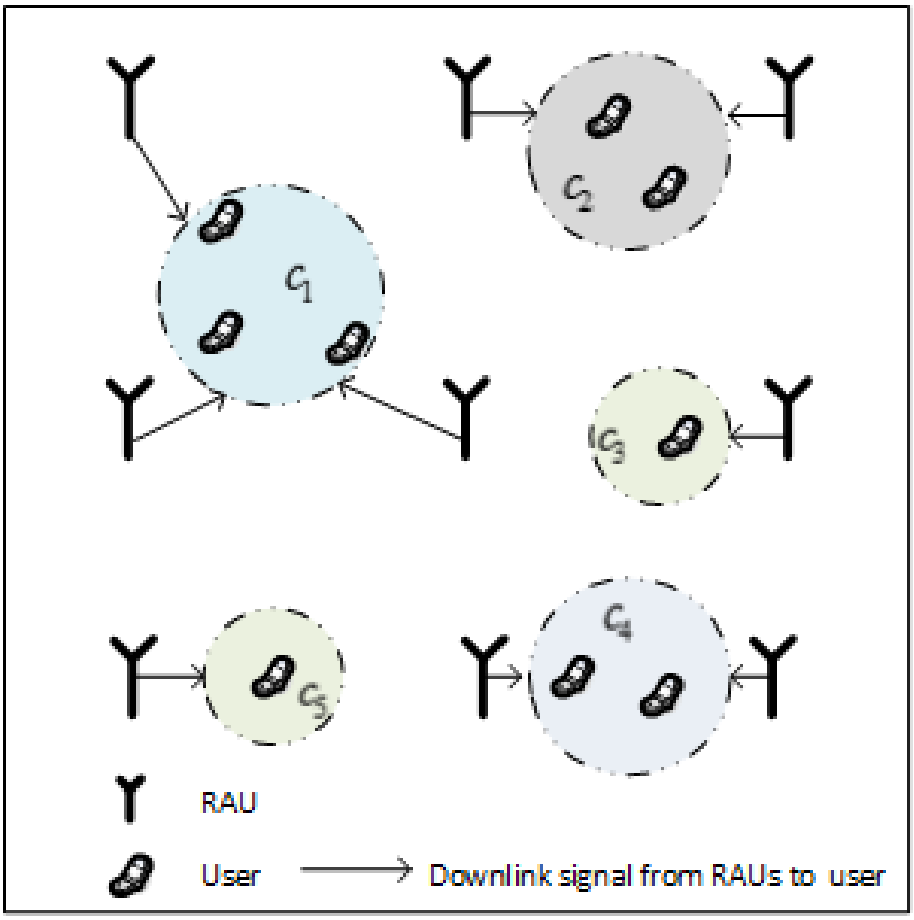

Figure 5.1: DAS architecture in cell.

In the TDD system, the CU estimates the CSI in the uplink time slot and then uses it to derive the precoder matrix for downlink transmission. Let τ denotes the transmission delay between the time slot when the CSI is estimated and the time slot when the estimated CSI is used for downlink precoding. Taking into account the fact that large scale fading changes much slower than the small scale fading, we modify the model in [60, 61] given by

$$\mathbf{h}_k(t) = \rho \mathbf{h}_k(t-\tau) + \sqrt{(1-\rho^2)}\mathbf{e}_k(t) \tag{5.4}$$

where $\mathbf{h}_k(t-\tau) = \mathbf{l}_k(t-\tau) \cdot \tilde{\mathbf{h}}_k(t-\tau)$ is the estimated channel vector, where its element is obtained from (5.3), $\mathbf{e}_k(t) = \mathbf{l}_k(t-\tau) \cdot \tilde{\mathbf{e}}_k(t)$ is the

error in the estimate that is uncorrelated with $\hat{\mathbf{h}}_k$ and ρ is the correlation coefficient between the actual channel gain and its estimate [53], which is given by $\rho = \mathbb{E}[h_{k,j}(t)h_{k,j}^H(t-\tau)]/\sqrt{\mathbb{E}[|h_{k,j}(t)|^2|h_{k,j}(t-\tau)|^2]} = J_0(2\pi f_d \tau)$, where $J_0(\cdot)$ is the zeroth-order Bessel function of the first kind and $f_d = \frac{v}{c} f_c$. The parameter $\rho \in [0,1]$ reflects the accuracy or quality of the channel estimate, i.e., $\rho = 1$ corresponds to perfect CSI, whereas for $\rho = 0$ the CSI is completely uncorrelated with the actual channel.

For a TDD system, the CU designs the precoding matrix based on the estimated channel at time $t-\tau$. In this paper, we adopt ZF precoding which completely eliminates interference, i.e., $\mathbf{h}_k(t-\tau)\mathbf{w}_i(t-\tau) = 0$, $\forall i \in \mathcal{K}\backslash\{k\}$. The precoding matrix $\mathbf{W}$ is the pseudoinverse of $\mathbf{H}$ [49], i.e.,

$$\begin{aligned}\mathbf{W}(t) &= \tilde{\mathbf{W}}(t-\tau) \\ &= \mathbf{H}^H(t-\tau)(\mathbf{H}(t-\tau)\mathbf{H}^H(t-\tau))^{-1}\end{aligned} \tag{5.5}$$

With perfect CSI ($\tau = 0$), $\mathbf{h}_k(t)\mathbf{w}_i(t) = 0$, $\forall i \in \mathcal{K}\backslash\{k\}$, and the symbol of the desired user is perfectly obtained due to the IUI elimination. On the other hand, since the CSI is imperfect for a non-zero delay ($\tau > 0$), there remains the residual interference, i.e., $\mathbf{h}_k(t)\mathbf{w}_i(t) = \sqrt{(1-\rho^2)}\mathbf{e}_k(t)\mathbf{w}_i(t)$. Due to this mismatch, the desired user's symbol is interfered with the other users' symbols due to the presence of residual interference.

The received SINR of user k at time t is given by

$$\gamma_k(t) = \frac{p_k(t)|\mathbf{h}^k(t)\mathbf{w}_k(t)|^2}{\sigma^2 + \sum_{\substack{i\in\mathcal{K} \\ i\neq k}} p_i(t)|\mathbf{h}^k(t)\mathbf{w}_i(t)|^2} \tag{5.6}$$

The achievable user rate (R_k) at time t is

$$\mathrm{R}_k(t) = \log_2(1+\gamma_k(t)),\ \forall k \in \mathcal{K} \tag{5.7}$$

The system sum rate (R) at time t is then obtained as

$$\begin{aligned} R(t) &= \sum_{k\in\mathcal{K}} R_k(t) \\ &= \sum_{k\in\mathcal{K}} \log_2(1+\gamma_k(t)) \end{aligned} \tag{5.8}$$

In DAS, all RAUs are geographically separated and have individual power amplifier and transceiver architectures. So the per antenna power constraint becomes more relevant than the total power constraint. We formulate the sum rate maximization problem at time t as follows:

$$\max_{\{\mathbf{w}_k\}} \sum_{k=1}^{K} \log_2(1+\gamma_k(t)(\mathbf{w}_k)) \tag{5.9a}$$

$$\text{s.t } \max_{j} \sum_{k=1}^{K} \left[\mathbf{w}_k(t) p_k(t) \mathbf{w}_k(t)^H\right]_{j,j} \leq P \tag{5.9b}$$

$$\gamma_k(t)(\mathbf{w}_k) \geq \gamma_0 \ \forall k \tag{5.9c}$$

where $P = \frac{P_t}{N_t}$ is the maximum transmit power of each RAU, P_t is the total transmit power in the cell and γ_0 is target SINR which is common for all users. (5.9b) is a per antenna power constraint and (5.9c) is quality of service (QoS) constraint.

The problem (5.9) may be infeasible as (5.9b) and (5.9c) give the upper and lower bounds of the transmit power respectively. Assigning all RAUs to all the users may increase infeasibility because it increases the dimension of channel matrix. However, it incurs huge computational complexity due to its large dimension of channel matrix. This gives us to select a subset of RAUs for each user. The problem (5.9) is difficult to solve directly due to i) non-convex cost function and constraint and ii) the computational complexity of designing a large precoding matrix. The cost function and constraint can be relaxed to the convex by iterative transmission algorithm [113–115]. However, the result may not reduce the computational complexity of optimization as shown in fig. 3.5. Therefore, we will resort to a sub-optimum approach, which is simple

but effective. One possible approach is to decompose the original problem into multiple sub-problems which carry out a channel-gain-based antenna selection and an interference-based user clustering separately in order to reduce the computational complexity.

As it can be seen from (5.4), the amount of the residual interference highly depends on the user mobility. The impact of residual interference on the system sum rate can be reduced by dividing users into a number of groups based on the mobility speed. Each group consists of a set of users who exhibit similar mobility speeds. Within a mobility group, proposed feedback time slot can be allocated to reduce the impact of the residual interference. For example, the high mobility user group naturally implies to the large amount of the residual interference because the channel significantly varies during the feedback interval. If the system allocates the shorter feedback interval, the accuracy of the channel estimation increases and reduces the residual interference. However, in the DAS, the user experiences different channels from RAUs due to different path loss. This motivates us to consider antenna selection among RAUs and select users by user clustering within the mobility group. This will also reduce the system computational complexity while designing precoding matrix. All clusters are served simultaneously using the same frequency resource and suffer from inter-group-inter-cluster interference. This interference can be minimized by merging the neighbouring group clusters to form cooperative cluster based on the particular needs of a given user. The cooperative cluster consists of subset of users of its own group and has a set of users of the other group to coordinate interference.

5.3 Cooperative Cluster Formation

The cooperative cluster c is formed to serve the set of users $\mathcal{C}_c$ while considering the non-negligible interference. The cooperation cluster formation consists of two phases, namely, antenna selection phase and user clustering phase. In the antenna selection phase, each user is assigned to a subset of the RAUs based on the estimated channel gain. In the

user clustering phase, one or more than one user-RAU pairs are selected to form a cooperative cluster. This clustering is performed based on the cluster SINR threshold (γ_c) so that the inter-cluster interferences are small enough to split the original problem (5.9) into the cluster-based sub-problems. In order to adapt to dynamic nature of the channel, the cooperative cluster formation is carried out once the CSI is obtained at the uplink time slot.

5.3.1 Antenna Selection (AS) Phase

Antenna Selection is a powerful signal processing technique that can reduce the cost and complexity of radio frequency (RF) chains associated with each RAU, but at the same time preserves the diversity and multiplexing gains obtained from the actual system. Also it reduces the signalling burden overhead at the CU.

Antenna selection is carried out at the CU based on the estimated channel. At the uplink transmit slot, the CU estimates CSI for all users from all RAUs. Multiple RAUs are assigned to a user in an iterative fashion. Let N_k be a predetermined number of RAUs that are supposed to be assigned to user k. The user k^* and RAU j^* are selected as follows

$$(k^*, j^*) = \underset{j \in \mathcal{N},\ k \in \mathcal{K}}{\arg\max} |h_{k,j}(t-\tau)|^2 \tag{5.10}$$

Then, RAU j^* is removed from RAU set. This procedure is repeated until all users are assigned to the RAUs as shown in Fig 5.2. The channel gain based AS is summarized in Algorithm 2.

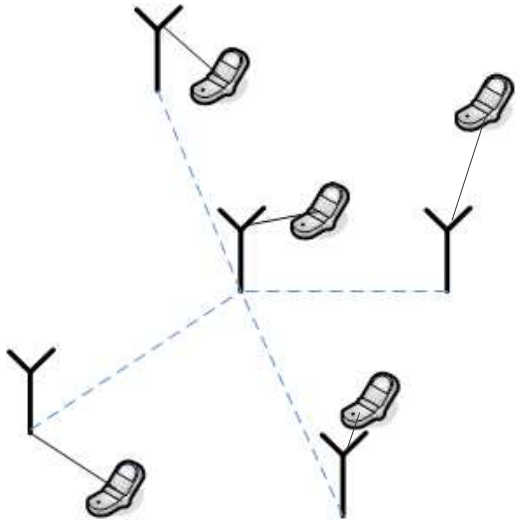

Figure 5.2: Illustration of antenna selection where user is assigned to RAU based on channel gain.

Algorithm 2 AS algorithm

Initialize $\mathcal{K} = \{1, \cdots, k, \cdots, K\}$ and $\mathcal{N} = \{1, \cdots, j, \cdots, N_t\}$, $\mathcal{N}_k = \emptyset$.
while $\mathcal{K} \neq \emptyset$ **do**
  Select the pair of user k^* and RAU j^* as $(k^*, j^*) = \arg\max_{j \in \mathcal{N},\ k \in \mathcal{K}} |h_{k,j}(t-\tau)|^2$.
  Update $\mathcal{N}_k \leftarrow \mathcal{N}_k \cup j^*$ and $\mathcal{N} \leftarrow \mathcal{N} \backslash j^*$.
  if $|\mathcal{N}_k| = N_k$ **then**
    Update $\mathcal{K} \leftarrow \mathcal{K} \backslash k^*$.
  end
end

5.3.2 User Clustering (UC) Phase

Different users may move at different speed. It is assumed the MSI is perfectly known at the CU. When a user moves or the transmission delay increases, the correlation between actual channel and estimated channel becomes small and degrades the performance. It can be seen from (5.4), the amount of the residual interference highly depends on the correlation of the channel. Therefore, the residual interference decreases as the correlation of the channel increases. Based on the autocorrelation

of channel, the users are classified into groups as follows:

$$\begin{aligned} 0 \leq \text{speed} \leq v_1 &\qquad \text{Low mobility} \\ v_1 < \text{speed} \leq v_2 &\qquad \text{Medium mobility} \\ v_2 < \text{speed} \leq v_3 &\qquad \text{High mobility} \end{aligned} \tag{5.11}$$

where v_1, v_2 and v_3 are the speeds of users and are determined based on the autocorrelation of channel.

After the antenna selection phase, each group selects the first user k (target user) and its associated RAU which has the highest channel gain. The next user i is selected from the remaining unselected pairs and compute a minimum SINR. The SINR is calculated under the assumption of maximum power transmission and maximum ratio combining [78] and given as:

$$\gamma_{k,i} = \min \left\{ \frac{\sum_{j \in \mathcal{N}_k} |h_{k,j}|^2 P}{\sigma^2 + \sum_{j' \in \mathcal{N}_i} |h_{kj'}|^2 P}, \frac{\sum_{j' \in \mathcal{N}_i} |h_{ij'}|^2 P}{\sigma^2 + \sum_{j \in \mathcal{N}_k} |h_{ij}|^2 P} \right\} \tag{5.12}$$

where $\mathcal{N}_k$ is a set of RAUs to serve user k.

If two users are located close to each other, the corresponding SINR becomes low due to the strong IUI as shown in Fig. 5.3. Then these neighbouring users are merged and form a cluster as shown in Fig. 5.4. Let $\mathcal{C}_c$ denotes the set of users in the c-th cluster and $\mathcal{C}_c \cap \mathcal{C}_{c'} = \emptyset$, where $c \neq c^{'}$. With minimum SINR γ_c, the selected user i will be incorporated into cluster c if their SINR is lower than or equal to γ_c as follows

$$\mathcal{C}_c = \mathcal{C}_c \cup i, \text{ if } D(\mathcal{C}_c, i) \leq \gamma_c \tag{5.13}$$

where the distance metric between two clusters is defined as

$$D(\mathcal{C}_c, \mathcal{C}_{c'}) = \min_{k \in \mathcal{C}_c, i \in \mathcal{C}_{c'}} \gamma_{k,i} \tag{5.14}$$

This process is repeated until all the users are assigned to one of the clusters. The proposed user clustering (UC) algorithm is summarized in Algorithm 3.

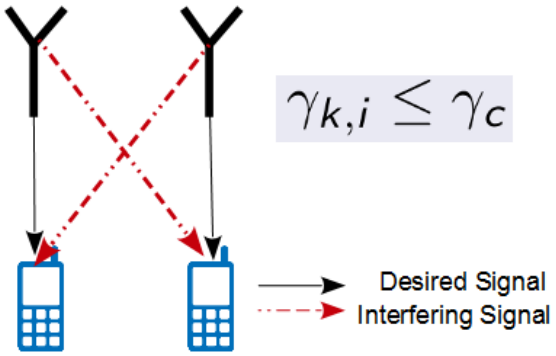

Figure 5.3: An example that strong cross link causes large interference.

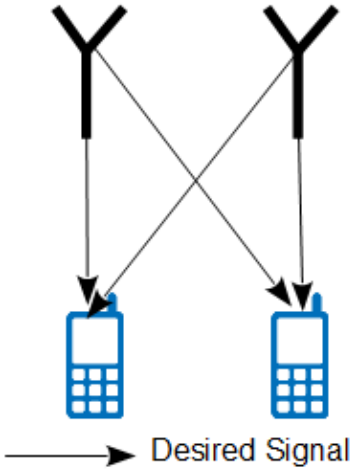

Figure 5.4: An example of user clustering where strong cross link provide cooperative gain.

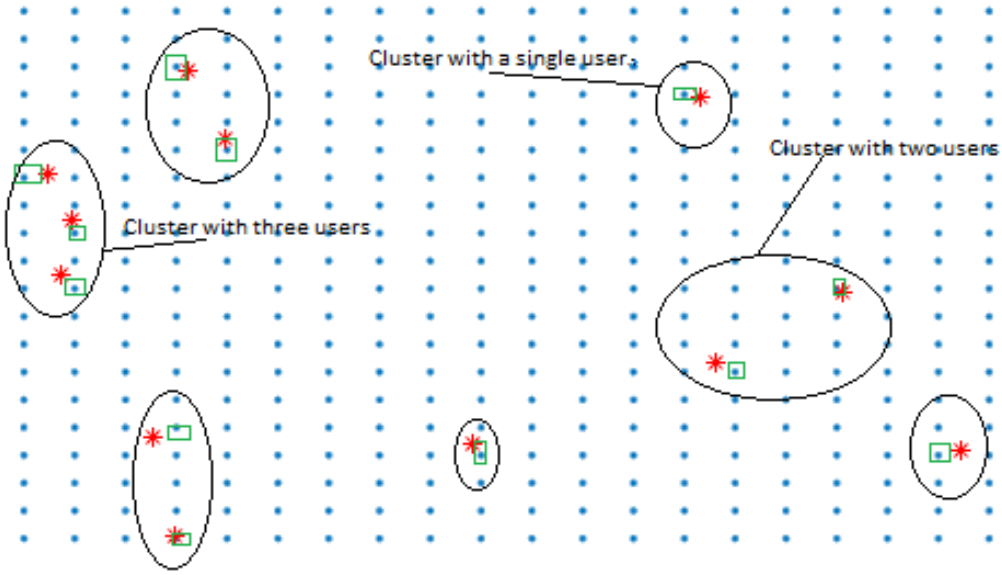

Figure 5.5: Illustration of cooperative clustering for 12 users and 400 RAUs where clustering threshold is 20dB.

Algorithm 3 UC algorithm

Initialize distance $d_c = 0$, cluster $\mathcal{C}_c = \{c\}$ where $c \in \mathcal{C}$ and given γ_c.
while $d_c \leq \gamma_c$ **do**
  find the distance of closest pair of cluster $\mathcal{C}_c$ and $\mathcal{C}_{c'}$, i.e., $d_c = \min_{k,i \in \mathcal{K},\ k \neq i} D(\mathcal{C}_c, \mathcal{C}_{c'})$.
  if $d_c < \gamma_c$ **then**
    merge cluster $\mathcal{C}_c \leftarrow \mathcal{C}_c \cup i$
  end
end

The performance of the system is severely degraded by inter-group-inter-cluster interference, which is uncoordinated. In the uncoordinated case, if the SINR of two interfering users of the neighbouring clusters are smaller than the cluster SINR threshold, the neighbouring clusters are merged into a cooperative cluster, as shown as Fig. 5.5.

5.3.3 Cluster based Sub-problem Formulation

Let $\mathcal{C}_c$ be the set of users in the cluster c, $\mathcal{N}_c$ be a subset of RAUs which serves $\mathcal{C}_c$. The received signal $y_{k,c}(t)$ at user k of cluster c at time t is

expressed as

$$\begin{aligned} y_{k,c}(t) &= \mathbf{h}_{c,c}^{k}(t)\mathbf{w}_{k,c}(t)\sqrt{p_c(t)}s_k(t) \\ &+ \mathbf{h}_{c,c}^{k}(t)\sum_{i\in\mathcal{C}_c, i\neq k}\mathbf{w}_{i,c}(t)\sqrt{p_c(t)}s_i(t) \\ &+ \sum_{j\in\mathcal{C}, j\neq c}\mathbf{h}_{c,j}^{k}(t)\mathbf{W}_j(t)\sqrt{\mathbf{P}_j(t)}\mathbf{s}_j(t) + n_c^k(t) \end{aligned} \tag{5.15}$$

where $\mathbf{h}_{c,c}^{k} \in \mathbb{C}^{1\times|\mathcal{N}_c|}$ is a channel vector from RAUs of cluster c to user k in the cluster c, $\mathbf{W}_j \in \mathbb{C}^{|\mathcal{N}_j|\times|\mathcal{C}_j|}$ denotes the precoding matrix for cluster j, $\mathbf{h}_{c,j}^{k}$ is interfering channel vector from RAUs of cluster j to user k of cluster c. $\mathbf{P}_j \in \mathbb{R}^{|\mathcal{C}_j|\times|\mathcal{C}_j|}$ is a diagonal matrix of power normalization factor of each RAU of cluster j. Same power normalization factor p for every RAU lies in the same cluster.

The achievable rate for user k of cluster c at time t is

$$R_{k,c}(t) = \log_2(1+\gamma_{k,c}(t)) \tag{5.16}$$

where

$$\gamma_{k,c}(t) = \frac{p_c(t)|\mathbf{h}_{c,c}^{k}(t)\mathbf{w}_{k,c}(t)|^2}{\sigma^2 + \mathrm{I}_{\text{intra}} + \mathrm{I}_{\text{inter}}} \tag{5.17}$$

where $\mathrm{I}_{\text{intra}} = \sum_{i\neq k} p_c(t)|\mathbf{h}_{c,c}^{k}(t)\mathbf{w}_{i,c}(t)|^2$
and $\mathrm{I}_{\text{inter}} = \sum_{j\in\mathcal{C}, j\neq c}|\mathbf{h}_{c,j}^{k}(t)\mathbf{W}_j(t)\sqrt{\mathbf{P}_j(t)}|^2$.

In order to maximize the sum rate, we consider the cooperative clustering. Using antenna selection and user clustering, we split the original problem (5.9) into sub-problem formulation that maximizes the sum rate of cluster c at time t

$$\max_{\{\mathbf{w}_{k,c}\}} \sum_{k\in\mathcal{C}_c} \log_2\left(1+\gamma_{k,c}\left(\mathbf{w}_{k,c}\right)\right) \tag{5.18a}$$

$$\text{s.t } \max_{j} \sum_{k\in\mathcal{C}_c} \left[\mathbf{w}_{k,c}p_c\mathbf{w}_{k,c}^{H}\right]_{j,j} \leq P \tag{5.18b}$$

$$\gamma_k\left(\mathbf{w}_{k,c}\right) \geq \gamma_0 \ \forall k \tag{5.18c}$$

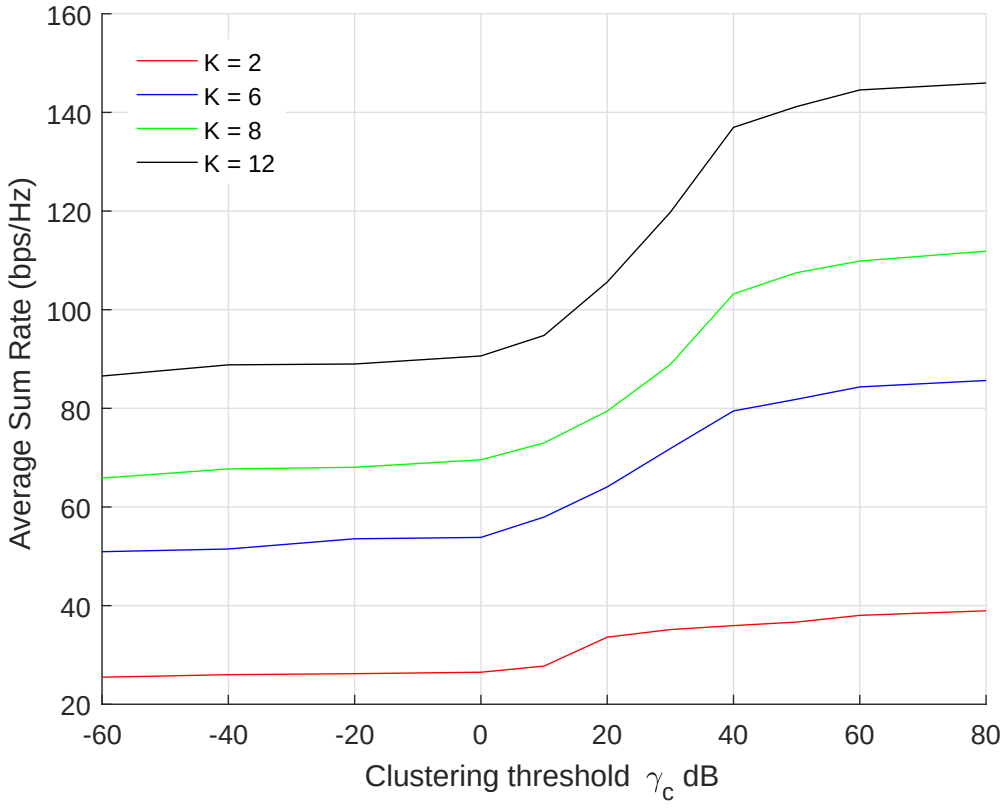

Figure 5.6: Illustration of Average sum rate of different users mobility with various clustering threshold where $N_t = 400$ and user target SINR is 50 dB at feedback time slot.

To satisfy QoS constraint (5.18c), an iterative antenna selection algorithm. In the iterative antenna selection algorithm is proposed, a RAU is assigned to those users of the cluster whose SINR is less than target SINR, i.e., $\gamma_k < \gamma_0$. The iterative process is repeated until all the users of the cluster satisfy the QoS constraint. The number of users within a cluster depends on the clustering threshold. If the cluster SINR threshold is small, then the system forms single-user clusters with high probability. For the single-user cluster, a pair of user and RAUs is selected which has the highest channel gain. If the cluster SINR threshold is high, the system forms one cluster with high probability. In the one cluster, all users are jointly served using MU-MIMO precoding. Fig. 5.6

illustrates the average sum rate as a function of clustering threshold γ_c, where $N_t = 400$ and $\gamma_o = 50$ dB. The performance of proposed cooperative clustering is evaluated through simulations. The user speed is randomly determined within the range of 0 to 15 m/s. The user is initially distributed randomly and uniformly within a cell. For a low clustering threshold $\gamma_c = -60$ dB, all the clusters become single user clusters with high probability. The single-user cluster consists of one pair of user and its associated RAU. For the single-user cluster, the RAU always transmits the signal with maximum power of RAU due to per antenna power constraint. The SINR is mainly affected by inter-cluster interference which limits the system sum rate. The feedback time slot of a cluster is allocated based on the user's speed. When the clustering threshold increases, multi-user clusters are formed, where multiple users are jointly served by multiple RAUs. As the clustering threshold increases, cluster size increases and the number of clusters decreases to one. The SINR value is close to the signal to noise plus residual interference ratio due to the reduced inter-cluster interference. The processing complexity also increases with an enlarged clustering size as shown in Fig. 5.5. At the high clustering threshold regime with $\gamma_c = 80$ dB, the system forms one cluster with high probability. The feedback time slot of the cluster is allocated based on the fastest mobility user, to minimize the mismatch error. The SINR is close to SNR due to the elimination of inter-cluster interference. By increasing the clustering threshold, sum rate can be improved while the computational complexity also increases.

5.3.3.1 Optimal User Clustering

The main contribution of this thesis is to maximize the sum rate by designing the precoding. For example, The cellular network consists of three RAUs ($N_t = 3$) and three users ($K = 3$). Each user has one antenna ($N_r = 1$). Let user set be denoted by $\mathcal{K}$ where $\mathcal{K} = \{1, 2, 3\}$ and RAU set be denoted by $\mathcal{N}$ where $\mathcal{N} = \{1, 2, 3\}$. If the result of

optimization is

$$\mathbf{w}_1 = [w_1 10 w_1 3]^T$$
$$\mathbf{w}_2 = [w_2 10 w_2 3]^T$$
$$\mathbf{w}_2 = [0 w_3 20]^T$$

The users $\mathcal{K}_1 = \{1, 2\}$ and RAUs $\mathcal{N}_1 = \{1, 2\}$ form a cluster because the transmit precoding for users $\mathcal{K}_1 = \{1, 2\}$ is formed with RAUs $\mathcal{N}_1 = \{1, 2\}$. And user $\mathcal{K}_2 = \{3\}$ and RAU $\mathcal{N}_2 = \{3\}$ form another cluster. However, this result may not happen in terms of optimization. The optimal solution of (5.9) is to form one cluster where all users are jointly served by multiple RAUs by using MU-MIMO precoding. If the result of optimization forms one cluster, the entire basic cluster will be selected. The overall sum rate will be high. If users K and RUAs N_t increase, the computational complexity also increases as shown in fig. 3.5. In this section, we proposed antenna selection and user clustering algorithms whose performance is very close to the exhaustive search method with much lower complexity. For optimal user clustering, the exhaustive search algorithm is used to maximize the sum rate by searching over all possible antenna combinations. Fig. 5.7 illustrates the sum rate as a function of number of RAUs N_t, where $K = 4$ and $v = 0$ m/s. To compare the proposed clustering algorithm with exhaustive search, we consider user mobility as zero and the total RAUs is also reduced. In one cluster, all users are jointly served by selected RAUs, where intra-cluster interference is cancelled by ZF precoding. The system performance is only limited by noise. Therefore, the performance of proposed clustering algorithm is same as exhaustive search. To form multi-user clusters, the clustering threshold is considered as $\gamma_c = 15 and 20$ dB. As the clustering threshold increases, cluster size increases but the number of clusters decreases. The inter-cluster interference also reduces as the clustering threshold increases. The processing complexity also increases with an enlarged clustering size. Therefore, by increasing clustering threshold, the system performance is improved at the increasing price of complexity.

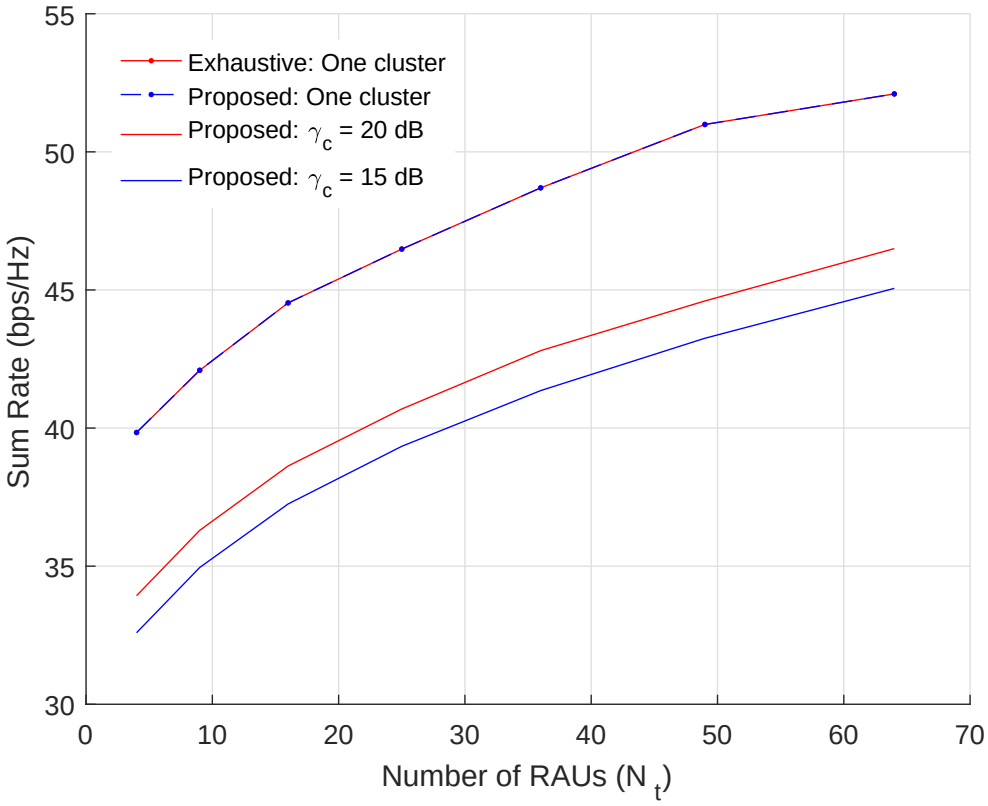

Figure 5.7: Comparison of sum rate of exhaustive search and proposed algrothim where $v = 0$ m/s and $K = 4$.

5.4 Feedback Interval Allocation

This section describes a uplink time slot allocation in order to balance the channel mismatch and the reduction of the number of downlink time slots. The feedback model and the frame structure of the TDD system was shown in Fig. 2.6. The channel remains constant during a time slot with length T_c. For simplicity, we assume there are N time slots in a time frame, i.e., $T = NT_c$ and the first time slot is always used for uplink channel estimation.

When the mobility speed increases or the transmission delay increases, the channel mismatch occurs which severely degrades the performance.

This motivates us to derive the feedback interval of the mobility user based on the autocorrelation of the channel coefficient. The autocorrelation, $R(\tau)$, of the channel is equal to the zeroth order Bessel function of the first kind, $J_0(.)$, which is given by

$$R(\tau) = J_0(2\pi f_d \tau) \tag{5.19}$$

where f_d is the maximum Doppler shift and τ is a transmission delay, i.e., $\tau = nT_c$, $n = \{1, \cdots, N\}$. As mentioned above, a long feedback interval limits the system performance. In order to overcome the problem, we introduce a minimum autocorrelation coefficient ρ_o. When the Doppler shift becomes larger as the user speed increases, the autocorrelation becomes smaller and finally smaller than the minimum autocorrelation value, i.e., $R(\tau) < \rho_o$. The next downlink time slot becomes uplink time slot to update the CSI, which increases the autocorrelation of the channel coefficient. The feedback interval T_f of a user becomes

$$T_f = (n-1)T_c, \text{ where } n = \{1, \cdots, N\} \tag{5.20}$$

Let N_u and N_d be number of uplink/feedback time slots and number of downlink time slots respectively, which are given by

$$N_u = \left\lceil \frac{NT_c}{T_f} \right\rceil \text{ and } N_d = N - N_u \tag{5.21}$$

Let T_u be uplink/feedback time slot of time frame T and given by

$$T_u = \left\lfloor 1 + (m-1)\frac{N}{N_u} \right\rfloor, \text{ where } m = \{1, \cdots, N_u\} \tag{5.22}$$

In the cooperative clustering, each cluster may have user with different range of mobility. Therefore, the feedback time slot of the cooperative cluster is allocated based on the fastest mobility user in order to minimize the mismatch error of the high mobility user.

Setting the minimum autocorrelation coefficient $\rho_o = 0.8$, the number of feedback time slots N_u and the number of downlink time slots N_d is calculated based on (5.21). Fig. 5.9 illustrates the feedback interval of different mobility users as a function of transmission delay. The

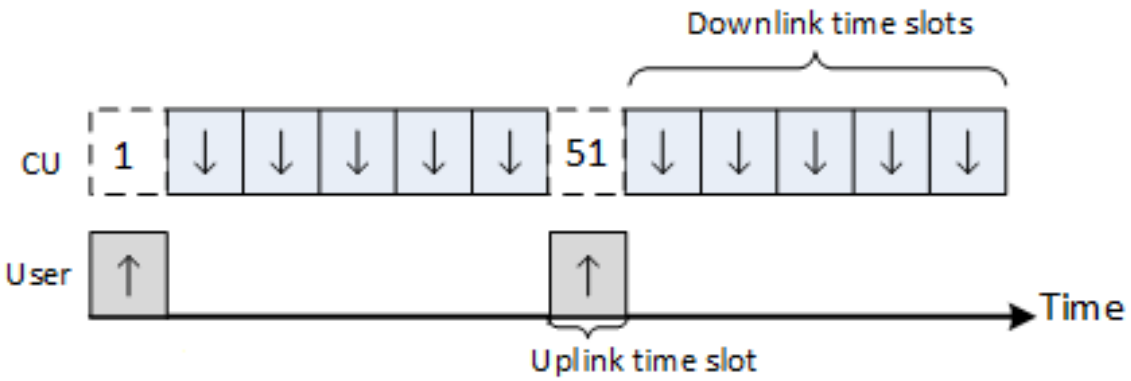

Figure 5.8: Illustration of feedback interval with user speed between 2 to 4 m/s where radio frame duration is 10 ms.

autocorrelation $R(\tau)$ of user with speed slower than 2 m/s is always higher than ρ_o. As the speed or the transmission delay increases, the autocorrelation $R(\tau)$ becomes lower than ρ_o, which results in the performance degradation. Thus, the system is required to update CSI by reducing the feedback interval, which is done by allocating the next time slot as uplink time slot when $R(\tau) < \rho_0$. For example, when the user speed is 4 m/s, the autocorrelation coefficient $R(\tau)$ becomes lower than the minimum autocorrelation coefficient ρ_o at $\tau = 5.0$ ms. Thus, the number of feedback interval becomes two, i.e., $N = 2$. The CSI and cooperative clustering are updated at $n = 1$ and $n = 51$ time slots as shown in Fig. 5.8. Therefore, when user speed increases, the number of uplink time slots increases and the feedback interval becomes smaller. Table 5.1 summarizes the uplink/feedback and downlink parameters for performance evaluation when $\rho_o = 0.8$.

In this thesis, recognizing the fact of centralized signal processing CU in DAS, we propose different feedback time slot in TDD transmission scheme. In the proposed system, a different transmission direction is assigned to different cooperative cluster. As shown in Fig. 5.10, RAU of each user communicates in downlink (uplink) and uplink (downlink) during the n $(n + 1)$ time slot. In the time slot n, there is a huge interference from RAU1 of UE1 to RAU2 of UE2, i.e., downlink-to-uplink

Table 5.1: Feedback parameters: $\rho_o = 0.8$

Speed (v m/s)	N_u	N_d	T_u
0 - 2	1	99	1^{st}
2 - 4	2	98	$1^{st}, 51^{st}$
4 - 6	3	97	$1^{st}, 35^{th}, 69^{th}$
6 - 9	4	96	$1^{st}, 26^{th}, 51^{st}, 76^{th}$
9 - 11	5	95	$1^{st}, 21^{st}, 41^{st}, 61^{st}, 81^{st}$
11 - 13	6	94	$1^{st}, 18^{th}, 35^{th}, 52^{th}, 69^{th}, 86^{th}$
13 - 15	7	93	$1^{st}, 16^{th}, 31^{st}, 46^{th}, 76^{th}, 91^{st}$

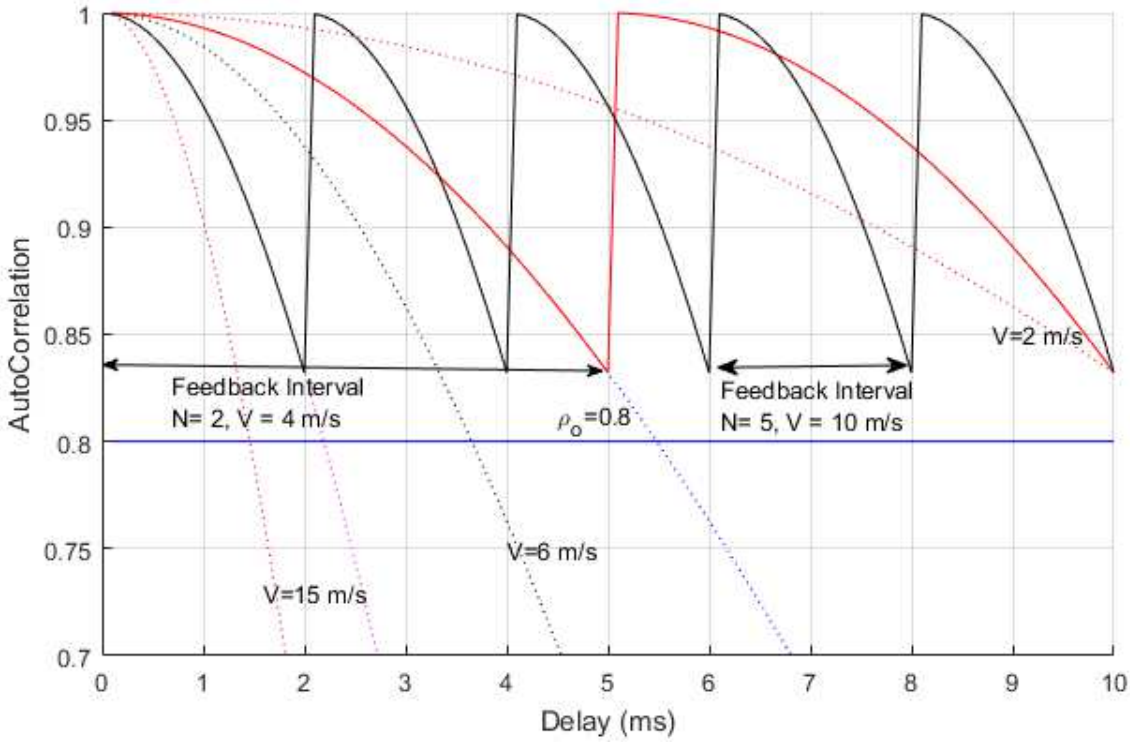

Figure 5.9: Illustration of feedback interval of different mobility users where minimum autocorrelation coefficient is 0.8.

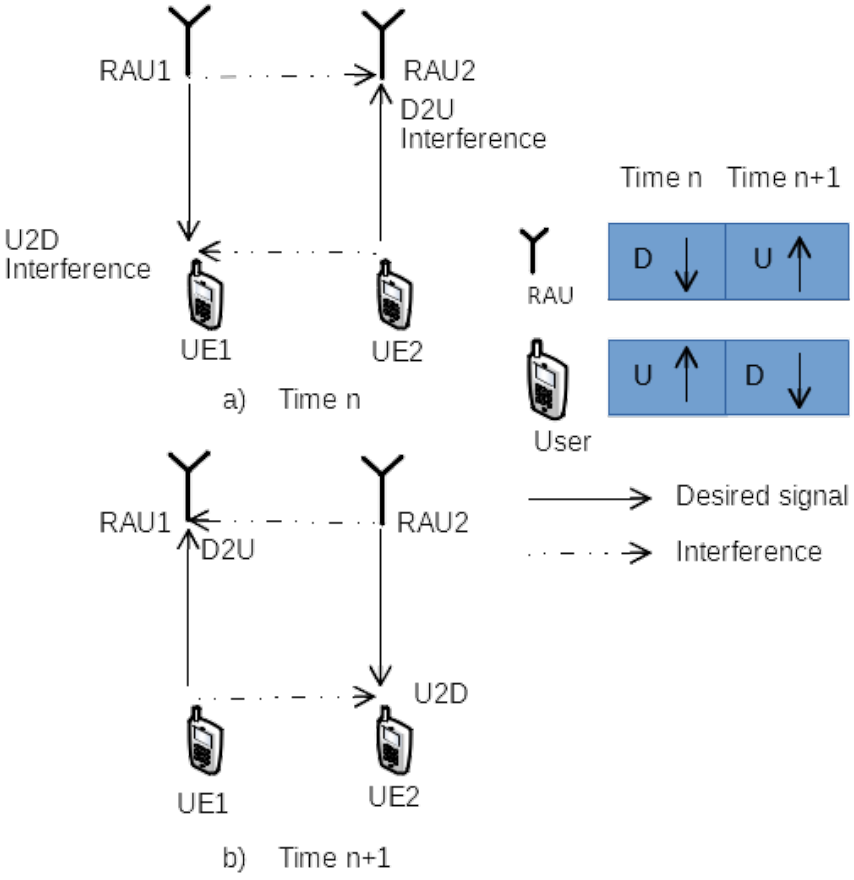

Figure 5.10: Illustration of time slot allocation.

(D2U) interference. However, the interference is perfectly known at CU so perfect interference cancellation is achievable. At the same time, there is an interference from the UE2 connected to RAU2 to the UE1 receiving signal from RAU1, i.e., uplink-to-downlink (U2D) interference. The U2D interference at UE1 may be insignificant due to low transmit power of user and high path attenuation between users [116]. In the time slot $n + 1$, the opposite case happens.

5.5 Downlink Rate Analysis

The ergodic sum rate R can be expressed as

$$R = \sum_{c=1}^{C} \sum_{k \in \mathcal{C}_c} \mathbb{E}[R_{k,c}] \tag{5.23}$$

The achievable ergodic rate of user k of the cluster c at time t can be written as

$$R_{k,c} = \mathbb{E}\left[\log_2\left(1 + \frac{p_k(t)|\mathbf{h}_{c,c}^k(t)\mathbf{w}_{k,c}(t)|^2}{\sigma^2 + \mathrm{I}_{\text{intra}} + \mathrm{I}_{\text{inter}}}\right)\right] \tag{5.24}$$

where $\mathrm{I}_{\text{intra}} = \sum_{i \neq k} p_i(t)[|\mathbf{h}_{c,c}^k(t)\mathbf{w}_{i,c}(t)|^2]$ and $\mathrm{I}_{\text{inter}} = \sum_{j \in \mathcal{C}, j \neq c}[|\mathbf{h}_{c,j}^k(t)\mathbf{W}_j(t)|^2 \mathbf{P}_j(t)]$. To achieve zero interference among users of cluster c, the precoding matrix $\mathbf{W}_c$ is chosen such that all off-diagonal elements of $\mathbf{H}_c\mathbf{W}_c$ are zero. In this thesis, we maximize the average sum rate of multiuser downlink systems which employ ZF under per-antenna power constraint. The power normalization factor p_c is given as

$$\begin{aligned} p_c(t) &= \frac{P}{\max\limits_j \left[\mathbf{W}_c(t)\mathbf{W}_c^H(t)\right]_{j,j}} \\ &= \frac{P}{\max\limits_j \left[\mathbf{H}_c^H(t-\tau)(\mathbf{H}_c(t-\tau)\mathbf{H}_c^H(t-\tau))^{-2}\mathbf{H}_c(t-\tau)\right]_{j,j}} \end{aligned} \tag{5.25}$$

It can be seen (5.25) that in order to obtain the distribution of $p_c(t)$, we need to find the joint distribution of diagonal elements of $\mathbf{H}_c^H(t-\tau)(\mathbf{H}_c(t-\tau)\mathbf{H}_c^H(t-\tau))^{-2}\mathbf{H}_c(t-\tau)$. However, this matrix has composite path loss of all users of cluster c, i.e., $\mathbf{H}_c = \mathbf{L}_c\tilde{\mathbf{H}}_c$. Thus, it is very difficult to compute its distribution due to the lack of the joint distribution of diagonal elements of a pseudo inverse matrix [117, 118].

We aim to analyse the average user rate performance of special case, i.e., single user clustering, where each user is served by its associated RAU $N_k = 1$, which is independent of the other clustering, as shown in

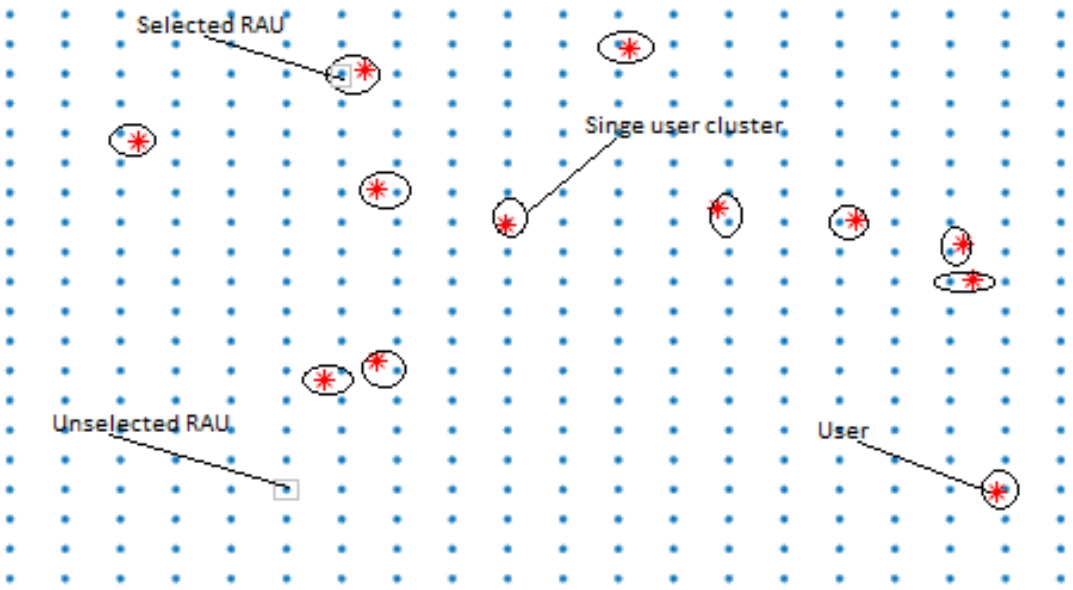

Figure 5.11: Illustration of single user clustering for 12 users and 400 RAUs.

Fig. 5.11. We consider the pdf of SINR to derive the closed form of the ergodic sum rate. In single user clustering, a pair of user and RAU is selected which has the strongest channel gain, where the total number of clusters is equal to the total number of users, i.e., $|\mathcal{K}| = C$. For user $k \in \mathcal{K}$, ZF precoding is calculated at time $t - \tau$ and given by

$$w_k(t) = h_{k,k}^H(t-\tau)(h_{k,k}(t-\tau)h_{k,k}^H(t-\tau))^{-1} \tag{5.26}$$

The power normalization factor at time $t - \tau$ is given by

$$\begin{aligned} p_k(t) &= P\frac{1}{w_k(t)w_k^H(t)} \\ &= P||h_{k,k}(t)||^2 \end{aligned} \tag{5.27}$$

The achievable ergodic rate of user k can be written as

$$R_k = \mathbb{E}\left[\log_2\left(1 + \frac{p_k(t)|h_{k,k}(t)w_k(t)|^2}{\sigma^2 + \mathrm{I}_{\text{inter}}}\right)\right] \tag{5.28}$$

where $\mathrm{I}_{\text{inter}} = \sum_{j\neq k} p_j(t)[|h_{k,j}(t)w_j(t)|^2]$ is the inter-cluster interference.

The received desired signal gain is given by

$$\begin{aligned}\gamma_{k,D} &= |h_{k,k}(t)w_k(t)\sqrt{p_k(t)}|^2 \\ &= P|(h^k_{k,k}(t-\tau) + e_k(t))w_k(t)|^2 \\ &\overset{(a)}{\approx} P\left(|h_{k,k}(t-\tau)|^2 + |e_k(t)\frac{w_k(t)}{||w_k(t)||}|^2\right) \\ &\approx a_{kk1}y_{kD1} + a_{kk2}y_{kD2} \end{aligned} \tag{5.29}$$

where $a_{kk1} = Pl_{k,k}\rho^2$, $y_{kD1} = |\tilde{h}_{k,k}(t-\tau)|^2$, $a_{kk2} = Pl_{k,k}(1-\rho^2)$, $y_{kD2} = |\tilde{e}_{k,k}(t)|^2$. Step (a) is obtained by neglecting the term containing both $h_{k,k}(t-\tau)$ and $e_k(t)$ [62].

We assume that $\tilde{h}_{k,j}$ is a Rayleigh fading channel modelled as i.i.d complex Gaussian with unit variance. Therefore, $|\tilde{h}_{k,j}|^2$ follows a chi-squared distribution with degree of freedom of 2.

Since $|\tilde{h}_{k,j}|^2$ follows the Chi-squared distribution, its pdf is given by [56]

$$f_{|\tilde{h}_{k,j}|^2}(x) = e^{-x}, x > 0 \tag{5.30}$$

As $\gamma_{k,D} = a_{kk1}y_{kD1} + a_{kk2}y_{kD2}$ follow the weighted Chi-squared distribution. The pdf of the $\gamma_{k,D}$ is

$$f_{\gamma_{k,D}}(\gamma) \approx \frac{1}{a_{kk1} - a_{kk2}}(e^{-\frac{\gamma}{a_{kk1}}} - e^{-\frac{\gamma}{a_{kk2}}}), \gamma > 0 \tag{5.31}$$

Appendix 6.2 shows the detailed derivation.

The interference plus noise is given by

$$\begin{aligned}\gamma_{k,I} &= \sigma^2 + \sum_{j\neq k} |h_{k,j}(t)w_j(t)\sqrt{p_j(t)}|^2 \\ &= \sigma^2 + P\sum_{j\neq k}\left|h_{k,j}(t)\frac{w_j(t)}{||w_j(t)||}\right|^2 \\ &= \sigma^2 + \sum_{j\neq k}\left(a_{kj}|\tilde{h}_{k,j}(t-\tau)|^2\right) \end{aligned} \tag{5.32}$$

where $a_{kj} = Pl_{k,j}$. The pdf of interference from RAU of user j to user k $a_{kj}|\tilde{h}_{k,j}|^2$ is given by

$$f_{\gamma_{k,j}}(\gamma) = \frac{1}{a_{kj}}(e^{-\frac{\gamma}{a_{kj}}}), \gamma > 0 \tag{5.33}$$

The moment generating function (MGF) associated with $\gamma_{k,j}$ is given by

$$\begin{aligned} M_{\gamma_{k,j}}(s) &= \int_0^\infty f_{\gamma_{k,j}}(\gamma) e^{s\gamma} d\gamma \\ &= \frac{1}{a_{kj}} \int_0^\infty \left(e^{-\frac{\gamma}{a_{kj}}}\right) e^{s\gamma} d\gamma \\ &= \frac{1}{(1 - a_{kj}s)} \end{aligned} \tag{5.34}$$

The MGF of interference of the k-th user $\sum_{j \neq k} \left(a_{kj}|\tilde{h}_{k,j}|^2\right)$ is given by

$$\begin{aligned} M_{\gamma_{k,I}}(s) &= \prod_{j \neq k} M_{\gamma_{k,j}}(s) \\ &= \prod_{j \neq k} \frac{1}{(1 - a_{kj}s)} \end{aligned} \tag{5.35}$$

The pdf of inter-cluster interference $f_{\gamma_{k,I}}(\gamma)$ is obtained by inverse Laplace transforming its MGF $M_{\gamma_{k,I}}(s)$ [119]. The pdf of the inter-cluster interference is

$$f_{\gamma_{k,I}}(\gamma) = \sum_{j \neq k} A_j \frac{1}{a_{kj}} e^{-\frac{\gamma}{a_{kj}}} \tag{5.36}$$

Appendix 6.2 shows the detailed derivation.

The pdf of noise plus interference of user k at time t $\gamma_{k,I}$ is

$$f_{k,NI}(\gamma) = \sum_{j \neq k} A_j \frac{1}{a_{kj}} e^{-\frac{\gamma - \sigma^2}{a_{kj}}} \tag{5.37}$$

Applying the Jacobian transformation to obtain pdf of signal to noise and interference ratio (γ_k) of user k at time t is given by

$$\begin{aligned}
f_{\gamma_k}(\gamma) &= \int_{\sigma^2}^{\infty} f_{\gamma_{k,D}}(\gamma\theta) f_{\gamma_{k,I}}(\theta)\theta d\theta \\
&\approx \int_{\sigma^2}^{\infty} \frac{1}{a_{kk1}-a_{kk2}} \left(e^{-\frac{\gamma\theta}{a_{kk1}}} - e^{-\frac{\gamma\theta}{a_{kk2}}}\right) \left(\sum_{j\neq k} \frac{A_j}{a_{kj}} e^{-\frac{\theta-\sigma^2}{a_{kj}}}\right) \theta d\theta \\
&= \sum_{j\neq k} \frac{A_j}{(a_{kk1}-a_{kk2})a_{kj}} e^{\frac{\sigma^2}{a_{kj}}} \int_{\sigma^2}^{\infty} e^{-\left(\frac{\gamma a_{kj}+a_{kk1}}{a_{kk1}a_{kj}}\right)\theta} \theta d\theta - \\
&\sum_{j\neq k} \frac{A_j}{(a_{kk1}-a_{kk2})a_{kj}} e^{\frac{\sigma^2}{a_{kj}}} \int_{\sigma^2}^{\infty} e^{-\left(\frac{\gamma a_{kj}+a_{kk2}}{a_{kk2}a_{kj}}\right)\theta} \theta d\theta \\
&= \sum_{j\neq k} \frac{A_j a_{kk1}}{(a_{kk1}-a_{kk2})} \frac{\sigma^2(a_{kk1}+\gamma a_{kj})+a_{kk1}a_{kj}}{(a_{kk1}+\gamma a_{kj})^2} e^{-\frac{\gamma\sigma^2}{a_{kk1}}} - \\
&\sum_{j\neq k} \frac{A_j a_{kk2}}{(a_{kk1}-a_{kk2})} \frac{\sigma^2(a_{kk2}+\gamma a_{kj})+a_{kk2}a_{kj}}{(a_{kk2}+\gamma a_{kj})^2} e^{-\frac{\gamma\sigma^2}{a_{kk2}}}
\end{aligned} \tag{5.38}$$

Using (5.38), the achievable ergodic rate of user k at time t is given by

$$\begin{aligned}
\mathbb{E}(R_k) &= \int_0^{\infty} \log_2(1+\gamma) f_{\gamma_k}(\gamma) d\gamma \\
&\approx \chi_1 \left[e^{\frac{\sigma^2}{a_{kk1}}} Ei\left(-\frac{\sigma^2}{a_{kk1}}\right) - e^{\frac{\sigma^2}{a_{kj}}} Ei\left(-\frac{\sigma^2}{a_{kj}}\right)\right] - \\
&\chi_2 \left[e^{\frac{\sigma^2}{a_{kk2}}} Ei\left(-\frac{\sigma^2}{a_{kk2}}\right) - e^{\frac{\sigma^2}{a_{kj}}} Ei\left(-\frac{\sigma^2}{a_{kj}}\right)\right]
\end{aligned} \tag{5.39}$$

where $\mathrm{Ei}(x) = -\int_{-x}^{\infty} \frac{e^{-t}}{t} dt$ denotes the exponential integral function [120].

So, the general expression of the downlink ergodic user rate at the user k ((5.39), derived in Appendix 6.2), where $\chi_1 = \frac{1}{\ln 2} \frac{a_{kk1}^2}{(a_{kk1}-a_{kk2})} \sum_{j\neq k} \frac{a_{kj}}{(a_{kj}-a_{kk1})} \left(\prod_{\substack{i\neq j \\ j\neq k}} \frac{1}{(a_{kj}-a_{ki})}\right)$ and $\chi_2 = \frac{1}{\ln 2} \frac{a_{kk2}^2}{(a_{kk1}-a_{kk2})} \sum_{j\neq k} \frac{a_{kj}}{(a_{kj}-a_{kk2})} \left(\prod_{\substack{i\neq j \\ j\neq k}} \frac{1}{(a_{kj}-a_{ki})}\right)$.

For the special case of general ergodic capacity with one user, i.e., $k = 1$ and $j = 0$, the ergodic user rate obtained by substituting the value of k and j in (5.39) and is written as

$$\mathbb{E}(R_1) \approx \frac{1}{\ln 2}\frac{1}{a_{111} - a_{112}}\left[a_{111}e^{\frac{\sigma^2}{a_{111}}}Ei\left(-\frac{\sigma^2}{a_{111}}\right) - a_{112}e^{\frac{\sigma^2}{a_{112}}} Ei\left(-\frac{\sigma^2}{a_{112}}\right)\right] \tag{5.40}$$

We consider the DAS with two single-user clusters case, i.e., $k = 1$ and $j = 1$. The ergodic user rate is obtained by substituting $k = 1$ and $j = 1$ in (5.39) and written as equation (5.41).

$$\mathbb{E}(R_1) \approx \frac{1}{\ln 2}\frac{1}{a_{111} - a_{112}}\left[\frac{a_{111}^2}{(a_{12} - a_{111})}\left\{e^{\frac{\sigma^2}{a_{111}}}Ei\left(-\frac{\sigma^2}{a_{111}}\right) - e^{\frac{\sigma^2}{a_{12}}}Ei\left(-\frac{\sigma^2}{a_{12}}\right)\right\} - \frac{a_{112}^2}{(a_{12} - a_{112})}\left\{e^{\frac{\sigma^2}{a_{112}}}Ei\left(-\frac{\sigma^2}{a_{112}}\right) - e^{\frac{\sigma^2}{a_{12}}}Ei\left(-\frac{\sigma^2}{a_{12}}\right)\right\}\right] \tag{5.41}$$

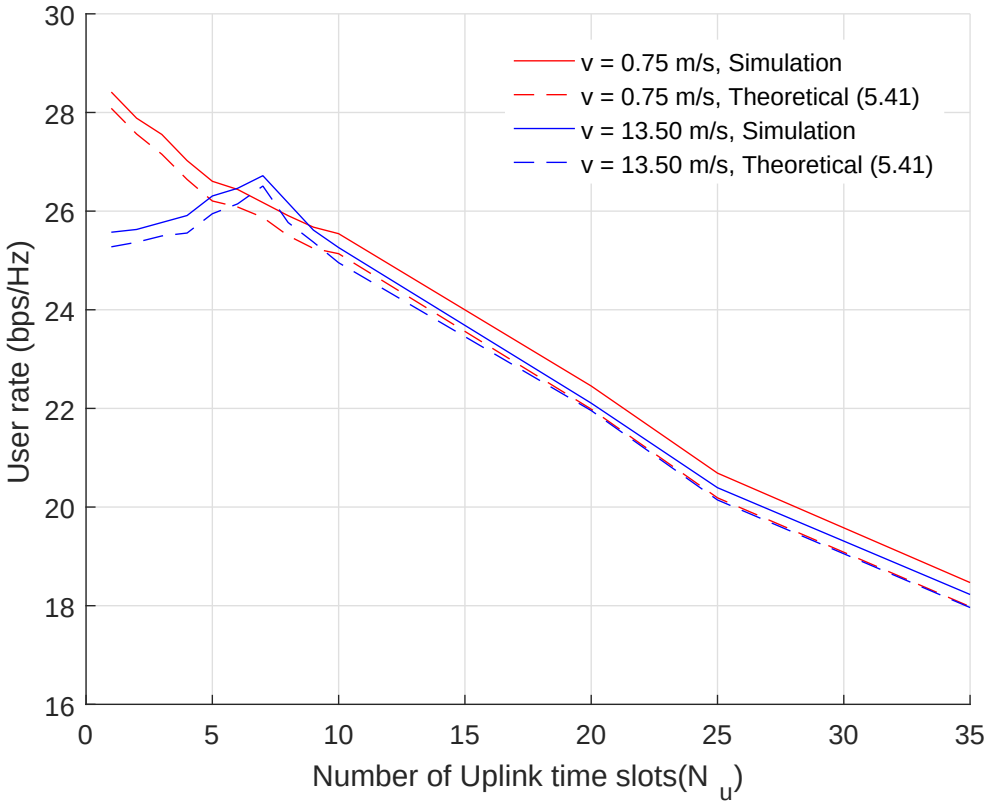

Figure 5.12: Illustration of Ergodic user rate of different mobility users over number of uplink time slots, N_u, where $\rho_o = 0.8$, $K = 2$ and $N_t = 400$.

Fig. 5.12 illustrates simulation and analytical results for the ergodic rate of single user clustering against the number of uplink time slots N_u. The user speed is fixed and $\rho_o = 0.8$ and $K = 2$. From this figure, it can be seen that our derived ergodic rate approximately matches with the simulation results. When $v = 0.75$ m/s, the autocorrelation coefficient of user is always higher than threshold value and the channel mismatch becomes small within the feedback interval. Therefore, the sum rate is highest at the least number of uplink time slots, i.e., $N_u = 1$. The user rate starts to decrease when the number of uplink time slots increases due to a reduction of the downlink time slots in the overall time slots. When $v = 13.50$ m/s, the channel mismatch becomes large within feedback interval and the autocorrelation becomes lower than the

threshold value. Therefore, the user rate increases up to $N_u = 7$ because the reduced feedback interval enables the more frequent CSI update. The user of the more accurate channel estimation for precoding derivation can compensate the reduction of the number of downlink time slots. However, the user rate starts to drop beyond $N_u = 7$. This is because the reduction of the number of downlink time slots becomes more significant while the improvement of CSI accuracy saturates. When the number of uplink time slots increases beyond $N_u = 10$, the user rate for both user speed remain similar due to the reduction of the downlink time slots in the overall time slots.

5.6 Numerical Results

It is assumed that the users have different speeds and its speed varies from 0 to 15 m/s. The MSI is perfectly known at the CU. The frame length is set as $T = 10$ ms which is divided into $N = 100$ time slots, and hence time slot length is $T_c = 0.1$ ms. The signal is transmitted at each downlink transmit slot. In the antenna selection, the number of RAUs assigned to user is one. Table 5.2 summarizes the MU-DAS system parameters for performance evaluation.

5.6.1 Average Sum Rate over User's Mobility

Fig. 5.13 illustrates the average sum rate as a function of user speed with the fixed initial location of users where $\gamma_c = 20$ dB and $\gamma_o = 50$ dB. Since the users are either at walking speed or stationary in the low mobility groups, the residual interference remains small even if the transmission delay increases. Thus, the sum rate is higher at the least number of uplink time slot. i.e., $N_u = 1$. The sum rate becomes higher at the high clustering threshold regime than the interference limited low clustering threshold regime. When user mobility increases, the residual interference increases as the transmission delay increases. The average sum rate is less than the average sum rate of the low mobility group due to channel mismatch error. At $N_u = 1$, the precoding matrix is updated

Table 5.2: Simulation Parameters

Parameter Settings	Value
Cell Model	square grid1 km^2
Carrier Frequency	2 GHz
Number of RAUs	$100 \leq N_t \leq 900$
Number of users	from 2 to 12
Users distribution	Uniform
Min dist. between RAU and user	from 1 to 10 m
Path loss exponent	3
Number of scatterers	64
Radio frame duration	10 ms
Time slot duration	0.1 ms
Total transmit power (P_t)	46 dBm
Noise power	-104 dBm
User speed range	0 m/s to 15 m/s
User target SINR	50 dB

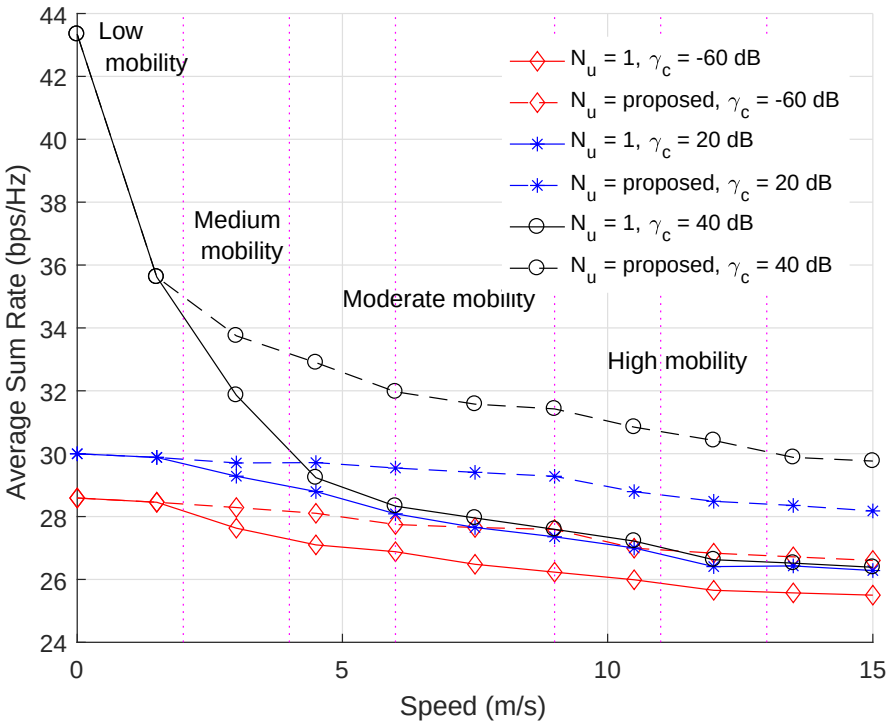

Figure 5.13: Illustration of Average sum rate over changing mobility of the users, where $\rho_o = 0.8$ $K = 2$ and $N_t = 400$.

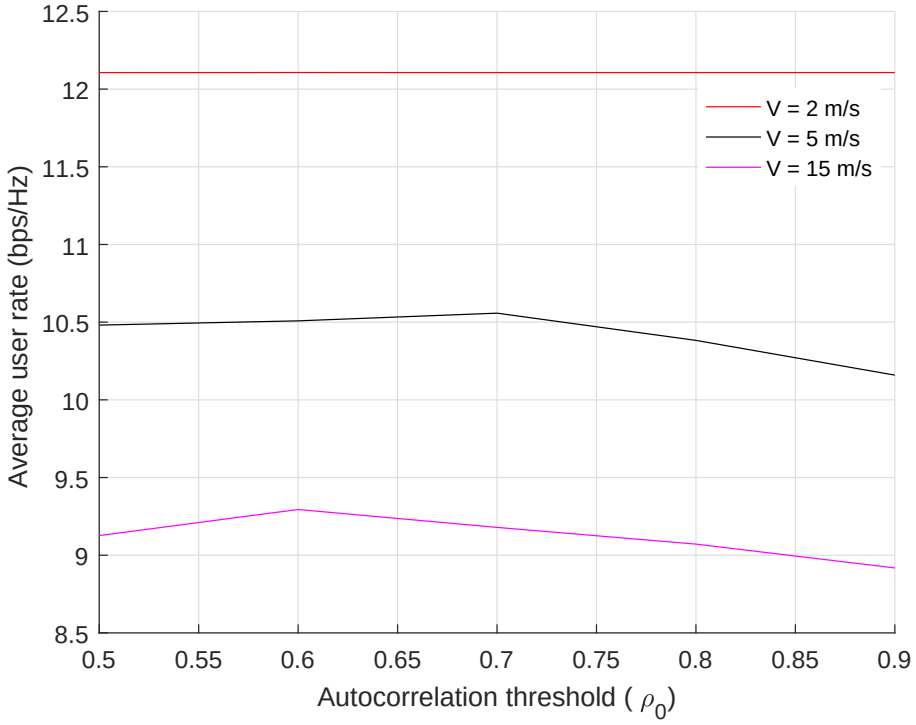

Figure 5.14: Illustration of Average user rate over autocorrelation threshold, where $K = 4$ and $N_t = 400$.

by once at $n = 1$ over feedback interval. By using proposed technique, the feedback interval is reduced based on table 5.1, the CSI is updated regularly at uplink time slot and reduced the residual interference. The SINR approximately is equal to signal to noise ratio (SNR) at high clustering threshold regime. Therefore, the average sum rate increases as clustering threshold increases and the high clustering threshold regime has a better average sum rate than the low clustering threshold regime.

Fig. 5.14 illustrates the impact of the user speed on the average user rate as a function of autocorrelation threshold when the proposed scheme is adopted. The autocorrelation is kept high due to slow channel variation when the user speed of 2 m/s, thus the average user rate is also kept high. As speed or transmission delay increases, the autocorrelation becomes much steeper than the user speed is 2 m/s as shown as Fig.

Table 5.3: Feedback parameters: adaptive autocorrelation threshold

N_u \ ρ_o	0.5	0.6	0.7	0.8	0.9
1	0-4	0-4	0-3	0-2	0-2
2	4-7	4-6	3-5	2-4	2-3
3	7-11	6-9	5-8	4-6	3-4
4	11-15	9-13	8-11	6-9	4-6
5		13-15	11-14	9-11	6-8
6			14-15	11-13	8-9
7				13-15	9-10
8					10-12
9					12-13
10					13-15
	Speed (v)				

5.9. Thus, the system is required to update CSI more frequently. For example, when the user speed is 15 m/s, the user rate exhibits the trend that it increases as the autocorrelation increases and finally reaches the optimal point at $R(\tau) = 0.6$. The reason is that the feedback interval becomes short or the number of uplink time slots increases, so the CSI updates more frequently, which reduces the channel mismatch error. However, the rate starts to decrease due to the reduction of the number of downlink time slots within a frame even though the CSI is updated more frequently. Fig. 5.14 motivates us to allocate individual autocorrelation threshold to different clusters. In cooperative clustering, the autocorrelation threshold is allocated based on fastest mobility user. Table 5.3 summarizes the uplink/feedback and autocorrelation threshold parameters for performance evaluation of different mobility user.

5.6.2 Average Sum Rate over the Number of Users

Fig.5.15 illustrates the ergodic sum rate of single user clustering for the DAS with $\gamma_c = -60$dB, $\gamma_o = 50$dB and $\rho_o = 0.8$. The initial location and speed of users are fixed for this illustration. The speeds are set to (0.5, 6.4, 14.9, 3.7, 5.6, 12.6, 1.8, 2.3, 5.2 and 5.7) m/s. When the

system selects two users, the first two sets of speed are allocated to two users and so on. From this figure, it can be seen that the derived ergodic sum rate nearly matches simulation result. The system with $N_u = 1$ updates the precoding vectors only once at $n = 1$ time slot and uses the same precoding vectors over the T_f feedback interval, which leads to that the channel mismatch error becomes bigger and bigger as the user speed or transmission delay increases. However, the system performance of the proposed scheme improves due to allocation of feedback time slot in cluster based on their speed, which updates the precoding vectors at every uplink time slots and reduces the mismatch error. Therefore, the performance of the proposed scheme outperforms the system with $N_u = 1$. The system with more number of RAUs, i.e., $RAU = 900$ outperforms the system with less number of RAUs, i.e., $RAU = 100$ due to less intra RAU distance. So, during the next uplink time slot, the user has more freedom to select RAU with the highest channel gain.

Fig. 5.16 illustrates the average sum rate of the DAS with and without MSI. The location and speed of users are randomly generated by a uniform distribution within a cell. It can be seen that the proposed feedback interval adaptation technique with knowledge of MSI outperforms the system without MSI. This is because the feedback interval can be adjusted based on MSI. Due to the cooperative clustering, the inter-cluster interference is less than clustering threshold. So, the data rate of user is mainly affected by the inter-cluster interference. However, without MSI, the CSI is updated at first time slot because the system cannot allocate feedback time slot due to the absence of mobility information. Thus, the data rate of user is mainly affected by residual interference and inter-cluster interference. The performance of the proposed feedback interval technique is also compared with a system with the number of feedback interval of one ($N_u = 1$). In proposed feedback interval adaptation technique, the CSI is updated at every feedback time slot and the residual interference is reduced, whereas, in $N_u = 1$, the CSI is updated at first time slot only. As expected, the adaptive autocorrelation threshold has superior performance to the fixed autocorrelation threshold, i.e.,

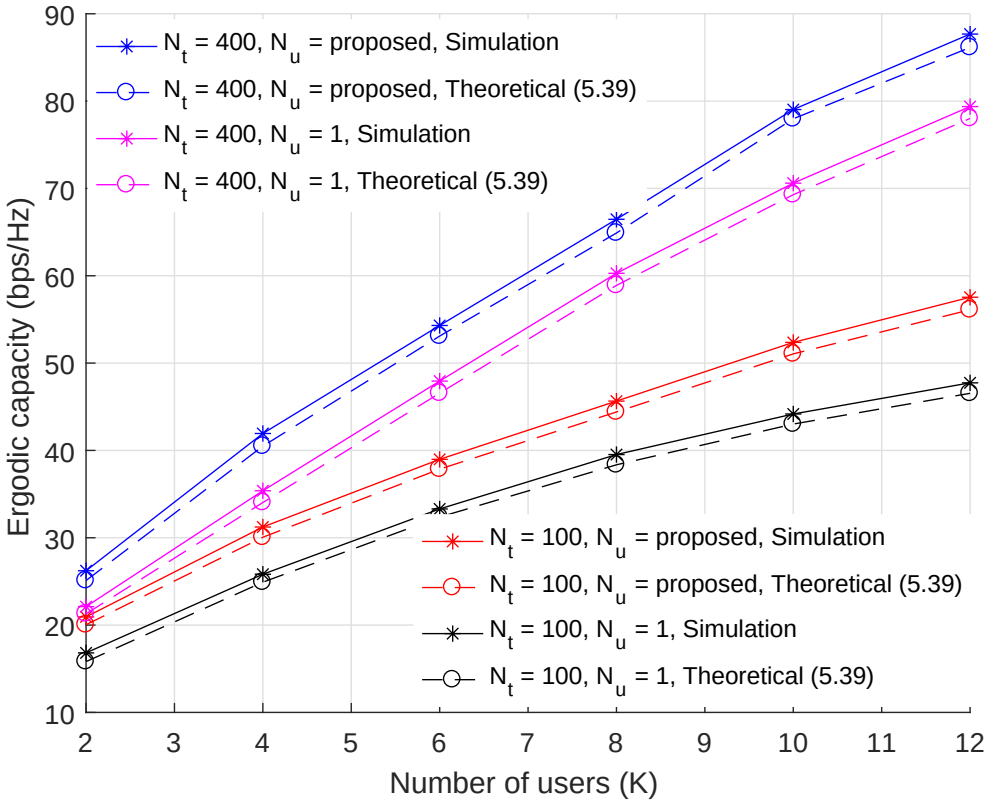

Figure 5.15: Illustration of Ergodic sum rate of different mobility users where user speed is fixed.

$\rho_o = 0.8$ due to the individual allocation of autocorrelation threshold in each cooperative clustering.

Fig. 5.17 illustrates the average sum rate for the DAS with and without cooperative clustering employing the proposed feedback interval technique with random user locations. Users' speeds are randomly generated by a uniform distribution within a cell. The performance of the proposed feedback interval technique is also compared to a system with and without channel error. It can be seen from Fig. 5.17 that the DAS with cooperative clustering outperforms the system without cooperative clustering due to the joint processing of the signal to cancel uncoordinated inter-cluster interference. The residual interference is reduced by

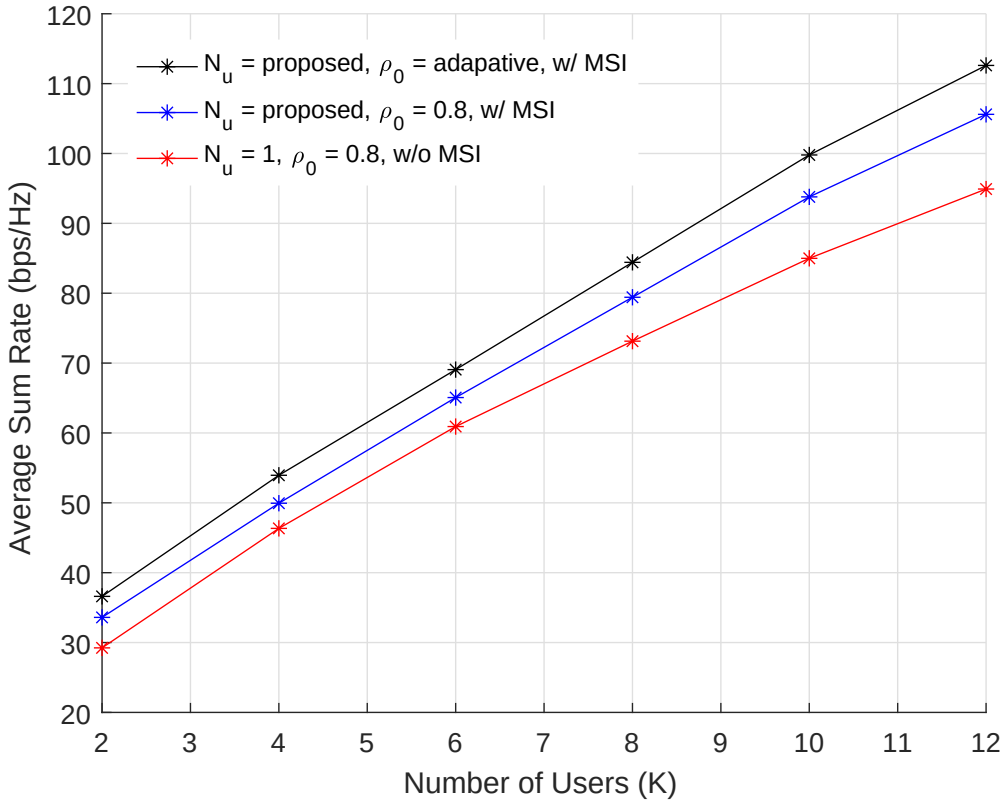

Figure 5.16: Illustration of Average sum rate of different users mobility with and without MSI where cooperative clustering is formed.

reducing the feedback interval. The SINR is mainly affected by noise and the inter-cluster interference which is smaller than the clustering threshold. Within the non-cooperative clustering, the average sum rate with and without channel error are similar. This is because the SINR is mainly affected by the inter-cluster interference, so that the system sum rate is limited.

5.6.3 Average Sum Rate over the Number of RAUs

Fig. 5.18 illustrates the average sum rate as a function of the number of RAUs. The total number of RAUs increases in the DAS leads to a significant increase in sum rate due to a larger number of degrees of freedom

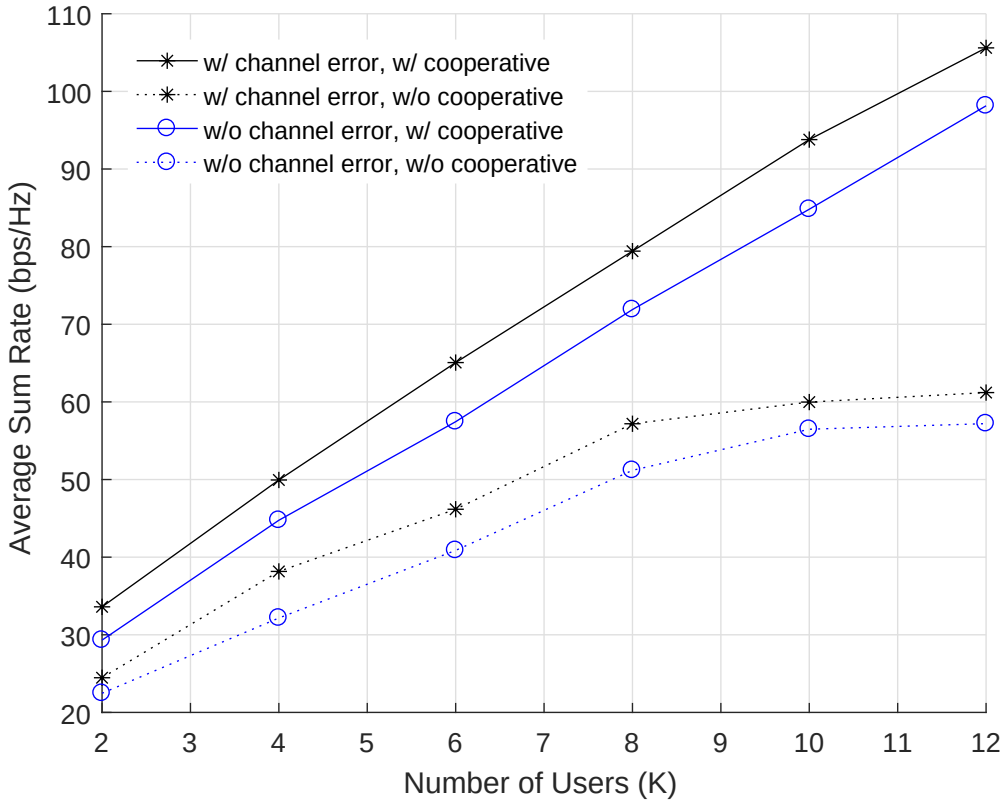

Figure 5.17: Illustration of Average sum rate of different users mobility with and without cooperative clustering where clustering threshold is 20dB and user target SINR 50 dB at feedback time slot.

(DoF). In the DAS, as the total number of RAUs increases, the path loss between the user and associated RAU decreases. As a result, the multiuser interference becomes more significant and the system performance gain is saturated.

5.7 summary

The sum rate of TDD downlink MU-DAS with the consideration of different user speed. A feedback interval reduction technique based on an autocorrelation of the channel is proposed to minimize the channel mismatch error. The channel gain based antenna selection and SINR thresh-

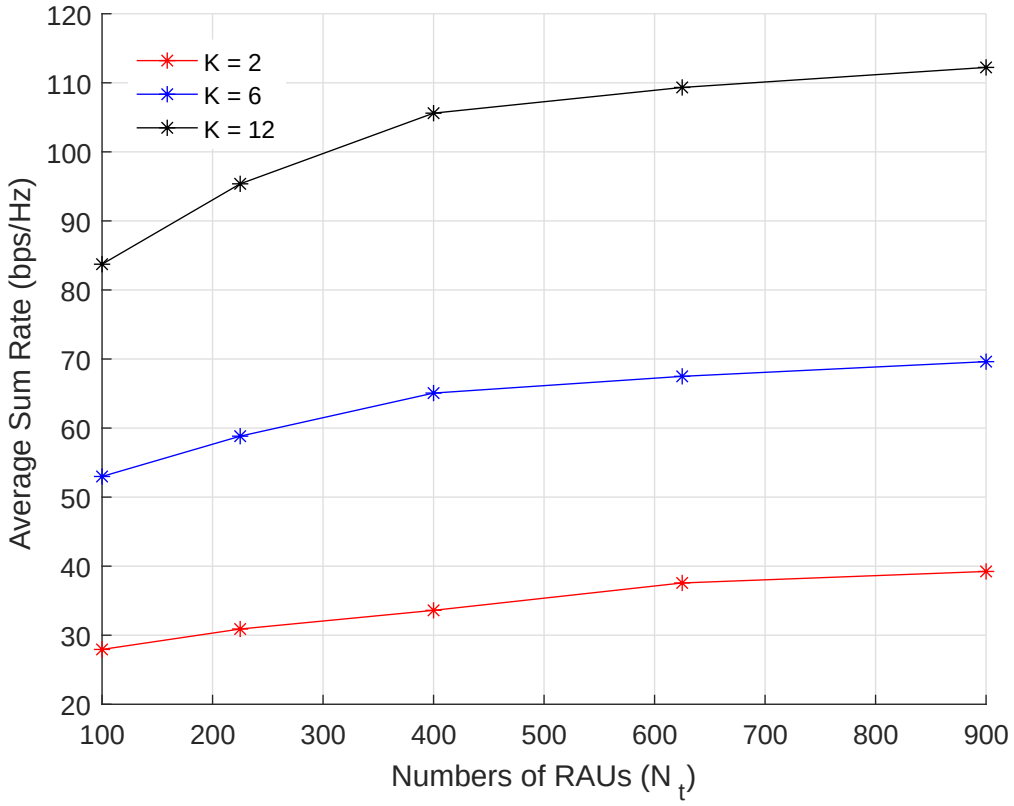

Figure 5.18: Illustration of Average sum rate of different users mobility over network size, N_t with various user speed.

old based user clustering is proposed to reduce the system computational complexity. To maximize the sum rate, the cooperative clustering is proposed where the feedback interval technique is implemented based on fastest mobility user. The numerical results have shown that the proposed technique can maximize the system sum rate in user movement environment. The numerical result has also shown that individual autocorrelation threshold value can be allocated to each cluster, to maximize the system sum rate. The proposed technique has good performance for wide range of speed and suitable for future wireless communication systems.

Chapter 6

Conclusions and Future Research

This thesis addresses coordinated transmission schemes in wireless interference networks and their performance limits. The focus has been put mainly on issues regarding channel mismatch error due to user mobility or transmission delay, user clustering to reduce computational complexity CSI feedback and adaptive transmission in TDD. These issues have been investigated in different wireless communication scenarios, summarized as follows.

6.1 Summary of Contributions

In chapter 3, the channel gaind based user clustering algorithm is proposed, which aims at reaching the performance obtained by the exhaustive-search algorithm (optimum method) but with lower complexity. Within a cluster, ZF precoding is used to cancel inter-user interference. The proposed algorithm also utilizes more transmit power than one cluster. The performance and complexity of the proposed algorithm have been validated and compared to two other algorithms; the exhaustive search algorithm and the single-user algorithm. The performance of proposed algorithm is compared with multi-user distributed and co-located MIMO. In chapter 4, the interference alignment technique is proposed to coordinate inter-cluster interference. In the DAS, each cluster receives different power level interference from the RAUs of the other clusters due to different large scale fading. The interference alignment is used to align strong

inter-cluster interferences into $N_r - 1$ dimension. The weak inter-cluster interference is treated as noise. The performance of the proposed algorithm is compared to other algorithms; single cluster algorithm, random user cluster and norm based cluster. The performance of single cluster is better than the proposed technique. This is because intra-cluster interference is cancelled by using block diagonalization precoding.
In chapter 5, the sum rate of TDD downlink MU-DAS is studied with the consideration of different user speed, while guaranteeing user's rate requirements and per antenna power constraints. The following conclusions are drawn:

1. In order to maximize the cell average sum rate, the problem was solved by channel gain based antenna selection and SINR threshold based user clustering to reduce the computational complexity of precoding matrix size.

2. Analytical expressions of single user clustering have been presented and verified through simulations.

3. The CSI was obtained by sending a uplink pilot from the users to the transmitter. However, frequent CSI updates are required at the transmitter as mobility increases or transmission delay increases. A feedback interval reduction technique based on an autocorrelation of the channel was proposed to minimize the channel mismatch error.

4. The proposed technique can maximize the system sum rate over a time varying channel in MU-DAS. The proposed scheme performance improves as the user speed increases.

6.2 Future Research

The work in this thesis only provides basic platform for mobility users. In the future, more realistic assumptions should be taken into consideration. Specifically, in this thesis, the user speed and direction is constant for each user. However, the user speed and direction may vary based on

practical environment. It is important to further characterize the downlink rate performance in a variable speed and direction of the user. The linear precoding technique ZF, is considered in this thesis. However, the optimization precoding design of a DAS in time-varying channel is an interesting topic that deserves attention in future study.

In this thesis, the maximum speed of user is 15 m/s which can be extended to higher speed by reducing time slot duration or changing carrier frequency. In future study, the downlink performance of high speed users in motorway or in high speed train is an interesting topic because the large-scale fading may not remain constant over the feedback interval. A global optimization in this environment, would lead to high computational complexity and high overhead for a DAS. To reduce the complexity, it is important to study to decompose the original problem into multiple sub-problems based on the concept of user clustering. Similarly, to reduce the overhead, it is important to further study how to optimize of uplink time slot without degrading the system performance.

Appendices

Appendix A

Derivation of (5.31)

The effective channel gain $\gamma_{k,D} = a_{kk1}y_{kD1} + a_{kk2}y_{kD2} = \gamma_{kD1} + \gamma_{kD2}$, the PDF of γ_{kD1} and γ_{kD2} are

$$f_{\gamma_{kD1}}(\gamma) = \frac{1}{a_{kk1}} e^{-\frac{\gamma}{a_{kk1}}} \text{and} f_{\gamma_{kD2}}(\gamma) = \frac{1}{a_{kk2}} e^{-\frac{\gamma}{a_{kk2}}} \tag{1}$$

The distribution of the effective channel gain $\gamma_{k,D} = \gamma_{kD1} + \gamma_{kD2}$ is given by

$$\begin{aligned} f_{\gamma_{k,D}}(\gamma) &= \int_0^\infty f_{\gamma_{kD1}}(\gamma - \gamma_{kD2}) f_{\gamma_{kD2}}(\gamma_{kD2}) d\gamma_{kD2} \\ &= \frac{1}{a_{kk1}a_{kk2}} \int_0^\infty e^{-\frac{\gamma-\gamma_{kD2}}{a_{kk1}}} e^{-\frac{\gamma_{kD2}}{a_{kk2}}} d\gamma_{kD2} \\ &= \frac{e^{-\frac{\gamma}{a_{kk1}}}}{a_{kk1}a_{kk2}} \int_0^\gamma e^{-\frac{a_{kk1}-a_{kk2}}{a_{kk1}a_{kk2}}\gamma_{kD2}} d\gamma_{kD2} \\ &= \frac{1}{a_{kk1} - a_{kk2}} \left(e^{-\frac{\gamma}{a_{kk1}}} - e^{-\frac{\gamma}{a_{kk2}}} \right) \end{aligned} \tag{2}$$

Appendix B

Derivation of (5.36)

The MGF of the inter-cluster interference for the user k-th is

$$\begin{aligned} M_{\gamma_{k,I}}(s) &= \prod_{j \neq k} \frac{1}{(1 - a_{kj}s)} \\ &= \frac{1}{1 - a_{k,1}s} \cdot \frac{1}{1 - a_{k,2}s} \cdots \frac{1}{1 - a_{k,K}s} \\ &= \frac{A_1}{1 - a_{k,1}s} + \frac{A_2}{1 - a_{k,2}s} + \cdots + \frac{A_K}{1 - a_{k,K}s} \\ &= \sum_{j \neq k} \left(\frac{A_j}{1 - a_{kj}s} \right) \end{aligned} \tag{3}$$

The coefficient A_j can be calculated through the method of undetermined coefficients, that is, multiplying $(1 - a_{kj}s)$ respectively to both sides of (3). Then we have

$$\begin{aligned} A_j &= M_{\gamma_{k,I}}(s) \cdot (1 - a_{kj}s) \Big|_{s=\frac{1}{a_{kj}}} \\ &= \left[(1 - a_{kj}s) \prod_{i \neq k, i \neq j} \frac{1}{(1 - a_{k,i}s)} \right] \Bigg|_{s=\frac{1}{a_{kj}}} \\ &= \left(\prod_{i \neq k, i \neq j} \frac{a_{kj}}{(a_{kj} - a_{ki})} \right) \end{aligned} \tag{4}$$

Since, the pair of the PDF and its corresponding MGF as,

$$\frac{A_j}{1 - a_{kj}s} \Longleftrightarrow A_j \frac{1}{a_{kj}} e^{-\frac{\gamma}{a_{kj}}} \tag{5}$$

Substituting (3) into (6.2), the PDF of the inter-cluster interference can be express as

$$f_{\gamma_{k,I}}(\gamma) = \sum_{j \neq k} A_j \frac{1}{a_{kj}} e^{-\frac{\gamma}{a_{kj}}} \tag{6}$$

where A_j is given by (4).

Appendix C

Derivation of (5.39)

The achievable ergodic rate of the user k is expressed as

$$\begin{aligned}\mathbb{E}(R_k) &= \int_0^\infty \log_2(1+\gamma) f_{\gamma_k}(\gamma) d\gamma \\ &\approx \int_0^\infty \log_2(1+\gamma) \left(B_1 \frac{\sigma^2(a_{kk1}+\gamma a_{kj}) + a_{kk1}a_{kj}}{(a_{kk1}+\gamma a_{kj})^2} \right. \\ &\left. e^{-\frac{\gamma\sigma^2}{a_{kk1}}} - B_2 \frac{\sigma^2(a_{kk2}+\gamma a_{kj}) + a_{kk2}a_{kj}}{(a_{kk2}+\gamma a_{kj})^2} e^{-\frac{\gamma\sigma^2}{a_{kk2}}} \right) d\gamma \end{aligned} \tag{7}$$

where $B_1 = \sum_{j\neq k} \frac{A_j a_{kk1}}{(a_{kk1}-a_{kk2})}$ and $B_2 = \sum_{j\neq k} \frac{A_j a_{kk2}}{(a_{kk1}-a_{kk2})}$.

(7) can be solved by using integration by parts. For simplicity, the first term of (7) is solved by using integration by parts as

$$\begin{aligned} C_{11} &= \int_0^\infty \log_2(1+\gamma) \left(B_1 \frac{\sigma^2(a_{kk1}+\gamma a_{kj}) + a_{kk1}a_{kj}}{(a_{kk1}+\gamma a_{kj})^2} e^{-\frac{\gamma\sigma^2}{a_{kk1}}} \right) d\gamma \\ &= B_1 \int_0^\infty \log_2(1+\gamma) \frac{1}{a_{kk1}} \frac{1}{1+\gamma\frac{a_{kj}}{a_{kk}}} \left(\sigma^2 + \frac{a_{kj}}{1+\gamma\frac{a_{kj}}{a_{kk}}} \right) e^{-\frac{\gamma\sigma^2}{a_{kk1}}} d\gamma \\ &= B_1 \frac{1}{\ln 2} \frac{\sigma^2}{a_{kj}-a_{kk1}} \int_0^\infty \left[\ln\left(1+\gamma\frac{a_{kj}}{a_{kk1}}\right) e^{-\frac{\sigma^2\gamma}{a_{kk1}}} \right. \\ &\left. - \ln(1+\gamma) e^{-\frac{\sigma^2\gamma}{a_{kk1}}} \right] d\gamma \end{aligned} \tag{8}$$

Based on the formula [120]

$$C_{11} = \chi_1 \left(e^{\frac{\sigma^2}{a_{kk1}}} Ei(-\frac{\sigma^2}{a_{kk1}}) - e^{\frac{\sigma^2}{a_{kj}}} Ei(-\frac{\sigma^2}{a_{kj}}) \right) \tag{9}$$

where $\chi_1 = \frac{1}{\ln 2}\frac{a_{kk1}^2}{(a_{kk1}-a_{kk2})}\sum_{j\neq k}\frac{a_{kj}}{(a_{kj}-a_{kk1})}\left(\prod_{\substack{i\neq j\\ j\neq k}}\frac{1}{(a_{kj}-a_{ki})}\right)$.
Similarly, the second term of (7) is solved as

$$C_{12} = \chi_2\left(e^{\frac{\sigma^2}{a_{kk2}}}Ei(-\frac{\sigma^2}{a_{kk2}}) - e^{\frac{\sigma^2}{a_{kj}}}Ei(-\frac{\sigma^2}{a_{kj}})\right) \tag{10}$$

where$\chi_2 = \frac{1}{\ln 2}\frac{a_{kk2}^2}{(a_{kk1}-a_{kk2})}\sum_{j\neq k}\frac{a_{kj}}{(a_{kj}-a_{kk2})}\left(\prod_{\substack{i\neq j\\ j\neq k}}\frac{1}{(a_{kj}-a_{ki})}\right)$.

Therefore, the achievable ergodic rate of user k at time t is expressed as

$$\begin{aligned}\mathbb{E}(R_k) \approx \chi_1\left[e^{\frac{\sigma^2}{a_{kk1}}}Ei\left(-\frac{\sigma^2}{a_{kk1}}\right) - e^{\frac{\sigma^2}{a_{kj}}}Ei\left(-\frac{\sigma^2}{a_{kj}}\right)\right] - \\ \chi_2\left[e^{\frac{\sigma^2}{a_{kk2}}}Ei\left(-\frac{\sigma^2}{a_{kk2}}\right) - e^{\frac{\sigma^2}{a_{kj}}}Ei\left(-\frac{\sigma^2}{a_{kj}}\right)\right]\end{aligned} \tag{11}$$

where $\mathrm{Ei}(x) = -\int_{-x}^{\infty}\frac{e^{-t}}{t}dt$ denotes the exponential integral function [120].

Bibliography

[1] A. Osseiran, F. Boccardi, V. Braun, K. Kusume, P. Marsch, M. Maternia, O. Queseth, M. Schellmann, H. Schotten, H. Taoka, H. Tullberg, M. A. Uusitalo, B. Timus, and M. Fallgren, "Scenarios for 5G mobile and wireless communications: the vision of the METIS project," *IEEE Commun. Mag.*, vol. 52, pp. 26–35, May 2014.

[2] Cisco, "Cisco visual networking index: gobal mobile data traffic forecast update." 2016-2021 White Paper, Mar. 2017.

[3] Ericsson, "Ericsson mobility report." White Paper, Nov. 2016.

[4] X. H. You, D. M. Wang, B. Sheng, X. Q. Gao, X. S. Zhao, and M. Chen, "Cooperative distributed antenna systems for mobile communications [Coordinated and Distributed MIMO]," *IEEE Wireless Commun.*, vol. 17, pp. 35–43, Jun. 2010.

[5] T. Marzetta, "Non cooperative cellular wireless with unlimited numbers of base station antennas," *IEEE Trans. Wireless Commun.*, vol. 9, pp. 3590–3600, Nov. 2010.

[6] F. Rusek, D. Persson, B. K. Lau, E. G. Larsson, T. L. Marzetta, O. Edfors, and F. Tufvesson, "Scaling up MIMO: Opportunities and challenges with very large arrays," *IEEE Signal. Process. Mag.*, vol. 30, pp. 40–60, Jan. 2013.

[7] J. Wang, H. Zhu, and N. J. Gomes, "Distributed antenna systems for mobile communications in high speed trains," *IEEE J. Sel. Areas Commun.*, vol. 30, pp. 675–683, Apr. 2012.

[8] H. Zhu and J. Wang, "Radio resource allocation in multiuser distributed antenna systems," *IEEE J. Sel. Areas Commun.*, vol. 31, pp. 2058–2066, Oct. 2013.

[9] L. Xiao, L. Dai, H. Zhuang, S. Zhou, and Y. Yao, "Information-theoretic capacity analysis in MIMO distributed antenna systems," in *The 57th IEEE Semiannual Vehicular Technology Conference, 2003. VTC 2003-Spring.*, vol. 01, pp. 779–782, Apr. 2003.

[10] H. Zhu and D. Toumpakaris, "Low-complexity resource allocation and its application to distributed antenna systems," *IEEE Wireless Commun.*, vol. 17, p. 44–50, Jun. 2010.

[11] X. You, D. Wang, P. Zhu, and B. Sheng, "Cell edge performance of cellular mobile systems," *IEEE J. Sel. Areas Commun.*, vol. 29, pp. 1139–1150, Jun. 2011.

[12] H. Zhu, "Performance Comparison Between Distributed Antenna and Microcellular Systems," *IEEE J. Sel. Areas Commun.*, vol. 29, pp. 1151–1163, Jun. 2011.

[13] H. Kim, S.-R. Lee, K.-J. Lee, and I. Lee, "Transmit schemes based on sum rate analysis in distributed antenna systems," *IEEE Trans. Wireless Commun.*, vol. 11, pp. 1201–1209, Mar. 2012.

[14] L. Dai, "A comparative study on uplink sum capacity with co-located and distributed antennas," *IEEE J. Sel. Areas Commun.*, vol. 29, pp. 1200–1213, Jun. 2011.

[15] A. Ghosh, N. Mangalvedhe, R. Ratasuk, B. Mondal, M. Cudak, E. Visotsky, T. A. Thomas, J. G. Andrews, P. Xia, H. S. Jo, H. S. Dhillon, and T. D. Novlan, "Heterogeneous cellular networks: From theory to practice," *IEEE Commun. Mag.*, vol. 50, pp. 54–64, Jun. 2012.

[16] J. Zheng, Y. Wu, N. Zhang, H. Zhou, Y. Cai, and X. S. Shen, "Optimal power control in ultra-dense small cell networks: A game-

theoretic approach," *IEEE Trans. Wireless Commun.*, vol. 16, pp. 4139–4150, Jul. 2017.

[17] C. L. I, C. Rowell, S. Han, Z. Xu, G. Li, and Z. Pan, "Toward green and soft: a 5G perspective," *IEEE Commun. Mag.*, vol. 52, pp. 66–73, Feb. 2014.

[18] A. Ghosh, T. A. Thomas, M. C. Cudak, R. Ratasuk, P. Moorut, F. W. Vook, T. S. Rappaport, G. R. MacCartney, S. Sun, and S. Nie, "Millimeter-wave enhanced local area systems: A high-data-rate approach for future wireless networks," *IEEE J. Sel. Areas Commun.*, vol. 32, pp. 1152–1163, Jun. 2014.

[19] S. G. Larew, T. A. Thomas, M. Cudak, and A. Ghosh, "Air interface design and ray tracing study for 5G millimeter wave communications," in *IEEE Globecom Workshops (GC Wkshps)*, pp. 117–122, Dec. 2013.

[20] J. Huang, C. X. Wang, R. Feng, J. Sun, W. Zhang, and Y. Yang, "Multi-frequency mmWave massive MIMO channel measurements and characterization for 5G wireless communication systems," *IEEE J. Sel. Areas Commun.*, vol. 35, pp. 1591–1605, Jul. 2017.

[21] D. Wang, J. Wang, X. H. You, Y. Wang, and M. Chen, "Spectral efficiency of distributed MIMO systems," *IEEE J. Sel. Areas Commun.*, vol. 31, pp. 2112–2127, Oct. 2013.

[22] S. I. on Distributed Broadband Wireless Communications *IEEE J. Sel. Areas Commun.*, vol. 29, Jul. 2011.

[23] H. Hu, Y. Zhang, and J. Luo, *Distributed Antenna Systems: Open Architecture for Future Wireless Communications.* CRC Press, 2007.

[24] C. M. R. Institute, "C-RAN: The road towards green RAN (Version 3.0)." White Paper, Jun. 2014.

[25] H. Zhu, "Performance comparison between distributed antenna and microcellular systems," *IEEE J. Sel. Areas Commun.*, vol. 29, pp. 1151–1163, Jun. 2011.

[26] H. Zhu, "On frequency reuse in cooperative distributed antenna systems," *IEEE Commun. Mag.*, vol. 50, pp. 85–89, Apr. 2012.

[27] W. Choi and J. G. Andrews, "Downlink performance and capacity of distributed antenna systems in a multicell environment," *IEEE Trans. Wireless Commun.*, vol. 6, pp. 69–73, Jan. 2007.

[28] J. Zhang and J. G. Andrews, "Distributed antenna systems with randomness," *IEEE Trans. Wireless Commun.*, vol. 7, pp. 3636–3646, Sept. 2008.

[29] J. Park, E. Song, and W. Sung, "Capacity analysis for distributed antenna systems using cooperative transmission schemes in fading channels," *IEEE Trans. Wireless Commun.*, vol. 8, pp. 586–592, Feb. 2009.

[30] A. M. Saleh, A. J. Rustako, and R. S. Roman, "Distributed antenna for indoor radio communications," *IEEE Trans. Commun.*, vol. 35, pp. 1245–1251, Dec. 1987.

[31] H. Osman, H. Zhu, D. Toumpakaris, and J. Wang, "Achievable rate evaluation of in-building distributed antenna systems," *IEEE Trans. Wireless Commun*, vol. 12, pp. 3510–3521, Jul. 2013.

[32] T. Alade, H. Zhu, and J. Wang, "Uplink spectral efficiency analysis of in-building distributed antenna systems," *IEEE Trans. Wireless Commun.*, vol. 14, pp. 4063–4074, Jul. 2015.

[33] K. Morita and H. Ohtsuka, "The new generation of wireless communications based on fiber-radio technologies," *IEICE Trans. Commun.*, vol. E76-B, pp. 1061–1068, Sept. 1993.

[34] J. Wang and L. B. Milstein, "CDMA overlay situations for microcellular mobile communications," *IEEE Trans. Commun.*, vol. 43, pp. 603–614, Feb./Mar./Apr. 1995.

[35] K. J. Kerpez, "A radio access system with distributed antennas," *IEEE Trans. Veh. Tech.*, vol. 5, pp. 265–275, May 1996.

[36] M. Z. Win, M. Chiani, and A. Zanella, "On the Capacity of Spatially Correlated MIMO Rayleigh Fading Channels," *IEEE Trans. Info. Theory*, vol. 49, pp. 2363–2371, Oct. 2003.

[37] W. Yu and T. Lan, "Transmitter optimization for the multi-antenna downlink with per-antenna power constraints," *IEEE Trans. Signal Process.*, vol. 55, pp. 2646–2660, Jun. 2007.

[38] W. Roh and A. Paulraj, "Performance of the distributed antenna systems in a multi-cell environment," in *The 57th IEEE Semiannual Vehicular Technology Conference, 2003. VTC 2003-Spring.*, vol. 1, p. 587–591, Apr. 2003.

[39] W. Feng, X. Zhang, S. Zhou, J. Wang, and M. Xia, "Downlink power allocation for distributed antenna systems with random antenna layout," in *2009 IEEE 70th Vehicular Technology Conference Fall*, pp. 1–5, Sept. 2009.

[40] G. R. Group, "Long Term Evolution, Evolved Universal Terrestrial Radio Access (E-UTRA) Physical Layer, General Descriptions. 3GPP TS 36.201), ETSI TS 36.201 (2011-01)," 2003.

[41] D. Gesbert, M. Kountouris, R. Heath, C.-B. Chae, , and T. Salzer, "Shifting the MIMO paradigm," *Trans. Sig. Process. Mag.*, vol. 24, p. 36 – 46, Sept. 2007.

[42] L. Dai, S. Zhou, and Y. Yao, "Capacity analysis in CDMA distributed antenna systems," *IEEE Trans. Wireless Commun.*, vol. 04, pp. 2613–2620, Nov. 2005.

[43] R. Heath, S. Peters, Y. Wang, and J. Zhang, "A current perspective on distributed antenna systems for the downlink of cellular systems," *IEEE Commun. Mag.*, vol. 51, pp. 161–167, Apr. 2013.

[44] N. Jindal, "Mimo broadcast channels with finite-rate feedback," *Trans. Inform. Theory*, vol. 52, p. 5045 – 5060, Nov. 2006.

[45] T. Yoo and A. Goldsmith, "On the optimality of multiantenna broadcast scheduling using zero-forcing beamforming," *IEEE J. Sel. Areas Commun.*, vol. 24, pp. 528–541, Mar. 2006.

[46] D. W. Bliss, K. W. Forsythe, I. Hero, A. O., and A. F. Yegulalp, "Environmental issues for MIMO capacity," *IEEE Trans. Sig. Process.*, vol. 50, p. 2128–2142, Sept. 2002.

[47] P. Kyritsi, R. A. Valenzuela, and D. C. Cox, "Channel and capacity estimation errors," *IEEE Commun. Lett.*, vol. 06, p. 517–519, Dec. 2002.

[48] T. Yoo and A. Goldsmith, "Capacity of fading MIMO channels with channel estimation error," in *2004 IEEE Int. Conf. Commun.*, vol. 2, p. 808–813, Jun. 2004.

[49] A. Wiesel, Y. C. Eldar, and S. Shami, "Zero-Forcing precoding and generalized inverses," *IEEE Trans. Signal Processing*, vol. 56, pp. 4409–4418, Sep. 2008.

[50] B. Bandemer, M. Haardt, and S. Visuri, "Linear MMSE multi-user MIMO downlink precoding for users with multiple antennas," in *Personal, Indoor and Mobile Radio Communications*, pp. 1–5, Sept. 2006.

[51] A. Goldsmith, *Wireless Communications*. Cambridge University Press, 2005.

[52] P. Dent, G. E. Bottomley, and T. Croft, "Jakes fading model revisited," *IEEE Electron. lett.*, vol. 29, pp. 1162–1163, Jun. 1993.

[53] R. Clarke, "A statistical theory of mobile radio reception," *Bell Syst. Tech. J.*, pp. 957–1000, Jul. 1968.

[54] R. Iqbal, T. D. Abhayapala, and T. A. Lamahewa, "Generalised clarke model for mobile-radio reception," *IET Communications*, vol. 3, pp. 644–654, Apr. 2009.

[55] W. C. Jakes, *Microwave Mobile Communications*. Wiley-IEEE Press, 1st ed. ed., 1974.

[56] J. G. Proakis and M. Salehi, *Digital Communications*. London: McGraw-Hill, 5th ed. ed., 2008.

[57] T. L. Marzetta and B. M. Hochwald, "Fast transfer of channel state information in wireless systems," *IEEE Trans. Sign. Proces.*, vol. 54, pp. 1268–1278, Apr. 2006.

[58] I. Sohn, K. B. Lee, and Y. S. Choi, "Comparison of decentralized time slot allocation strategies for asymmetric traffic in TDD systems," *IEEE Trans. Wireless Commun.*, vol. 08, pp. 2990–3003, Jun. 2009.

[59] P. Komulainen, A. Tolli, and M. Juntti, "Effective CSI signaling and decentralized beam coordination in TDD multi-cell MIMO systems," *IEEE Trans. Sign. Proces.*, vol. 61, pp. 2204–2218, May 2013.

[60] C. Wang and R. D. Murch, "Adaptive downlink multi-user MIMO wireless systems for correlated channels with imperfect CSI," *IEEE Trans. Wireless Commun.*, vol. 5, pp. 2435–2446, Sept. 2006.

[61] S. Haykin, *Adaptive Filter Theory*. Englewood Cliffs, USA: Prentice-Hall, 3rd ed. ed., 1996.

[62] D. Jaramillo-Ramirez, M. Kountouris, and E. Hardouin, "Coordinated multi-point transmission with quantized and delayed feedback," in *IEEE GLOBECOM*, pp. 2391–2396, Dec. 2012.

[63] D. Jaramillo-Ramirez, M. Kountouris, and E. Hardouin, "Coordinated multi-point transmission with imperfect channel knowledge and other cell interference," *IEEE Trans. Wireless Commun.*, vol. 14, pp. 1882–1896, Apr. 2015.

[64] S. Pandula and B.-P. Paris, "Performance analysis of mimo receivers under imperfect CSIT," *IEEE Inform. Sciences and Systems*, pp. 107–112, Mar. 2007.

[65] G. Primolevo, O. Simeone, and U. Spagnolini, "Effects of imperfect channel state information on the capacity of broadcast OSDMA-MIMO systems," in *IEEE Workshop on Sig. Proc. Advances in Wireless Commun.*, pp. 546–550, Jul. 2004.

[66] H. Shirani-Mehr, G. Caire, and M. J. Neely, "MIMO downlink scheduling with non-perfect channel state knowledge," *IEEE Trans. Commun.*, vol. 58, pp. 2055–2066, Jul. 2010.

[67] A. Muller, E. Bjornson, R. Couillet, and M. Debbah, "Analysis and management of heterogeneous user mobility in large-scale downlink systems," *IEEE Asilomar*, pp. 773–777, Nov. 2013.

[68] J. Niu, D. Lee, T. Su, G. Y. Li, and X. Ren, "User classification and scheduling in LTE downlink systems with heterogeneous user mobilities," *IEEE Trans. Wireless Commun.*, vol. 12, pp. 6205–6213, Dec. 2013.

[69] A. Vakili, M. Sharif, and B. Hassibi, "The effect of channel estimation error on the throughput of broadcast channels," in *2006 IEEE International Conference on Acoustics Speech and Signal Processing Proceedings*, vol. 04, pp. 29–32, May 2006.

[70] M. Kobayashi, G. Caire, and D. Gesbert, "Transmit diversity versus opportunistic beamforming in data packet mobile downlink transmission," *IEEE Trans. Commun.*, vol. 55, pp. 151–157, Jan. 2007.

[71] J. So and J. Cioffi, "Feedback reduction scheme for downlink multiuser diversity," *IEEE Trans. Wireless Commun.*, vol. 08, pp. 668–672, Feb. 2009.

[72] M. Bashar, M. Eslami, and M. J. Dehghani, "Threshold-based CSI feedback reduction for time-varying multiple-input multiple-output broadcast channels," *IEEE Trans. Wireless Commun.*, vol. 08, pp. 1616–1625, Feb. 2014.

[73] U. Salim and D. Slock, "How much feedback is required for TDD multi-antenna broadcast channels with user selection?," *EURASIP J. Adv. in Signal Process.*, 2010.

[74] Samsung, "3GPP TSG RAN WG1 Meeting 68, R1-120196, Performance evaluation of dynamic TDD reconfiguration." Dresden, Germany, Feb. 2012.

[75] CATT, "3GPP TSG RAN WG1 Meeting 68, R1-120118, Evaluation on TDD UL-DL reconfiguration for isolated Pico scenario." Dresden, Germany, Feb. 2012.

[76] Z. Shen, A. Khoryaev, E. Eriksson, and X. Pan, "Dynamic uplink-downlink configuration and interference management in TD-LTE," *IEEE Commun. Mag.*, vol. 50, pp. 51–59, Nov. 2012.

[77] M. Costa, "Writing on dirty paper (corresp.)," *IEEE Trans. Inform. Theory*, vol. 29, pp. 439–441, May 1983.

[78] J. Joung, Y. K. Chia, and S. Sun, "Energy-efficient, large-scale distributed-antenna system (L-DAS) for multiple users," *IEEE J. Sel. Top. Sign. Proces.*, vol. 8, pp. 954–965, Oct. 2014.

[79] R. W. Heath, T. Wu, Y. H. Kim, and A. C. K. Soong, "Multiuser mimo in distributed antenna systems," in *Proc. Asil. Conf. Signal, Syst., Comput.*, pp. 1202–1206, Nov. 2010.

[80] L.-L. Yang, "Performance of mmse multiuser detection in cellular ds-cdma systems using distributed antennas," in *Veh. Tech. Conf.*, vol. 01, pp. 274–278, May 2006.

[81] W. Yu, "Sum-capacity computation for the gaussian vector broadcast channel via dual decomposition," *IEEE Trans. Inform. Theory*, vol. 52, pp. 754–759, Feb. 2006.

[82] Z. Tu and R. S. Blum, "Multiuser diversity for a dirty paper approach," *IEEE Communications Letters*, vol. 07, pp. 370–372, Aug. 2003.

[83] G. Dimic and N. D. Sidropoulos, "Low-complexity downlink beamforming for maximum sum capacity," in *2004 IEEE International Conference on Acoustics, Speech, and Signal Processing*, vol. 4, pp. 701–704, May 2004.

[84] S. Venkatesan and H. Huang, "System capacity evaluation of multiple antenna systems using beamforming and dirty paper coding," *Bell Labs*.

[85] G. Caire and S. Shamai, "On the achievable throughput of a multiantenna gaussian broadcast channel," *IEEE Trans. Inform. Theory*, vol. 49, p. 1691–1706, Jul. 2003.

[86] H. Viswanathan, S. Venkatesan, and H. Huang, "Downlink capacity evaluation of cellular networks with known-interference cancellation," *IEEE J. Select. Areas Commun.*, vol. 21, p. 802–811, Jun. 2003.

[87] M. Bengtsson and B. Ottersten, "Optimal and suboptimal transmit beamforming," in *Handbook of Antennas in Wireless Communications*, CRC Press, 2001.

[88] M. Schubert and H. Boche, "Solution of the multiuser downlink beamforming problem with individual sinr constraints," *IEEE Trans. Veh. Tech.*, vol. 53, pp. 18–28, Jan. 2004.

[89] A. B. Gershman, N. D. Sidiropoulos, S. Shahbazpanahi, M. Bengtsson, and B. Ottersten, "Convex optimization-based beamforming," *IEEE Sig. Process. Mag.*, vol. 27, pp. 62–75, May 2010.

[90] K. Karakayali, R. Yates, G. Foschini, and R. Valenzuela, "Optimum zero-forcing beamforming with per-antenna power constraints," in *2007 IEEE International Symposium on Information Theory*, pp. 101–105, Jun. 2007.

[91] M. A. Maddah-Ali, A. S. Motahari, and A. K. Khandani, "Communication over mimo x channels: Interference alignment, decomposition, and performance analysis," *IEEE Transactions on Information Theory*, vol. 54, pp. 3457–3470, Aug. 2008.

[92] V. Cadambe and S. Jafar, "Interference alignment and degrees of freedom of the k-user interference channel," *IEEE Trans. Inf. Theory*, vol. 54, pp. 3425–3441, Aug. 2008.

[93] V. Cadambe and S. Jafar, "Can 100 speakers talk for 30-minutes each in one room within one hour and with zero interference to each other's audiance?," in *2007 Annual Allerton Conference on Communications, Control and Computing*, p. 1141–1148, 2007.

[94] S. Jafar, "Interference alignment: A new look at signal dimensions in a communication network," *Foundations and Trends in Communications and Information Theory*, vol. 7, no. 1, p. 1–134, 2011.

[95] S. A. Jafar and S. Shamai, "Degrees of freedom region of the mimo x channel," *IEEE Transactions on Information Theory*, vol. 54, pp. 151–170, Jan. 2008.

[96] O. E. Ayach, S. W. Peters, and R. W. Heath, "The practical challenges of interference alignment," *IEEE Wireless Communications*, vol. 20, pp. 35–42, Feb. 2013.

[97] A. F. Molisch and M. Win, "MIMO systems with antenna selection," *IEEE Microw. Mag.*, vol. 05, pp. 46–56, Mar. 2004.

[98] S. Sanayei and A. Nosratinia, "Antenna selection in MIMO systems," *IEEE Commun. Mag.*, vol. 42, pp. 68–73, Oct. 2004.

[99] J.-K. Lain, "Joint transmit/receive antenna selection for MIMO systems: a real valued genetic approach," *IEEE Commun. Lett.*, vol. 15, pp. 58–60, Jan. 2011.

[100] A. Gorokhov, D. A. Gore, and A. J. Paulraj, "Receive antenna selection for MIMO flat-fading channels: Theory and algorithms," *IEEE Trans. Inf. Theory*, vol. 49, pp. 2687–2696, Oct. 2003.

[101] A. F. Molisch, M. Z. Win, Y.-S. Choi, and J. H. Winters, "Capacity of MIMO systems with antenna selection," *IEEE Trans. Wireless Commun.*, vol. 4, pp. 1759–1772, Jul. 2005.

[102] L. Zhou and M. Shimizu, "Fast recursive algorithm for efficient transmit antenna selection in spatial multiplexing systems," in *2009 IEEE 70th Vehicular Technology Conference Fall*, pp. 1–5, Sept. 2009.

[103] C. Chen, "A computationally efficient near-optimal algorithm for capacity maximization based joint transmit and receive antenna selection," *IEEE commun. Lett.*, vol. 14, pp. 402–405, May 2010.

[104] R. Vaze and H. Ganapathy, "Sub-modularity and antenna selection in MIMO systems," *IEEE commun. Lett.*, vol. 16, pp. 1446–1449, Sept. 2012.

[105] R. Chen, R. Heath, and J. Andrews, "Transmit selection diversity for unitary precoded multiuser spatial multiplexing systems with linear receivers," *IEEE Trans. Signal Process.*, vol. 55, pp. 1159–1171, Mar. 2007.

[106] R. W. Heath and D. J. Love, "Transmit antenna selection for decision feedback detection in MIMO fading channels," *IEEE Trans. Signal Process.*, vol. 53, pp. 3042–3056, Aug. 2005.

[107] A. F. M. M. Z. Win, , and J. H. Winters, "Reduced-complexity transmit/receive-diversity systems," *IEEE Trans. Signal. Process.*, vol. 51, pp. 2729–2738, Nov. 2003.

[108] K. Dong, N. Prasad, X. Wang, , and S. Zhu, "Adaptive antenna selection and tx/rx beamforming for large-scale MIMO systems in 60ghz channels," *EURASIP J. Wireless Commun. Netw.*, vol. 11, p. 59, Aug. 2011.

[109] J. Starr, O. E. Ayach, and R. W. H. Jr., "Interference alignment in distributed antenna systems," *CoRR*, vol. abs/1305.2459, 2013.

[110] R. Tresch and M. Guillaud, "Clustered interference alignment in large cellular networks," in *2009 IEEE 20th International Symposium on Personal, Indoor and Mobile Radio Communications*, pp. 1024–1028, Sept. 2009.

[111] S. W. Peters and R. W. Heath, "User partitioning for less overhead in mimo interference channels," *IEEE Trans. .Wireless Commun.*, vol. 11, pp. 592–603, Feb. 2012.

[112] H. Wang, L. Li, L. Song, and X. Gao, "A linear precoding scheme for downlink multiuser mimo precoding systems," *IEEE Communications Letters*, vol. 15, pp. 653–655, Jun. 2011.

[113] W. Feng, Y. Wang, N. Ge, J. Lu, and J. Zhang, "Virtual MIMO in multi-cell distributed antenna systems: Coordinated transmissions with large-scale CSIT," *IEEE J. Sel. Areas Commun.*, vol. 31, pp. 2067–2081, Oct. 2013.

[114] L. Zheng and C. W. Tan, "Maximizing sum rates in cognitive radio networks: Convex relaxation and global optimization algorithms," *IEEE J. Sel. Areas Commun.*, vol. 32, pp. 667–680, Mar. 2014.

[115] S. Boyd and L. Vandenberghe, *Convex Optimization*. New York, USA: Cambridge Univ. Press, 2004.

[116] K. Adachi and S. Sun, "An asymmetric TDD distributed massive antenna system," in *2013 IEEE/CIC International Conference on Communications in China (ICCC)*, pp. 583–587, Aug. 2013.

[117] Z. Zhang, "Pseudo-inverse multivariate/matrix-variate distributions," *J. Multivariate Analysis*, vol. 98, pp. 1684 – 1692, Sept. 2007.

[118] S. R. Lee, J. S. Kim, S. H. Moon, H. B. Kong, and I. Lee, "Zero-forcing beamforming in multiuser MISO downlink systems under per-antenna power constraint and equal-rate metric," *IEEE Trans. Wireless Commun.*, vol. 12, pp. 228–236, Jan. 2013.

[119] M. K. Simon and M.-S. Alouini, *Digital Communication over Fading Channels*. New York: John Wiley, 2000.

[120] I. Gradshteyn and I. Ryzhik, *Table of Integrals, Series, and Products*. London: Academic Press, 2003.